

2014

Study On The High Temperature Performance Of Bio Modified Rubber Asphalt (Bmr)

Amadou M. Bocoum
North Carolina Agricultural and Technical State University

Follow this and additional works at: <https://digital.library.ncat.edu/theses>

Recommended Citation

Bocoum, Amadou M., "Study On The High Temperature Performance Of Bio Modified Rubber Asphalt (Bmr)" (2014). *Theses*. 217.
<https://digital.library.ncat.edu/theses/217>

This Thesis is brought to you for free and open access by the Electronic Theses and Dissertations at Aggie Digital Collections and Scholarship. It has been accepted for inclusion in Theses by an authorized administrator of Aggie Digital Collections and Scholarship. For more information, please contact iyanna@ncat.edu.

Study on the High Temperature Performance of Bio Modified Rubber Asphalt (BMR)

Amadou M Bocoum

North Carolina A&T State University

A thesis submitted to the graduate faculty
in partial fulfillment of the requirements for the degree of

MASTER OF SCIENCE

Department: Civil, Architectural and Environmental Engineering

Major: Civil Engineering

Major Professor: Dr. Elham H. Fini

Greensboro, North Carolina

2014

The Graduate School
North Carolina Agricultural and Technical State University
This is to certify that the Master's Thesis of

Amadou M Bocoum

has met the thesis requirements of
North Carolina Agricultural and Technical State University

Greensboro, North Carolina

2014

Approved by:

Elham H. Fini, PhD
Major Professor

Nabil Nassif, PhD
Committee Member

Robert Powell, M.S
Committee Member

Sameer Hamoush, PhD
Department Chair

Dr. Sanjiv Sarin
Dean, The Graduate School

Biographical Sketch

Amadou M Bocoum was born on 19th of March, 1974 in Kayes, Mali. He earned the Bachelor Degree from in Civil Engineering from National School of Engineering Mali Bamako, in 1999. He worked with different construction companies before moving into the USA, to take his education to the higher level. In order to pursue his interest and desire to experience the world class education, he started his graduate studies at North Carolina A & T State University from fall 2012 under the guidance of Dr. Elham H. Fini. Based on his research results, Amadou has developed a paper which was submitted to Journal of International Society of Asphalt Pavements. He also presented his research results via a poster during a poster competition at NC A&T State.

Dedication

Dedicated to my parents Mr Mamadou Bocoum & Binta Bocoum.

Acknowledgments

This thesis could not have been written without Dr Fini, who not only served as my supervisor but also encouraged and challenged me throughout my academic program. She never accepted less than my best efforts. She gives me the opportunities to join her research team, and supported me. It has been a life learning experience Thank you.

I would like to acknowledge and extend my heartfelt gratitude to Dr Sameer Amoush who supported me tirelessly throughout my program, to my committee members who shared their expertise and personal experience with me: Dr Nabil Nassif, and Mr Robert Powell. To Dr Taher Abu Lebdeh, who always helped, and advise me.

Most especially to my family, my friend, Boubacar Traore words alone cannot express what I owe them for their encouragement and financial support. Thanks to all the Simlab group reseach, to Mr Faroukh Mirzaefard the laboratory manager, and all others friends who assisted me throughout this research.

What are collected in this thesis are materials that I found in articles or in books. A special thanks to the authors mentioned in the bibliography page.

I especially thank God, who made all things possible.

Table of Contents

List of Figures	x
List of Tables	xiii
Abstract	1
CHAPTER 1 Introduction	2
1.1 Problem Statement	4
1.2 Objectives	4
1.3 Methodology	5
1.4 Organization.....	6
CHAPTER 2 Literature Review	8
2.1 Tires.....	8
2.2 Assessment of the Present Situation.....	11
2.2.1 Generation of scrap tire.....	11
2.2.2 Recycling alternatives.....	12
2.3 Scrap Tires and Crumb Rubber.....	13
2.4 Ambient Grinding	15
2.5 Cryogenic Grinding	16
2.6 Tire Pyrolysis	18
2.7 Tire Derived Product	18
2.8 Asphalt.....	19
2.8.1 Definition and terminology	19
2.8.2 History	19
2.8.3 Uses	19

2.8.4 Refining asphalt.....	20
2.8.5 Asphalt cement behavior.....	22
2.8.6. Asphalt-rubber cement and asphalt-rubber mixture - application and performance	24
2.8.7. Asphalt-rubber manufacturing processes.....	26
2.8.8 Performance record.....	29
2.9 Ongoing Research on High Temperature Properties.....	31
2.10 Bio-Binder.....	34
2.10.1. Problems with swine manure	34
2.10.2. Production	35
2.10.3. Chemical characterization of bio-binder.....	39
CHAPTER 3 Materials Preparation and Test Procedures.....	40
3.1 Materials Description.	40
3.1.1 Base binder asphalt.....	40
3.1.2 Crumb rubber modifier (CRM)	41
3.1.3 Bio-binder	43
3.2 Modified Binder Preparation	43
3.3 Blending Process	46
3.4 Test Procedure.....	46
3.4.1 Viscosity testing	46
3.4.2 Temperature susceptibility.....	48
3.4.3 Shear susceptibility.....	48
3.4.4 Dynamic shear rheometer (DSR)	48
3.4.5 Specimens' master curves.....	51

3.4.6 Rolling thin film oven (RTFO)	51
CHAPTER 4 Results and Discussion	53
4.1 Bio Modified Rubber and Non-Modified Binders Viscosity Testing	53
4.2 Viscosity Temperature Susceptibility.....	58
4.3 Shear susceptibility.....	61
4.4 Dynamic Shear Rheometer (DSR) Results Before and After RTFO	64
4.5 Effect of Temperature on Parameter $G^*/\sin(\delta)$ Un-Aged and Aged Specimens	67
4.6 Effect of Temperature on Parameter (δ) Un-Age and Aged Specimens	70
CHAPTER 5 Summary and Conclusions	76
References	79
Appendix	86

List of Figures

Figure 1.1 Algorithm of the experiment plan	6
Figure 2.1 Cross-section of a high-performance tire (Discount Tire).....	8
Figure 2.2 One of the world largest dump tires (EPA) Hudson Colorado	10
Figure 2.3 Current uses of scrap tires (US environmental and protection service, 2013)	11
Figure 2.4 Ambient scrap tire processing plant schematics (Reschner, 2006).....	17
Figure 2.5 Cryogenic scrap tire processing plant schematics (Reschner, 2006)	17
Figure 2.6 National asphalt road and oil production (US energy information agency, 2014)	20
Figure 2.7 Typical barrel of crude oil	21
Figure 2.8 A commonly used fractionation scheme for crude oil (SARA)(Barman, Cebolla, & Membrado, 2000).....	22
Figure 2.9 Two asphalt-rubber applications (source: Clemson.edu)	26
Figure 2.10 Crumb rubber modified asphalt type processes (FHWA, 19941).....	27
Figure 2.11 Lagoon at NCA&T Farm (Swine Unit).....	35
Figure 2.12 A Sample of mixed manure with water	36
Figure 2.13 Canister	37
Figure 2.14 Running reactor producing bio-oil	37
Figure 2.15 Algorithm of bio-binder production.	38
Figure 3.1 Crumb Rubber Mesh Size 80-200 from Rubber Manufacturers.....	42
Figure 3.2 Bio-binder produced at NCA&T Farm.....	43
Figure 3.3 Sample Blending	46
Figure 3.4 Brookfield viscometer (RV-DVIII Ultra).....	47
Figure 3.5 Dynamic shear rheometer	50

Figure 3.6 DSR Sample (25mm in Diameter)	50
Figure 3.7 Rolling thin film oven (RTFO).	52
Figure 4.1 Viscosity vs temperature for control, 15% CRM, with Bio-binder at 10 rpm.....	56
Figure 4.2 Viscosity vs Temperature for control, 20% CRM, with Bio-binder at 10 rpm	57
Figure 4.3 Viscosity of all specimens at test temperature 135°C	58
Figure 4.4 Viscosity temperature susceptibility (VTS) for 15% concentration of CRM.....	59
Figure 4.5 Viscosity Temperature susceptibility (VTS) for 20% concentration of CRM.	60
Figure 4.6 Shear Susceptibility (SS) for 15%CRM with different percentages of Bio-binder at 150°C.....	62
Figure 4.7 Shear susceptibility (SS) for 20%CRM with different percentages of Bio-binder at 150°C.....	63
Figure 4.8 Master curves for PG64-22, 15%CRM, un-aged specimens	65
Figure 4.9 Master curves for PG64-22, 20%CRM, un-aged specimens	65
Figure 4.10 Master curves for PG64-22, 15%CRM, aged specimens	66
Figure 4.11 Master Curves for PG64-22, 20%CRM, Aged Specimens.....	66
Figure 4.12 Effect of temperature on $G^*/\sin\delta$, 15%CRM, un-aged specimens	68
Figure 4.13 Effect of temperature on $G^*/\sin\delta$, 15%CRM, un-aged specimens	68
Figure 4.14 Effect of temperature on $G^*/\sin\delta$, 20%CRM, un-aged specimens	69
Figure 4.15 Effect of temperature on $G^*/\sin\delta$, 20%CRM, aged specimens	69
Figure 4.16 Effect of temperature on phase angle (δ), un-aged 15%CRM.....	71
Figure 4.17 Effect of temperature on phase angle (δ), un-aged 20% CRM.....	72
Figure 4.18 Effect of temperature on parameter $\tan(\delta)$, RTFO 15%CRM	73
Figure 4.19 Effect of temperature on phase angle (δ) aged 20%CRM.....	73

Figure 4.20 Phase angle of binders at 64°C and a frequency of 1.67E+00, 15%CRM75

Figure 4.21 Phase angle of binders at 64°C and a frequency of 1.67E+00, 20%CRM75

List of Tables

Table 2.1 Typical Weight Distribution of the Components of a Tire	9
Table 2.2 Crumb Rubber Mesh Size by Market Category	14
Table 2.3 Crumb rubber gradations for asphalt-rubber (from asphalt rubber , an anchor to crumb rubber markets, 1999)	15
Table 2.4 Performance graded asphalt binder specification (from AASHTO, MP1).....	24
Table 2.5 Common abbreviations for forms of asphalt rubber (from white paper, 2011).....	26
Table 2.6 Comparison of SARA components of bio-binder and bituminous binder (Fini et al., 2011)	39
Table 2.7 Chemical composition of bio-binder and bituminous binder (Fini, et al., 2011).....	39
Table 3.1 Physical data of PG64-22 (from Asphalt Associates)	41
Table 3.2 Grading and Characteristics of Crumb Rubber Particles by Mesh Size	42
Table 3.3 Content of Binders Developed and Evaluated	45
Table 3.4 Factors Used for Frequency Sweeps	51
Table 4.1 Specimens' Average Viscosity at 120°C	53
Table 4.2 Specimens' Average Viscosity at 135°C	54
Table 4.3 Specimens' Average Viscosity at 150°C	54
Table 4.4 Slope for Different Specimens with 15%CRM (VTS)	60
Table 4.5 Slope for Different Specimens with 20%CRM (VTS)	61
Table 4.6 Slope for Different Specimens with 15%CRM (SS)	62
Table 4.7 Slope for Different Specimens with 20%CRM (SS)	63

Abstract

The objective of this study is to produce an environmentally friendly paving material with enhanced high temperature performance. To do so, feasibility of synthesis an alternative asphalt binder from scrap tire rubber and bio-binder is investigated in this paper. The newly developed bio modified rubber is a hybrid viscoelastic thermoplastic adhesive composed of ambient crumb rubber and bio-binder. Bio-binder is produced from thermochemical conversion of swine manure, and crumb rubber is obtained from grinding of scrap tire. It should be emphasized that the aforementioned ingredients are derived from waste materials. Using crumb rubber as paving material can alleviate problems facing the solid waste management industry related to disposal of scrap tire. On the other side, production of bio-binder reduces the need of lagoons to store swine manure, and decreases noxious odor originating from swine manure stored in lagoons. This study concentrates on the high temperature properties and temperature susceptibility of the bio modified rubber. To develop bio-modified rubber bio-binder were mixed with various percentages of ambient crumb rubber 80 mesh (0.177mm) ranging from 5 up to 50% by the weight of asphalt binder. Dynamic shear rheometer (DSR) was employed to measure the complex modulus (G^*) and phase angle (δ) of un-aged and aged bio-modified rubber. Aging was conducted using rolling thin film oven (RTFO). The rotational viscometer (RV) was used to quantify the bio-modified rubber binder's high temperature properties and pump-ability. It was found that bio-modified rubber binder's viscosity decreases by increasing the bio-binder percentages at specified temperature. In addition, the increase of bio-binder percentages showed to improve temperature susceptibility and resistance to rutting. As such it was concluded that alternative asphalt with enhanced high temperature properties could be produced using scrap tire and bio-binder rubber.

CHAPTER 1

Introduction

It is well documented that world natural resources are depleting. To face the problem, governments and local agencies are encouraging recycling and looking for alternative sustainable building materials. Rubber is a well-known material that is classified as natural or synthetic, based on its source. Natural rubber (NR), also called India rubber or caoutchouc, is an elastic hydrocarbon polymer originally obtained from the latex produced by certain plants. On the other hand, synthetic rubber (SR) is a polymer classified in many types of classes; it is made of raw material mainly derived from petroleum products and other raw materials such as natural gas (Encyclopaedia Britannica, 2014). Synthetic rubber is usually a copolymer, which is a polymer made with more than one monomer. This is also known as an elastomer (Encyclopaedia Britannica, 2014). The above mentioned materials are the main components of tires used in automobiles, aircraft, and heavy equipment. A typical passenger tire contains 15% to 19% vulcanized NR, 25% to 29% vulcanized SR, and other components such as carbon black. Carbon black is used to improve tire treads' rigidity and to minimize heat buildup in sidewalls (Shulman, 2000). At the end of their service life tires become a waste material requiring disposal. The least expensive disposal is a landfill, which is not a sustainable practice (EPA, 2012). According to the rubberized asphalt foundation, the tire recycling alternative with the highest potential to significantly reduce the United States' scrap tire problem is the use of tire rubber in asphalt highway construction (ra-foundation.org, 2013). The use of ground tire rubber or crumb rubber modifier (CRM) in asphalt offers the advantage of resource recovery and dates back many years in the United States, Canada and other countries (Liu, Cao, Fang, & Shang, 2009; Roberts, Kandha, Brown, & Dunning, 1989). The resulting product has commonly been called "asphalt-

rubber”(Liu et al., 2009). CRM is the second most-used polymer as an asphalt modifier, after styrene butadiene styrene (SBS) (Liu et al., 2009). From the literature, the properties that CRM introduces to hot mix asphalt (HMA) are higher crack resistance, reduced temperature susceptibility, noise reduction, and aging resistance (Dong, Li, & Wang, 2011). Furthermore, research has shown that the mix of asphalt with crumb rubber improves asphalt pavement’s resistance to permanent deformation, reduces the thickness of asphalt overlays, saves resources, and protects the environment (Cong, Xun, Xing, & Chen, 2013). It has been reported that acceptance of asphalt-rubber systems has been mainly regional, related to beneficial experience gained during experimental stages of use. A U.S. government regulation issued in 1997 required all fifty states to use scrap tire as a modifier at 20% of their total asphalt (Cong et al., 2013). Introducing 20% by weight crumb rubber to asphalt was problematic, due to poor compatibility between asphalt binder and the rigid crumb rubber. Additionally, the mix required a high processing temperature of over 190°C. This resulted in some engineering problems and environmental concerns (Cong et al., 2013). Also, asphalt rubber has been extensively used in warmer geographical areas, where rutting is one of the main pavement distresses caused by traffic loading (Wang, Dang, You, & Cao, 2012). In hot climate conditions, rutting is related to the high temperature properties of hot mix asphalt. To address the aforementioned problems, the main objective of this thesis is to produce an environmentally friendly paving material, bio-modified rubber (BMR), which has enhanced high-temperature rheological properties and can be used as a partial or total replacement for asphalt-binder. Bio-modified rubber (BMR) is a combination of bio-binder and ambient crumb rubber; both materials are derived from waste. Bio-binder is produced from thermochemical conversion of swine manure. Crumb rubber is obtained from a grinding process of scrap tire. Bio-oil is a “thick, black, energy-dense crude oil

that is remarkably similar to petroleum extracted from deep within the earth” (Fini et al., 2011). The estimated cost of bio-oil production is approximately \$0.13/L (\$0.54/gal) (Fini et al., 2011). The previous study shows that bio-binder is a promising candidate as an asphalt additive, based on a comparison of bio-binder properties (such as lower softening point) with properties of petroleum-asphalt binder. Furthermore, rheological and chemical similarities between bio-binder and asphalt binder make the two materials compatible.

1.1 Problem Statement

Asphalt binder resistance to deformation at intermediate and high temperatures significantly affects overall pavement resistance to rutting deformation under heavy traffic. To enhance asphalt resistance to deformation, researchers have used various modifiers and additives such as crumb rubber modifier (CRM). The physical effect of rubber is the main key factor in increasing asphalt-rubber viscosity, reducing its pumpability and workability, this in turn makes its application problematic. It is stated that bio-binder can be used as a binder additive. This study hypothesizes that addition of bio-binder to asphalt-rubber helps reduce the mixture viscosity without negatively impacting the mixture’s rheological properties. Introducing bio-binder into asphalt rubber produces a bio-modified rubber. In addition, it is hypothesized that by increasing bio-binder content, a higher percentage of crumb rubber can be added to asphalt without encountering pumpability problem. Moreover, bio-modified rubber will allow decreasing the mixing and compaction temperatures used in the asphalt-rubber industry.

1.2 Objectives

The new product, bio-modified rubber, is a hybrid viscoelastic thermoplastic adhesive. Since modification has occurred by introducing two products to the virgin asphalt binder, this study’s objectives are as follows:

- Evaluate the rheological properties and performance of bio-modified rubber.
- Determine the effects of different percentages of bio-binder on the rheological properties of asphalt-rubber produced with a base asphalt of PG64-22 (commonly used in North Carolina) and two different percentages (15% and 20%) of ambient ground tire rubber.
- Evaluate the mechanical properties of bio-modified rubber (BMR) and compare them with the properties of traditional rubberized asphalt, using a rotational viscometer (RV) on un-aged samples and a dynamic shear rheometer (DSR) on rolling thin-film oven (RTFO) aged samples.

1.3 Methodology

A research plan was formulated to achieve the aforementioned goals (Figure 1.1). The plan is organized as follows:

- Literature review
- Binder matrix preparation
- Binder testing
- Laboratory performance data analysis

The experimental plan formulated in this study uses different laboratory-produced Bio-asphalt modified rubber binders following the ASTM D8 definition and the Caltrans rubberized binder procedure (Caltrans, 2003). A detailed description of each mixture design and modification is given in Chapter 3. All binders produced were tested according to the Superpave performance graded asphalt binder specifications and testing procedures (U.S. Department of Transportation Federal Highway Administration, 1994). Tests performed to characterize the binders use a rotational Brookfield viscometer test on un-aged samples and a dynamic shear rheometer (DSR) test on rolling thin-film oven (RTFO) short-aged samples.

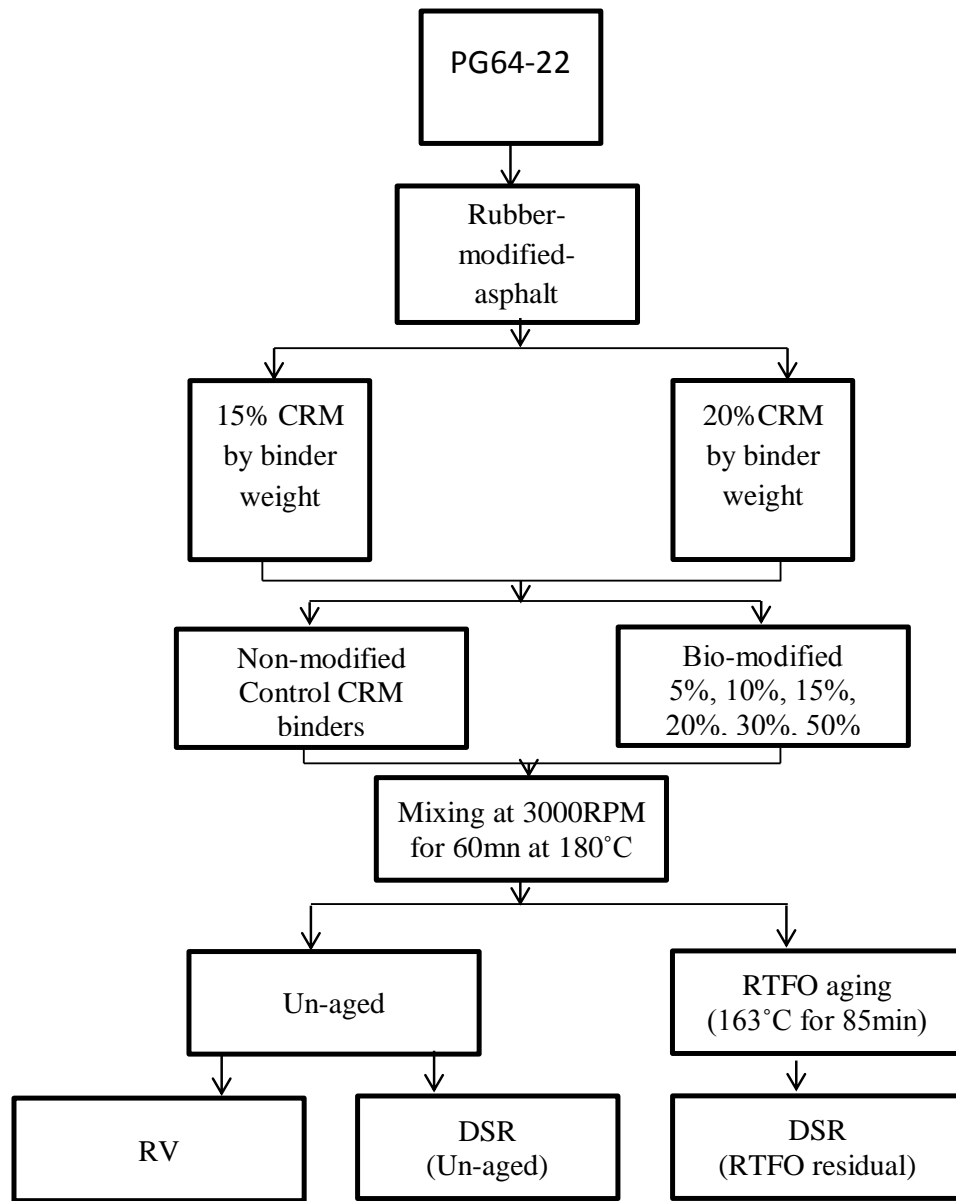


Figure 1.1 Algorithm of the experiment plan

1.4 Organization

This thesis consists of five chapters. Chapter 1 is the introduction. Chapter 2 is a literature review of tire, asphalt, and asphalt-rubber current practice, ongoing research on high-temperature properties of rubberized asphalt, and bio-binder. Chapter 3 describes laboratory investigations and test procedures; this chapter present tests conducted on bio-modified rubber

asphalt. Chapter 4 contains data analysis, including bio-modified -rubber, asphalt rubber, and virgin asphalt mechanical testing results. Chapter 5 discusses the conclusions and summary of the research, including recommendations for future work.

CHAPTER 2

Literature Review

2.1 Tires

A typical passenger tire contains respectively 15% to 19% vulcanized natural rubber, 25% to 29% synthetic rubber, and other components such as carbon black. Carbon black is used to improve tire treads' rigidity and to minimize heat buildup in sidewalls (Shulman, 2000). Another important component is steel, which provides rigidity and flexibility to the carcass. Nylon, rayon, and polyester are also used as textiles components (Rahman, 2004). A common weight distribution is given in Table 2.1 (Unapumnuk, 2006). Figure 2.1 shows the different components of a typical passenger tire

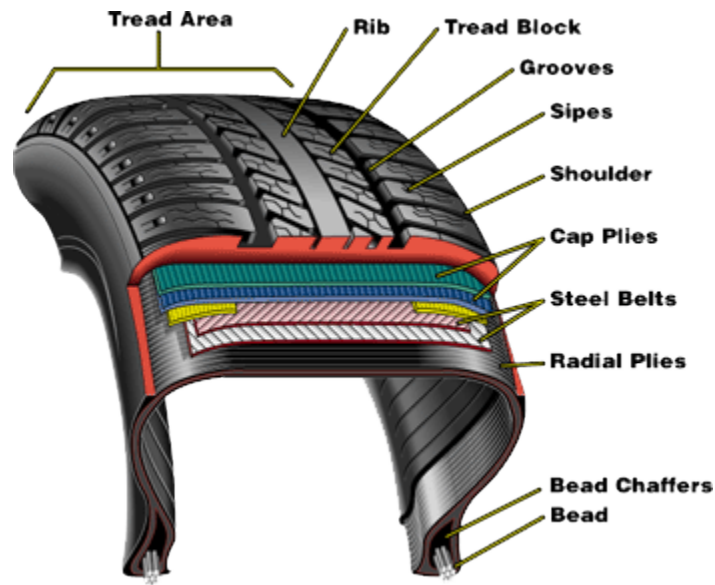


Figure 2.1 Cross-section of a high-performance tire (Discount Tire)

Table 2.1
Typical Weight Distribution of the Components of a Tire

Tire components	Percentage
Natural rubber	15-19
Carbon black	24-28
Synthetic rubber	25-29
Steel cords	9-13
Textile cords	9-13
Chemical additives	14-15

Tire production is growing proportional to demand around the world (Rubber Manufacturers Association, 2009). In America every year, two hundred ninety million old tires were generated in 2003 (U.S. Environmental Protection Agency., 2013). This is nearly one for every American (Rubberized Asphalt Foundation, 2013). Also there are 33.5 million tires that are retreaded and an estimated 10 million that are reused each year as second-hand tires. It is assessed that 7 percent of the discarded tires are presently being reprocessed into new products and 11 percent are converted to energy. Nearly 78 percent are being landfilled, stockpiled, or illegally dumped, with the remainder being exported (U.S. Environmental Protection Agency., 2013). For many years, waste tire recycling has drawn major attention, for several reasons. Tires' principal component is cured rubber styrene-butadiene-styrene, which can have many applications such as asphalt additives or a source of hydrocarbon. Another reason is the negative environmental impact of disposed tires, as mentioned by solid waste and tire experts: scrap tires provide breeding sites for mosquitoes that can spread diseases, and large tire piles often constitute fire hazards (EPA, 2013). A perennial challenge has been the space and cost required

for transporting and storing scrap tires (U.S. Environmental Protection Agency., 2006). According to the Rubberized Asphalt Foundation, the largest tire pile in the nation is in Sycamore, Ohio. Authorities estimate this location as having over eighty millions tires, piling up over twenty years. In second place is a location in Smithfield, Rhode Island, covering fourteen acres of land with over ten million tires (Rubberized Asphalt Foundation, 2010). Figure 2.2 is a picture of one of the world's largest tire dumps (EPA, 2013). Tire piles around the country entail serious environmental concerns. Among technologies developed for the recycling of scrap tires, the most familiar and widely used is the grinding process. Most grinding mechanisms produce different particle sizes of crumb rubber, separated from steel wire. The end product of grinding tire is named ground tire rubber (GTR) (EPA); it has been used mostly in the pavement industry since 1960 (Daryl, Susanna, Ryan, & Ludo, 2007). It was first implemented by Charles McDonald in Arizona (Shatnawi, 2011a). Current estimation of ground tire used in civil engineering projects is about 21percent of the quantity generated (EPA, 2013). In practice, two types of ground tire rubber derived from scrap tires are being used: ambient ground tire rubber and cryogenic ground tire rubber. Ground tire can be used as a basic stock for further processes like pyrolysis and devulcanization. Scrap tires are also used as supplemental fuel for power plants (Barla, Eleazer, & Whittle, 1993).



Figure 2.2 One of the world largest dump tires (EPA) Hudson Colorado

2.2 Assessment of the Present Situation

2.2.1 Generation of scrap tire. Since there is no industry group or governmental agency that monitors tire disposal in the United States, the best estimates that can be made are based on tire production (EPA 2013). The Rubber Manufacturers Association (RMA) estimates that about 290 million tires were generated in the U.S. in 2009 (Rubber Manufacturers Association, 2009). In recent years, statistics show an increase in scrap tires going into markets since 1990. Eleven states generate 90% of these tires. From Figure 2.3, about 60.9 million were recycled, 130.5 million were recovered for energy, and about 8.7 million were exported, leaving 26.1 million for landfilling, stockpiling, or illegal dumping.



Figure 2.3 Current uses of scrap tires (US environmental and protection service, 2013)

2.2.2 Recycling alternatives. Recycling alternatives include the use of whole tires, requiring no extensive processing; splitting or punching tires to make products; and finely grinding the tires to enable the manufacture of crumb rubber products. Some applications for each alternative are enumerated below:

- Whole tire applications: artificial reefs and breakwaters, playground equipment, erosion control, highway crash barriers
- Split or punched tire applications: floor mats, belts, gaskets, shoe soles, dock bumpers, seals, muffler hangers, shims, washers, and insulators
- Shredded tire applications: lightweight road construction material, playground gravel substitutes, sludge composting, ground rubber applications, rubber and plastic products like molded floor mats, mud guards, carpet padding, plastic adhesives, rubber railroad crossings, additives for asphalt pavements

All the tire recycling alternatives listed above are being used to some extent. However, the total usage of tires for recycling currently is estimated to be less than 8 percent of the annual generation (EPA, 2013). According to the EPA, the markets for most of the above products may be increased, but even if the markets are increased to their fullest extent, the total usage appears to be small compared to the number of tires generated each year. Ground rubber applications hold the greatest promise. The tire recycling alternative with the highest potential to significantly reduce the scrap tire problem of the United States is in asphalt highway construction (EPA, 2013).

There are two types of processes for using crumb rubber in pavements. One application, referred to as rubber modified asphalt concrete (RUMAC), involves replacing some of the aggregate in the asphalt mixture with ground tires. The second, called asphalt-rubber, defined by

the American Society of Testing Materials (ASTM) as “ a blend of asphalt cement, reclaimed tire rubber, and certain additives in which the rubber component is at least 15 percent by weight of the total blend and has reacted in the hot asphalt cement sufficiently to cause swelling of the rubber particles”(ASTM D8, 2014). Both systems are being evaluated by state agencies as well as the federal government.

Tires can be reclaimed into virgin asphalt as crumb rubber modifier, recycled asphalt pavement (CRM—RAP)(Kandhal, 1992), or as an aggregate in Portland cement (Nehdi & Khan, 2001). Recent progress in devulcanization facilitates recycling scrap tires into new tires. Devulcanization is rated as a highly effective method of transforming the structure of waste vulcanized rubber or elastomers for reuse as a virgin rubber substitute. It can be performed mechanically or chemically using devulcanising agents (Isayev, 2005). In chemical method of devulcanization, crumb rubber is mixed with a reagent in a simple reaction vessel. The reagent penetrates into the crumb rubber and reactively breaks the carbon-sulfur and sulfur-sulfur bonds that cross-link the linear polymers in the crumb rubber. The resulting mixture is conveyed to a filtration unit to separate it into a particulate solids stream and a liquid stream (Fan & Shafie, 2013)

The process can operate at low temperature under atmospheric pressure using a non-toxic, non-corrosive, renewable, and recyclable reagent (Fan & Shafie, 2013).

2.3 Scrap Tires and Crumb Rubber

Each year millions of tires become available for recycling into crumb rubber, for use in asphalt-rubber. Crumb rubber is the name given to any material derived by reducing scrap tires or other rubber into uniform granules, with the inherent reinforcing materials such as steel and

fiber removed along with any other inert contaminants such as dust, glass, and rock (Carlson & Zhu, 1999). The crumb rubber is made by first processing the scrap tires to an almost powder-like product named crumb rubber modified (CRM). The initial product consists of 2-inch chips of shredded scrap tires. The next step is to size the CRM into two different granulations: 3/4 inch and 1/4 inch. The final step is to grind the material to a size of 1mm (10mesh) or slightly larger, depending on the CRM to be used. The tire's wires and fibers are extracted from the rubber during the shredding process. Most crumb rubber particle sizes range between N°20 (1.2mm) and N°40 (0.42mm), while some particles may be a finer size of N°200 (0.075mm)(Way, Kaloush, & Biligiri, 2011). Table 2.2 shows the crumb mesh size range for each market category. Table 2.3 shows common gradations for rubber particle sizes used in asphalt by leading states; the percent passing range for each sieve size is given. A blank cell in Table 2.3 indicates an unused sieve (Carlson & Zhu, 1999).

Table 2.2
Crumb Rubber Mesh Size by Market Category

Market	Mesh Sizes
Molded and Extruded Products	4 - 100 mesh
Asphalt Modification	16 - 40 mesh
Sport Surfacing	1/4" - 40 mesh
Automotive Products	10 - 40 mesh
Tires	80 - 100 mesh
Rubber and Plastic blend	10 - 40 mesh
Construction	10 - 40 mesh

Table 2.3

Crumb rubber gradations for asphalt-rubber (from asphalt rubber, an anchor to crumb rubber markets, 1999)

Sieves (mm)	#8 (2.38)	#10 (2)	#16 (1.19)	#20 (0.841)	#30 (0.595)	#40 (0.4)	#50 (0.297)	#80 (0.177)	#100 (0.149)	#200 (0.074)
Arizona		100	75-100		25-100		0-45	0-10		0
California	100	95-100								0-3
Florida				100		85-100			50-30	

Two common technologies to produce crumb rubber are ambient grinding and cryogenic processing. The most common methods for producing crumb rubber are the crackermill process and micro-mill process, which produce ambient crumb rubber, and the cryogenic process, which produces a cryogenic crumb

2.4 Ambient Grinding

This process is conducted at ambient or room temperature; material is fed to a crackermill or granulator. The granulator downsizes the rubber particles by shearing and cutting action. Variable screens within the machine define the end product size. Rubber particles produced by a granulator have a cut surface shape and are rough in texture. On the other hand, rubber particles produced by a crackermill, a low velocity machine, usually have a long and narrow shape, and also have a high surface area (Way et al., 2011). Figure 2.4 is a detailed description of a typical ambient process scrap tire recycling facility. The tires are charged into the preliminary shredder A, which downsizes tires to a 2-inch particle size. The 2-inch particles then pass through a granulator B, to be further reduced to a size less than 3/8 inches; in this step, most fibers are separated from the rubber particles. The next step consists of freeing the rubber chips from steel and remaining fibers by using a magnetic device, a shaking screen, and wind sifters (Reschner, 2006). This process produces a sponge-like surface on the crumb rubber particles. Rubber

particles obtained from this process have greater surface area than the ones produced cryogenically for a given particle size. Increased surface area increases the reaction rate with hot asphalt (Roberts et al., 1989).

2.5 Cryogenic Grinding

Figure 2.5 shows a schematic of a cryogenic scrap tire processing plant. In this process, tires are fed into a shredder similar to the ambient process one, to be reduced typically to 2-inch chips. The rubber chips are then cooled to approximately -112°F (-80°C) using a tunnel chamber containing nitrogen. The cooled product is then reduced to smaller sizes of $\frac{1}{4}$ inch (6mm) or less by means of a hammer mill. Steel and fiber are removed by magnets and aspiration. The end product looks shiny and clean with small surface area (Reschner, 2006). Particles produced from this method have a reduced reaction rate, and the Australian Road Research Board states that this process manufactures undesirable particle structure and usually gives lower elastic recovery compared to ambient ground rubber (Roberts et al., 1989).

Example of an Ambient Scrap Tire Recycling System

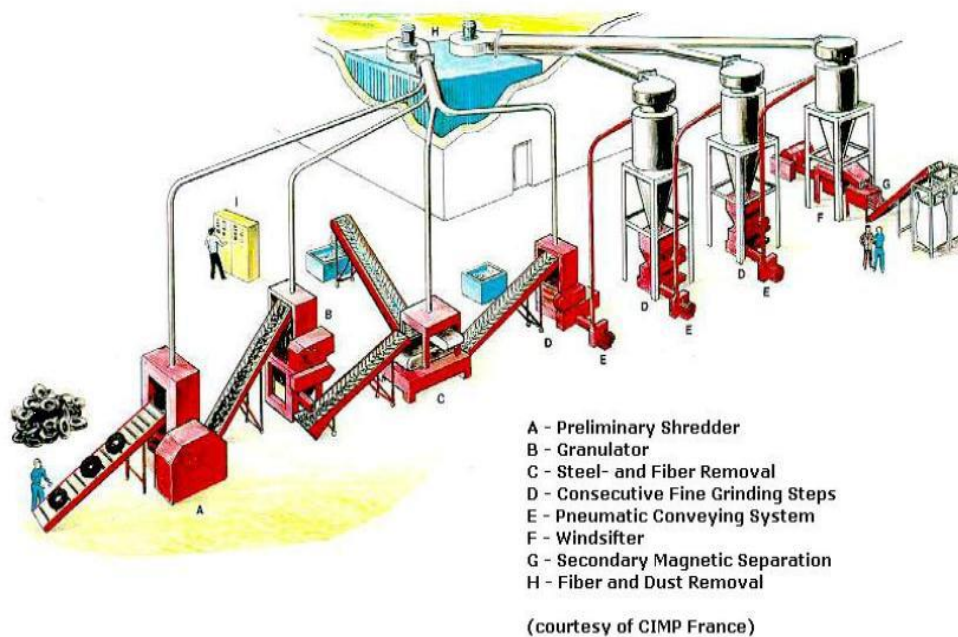


Figure 2.4 Ambient scrap tire processing plant schematics (Reschner, 2006)

Example of a Cryogenic Scrap Tire Recycling System

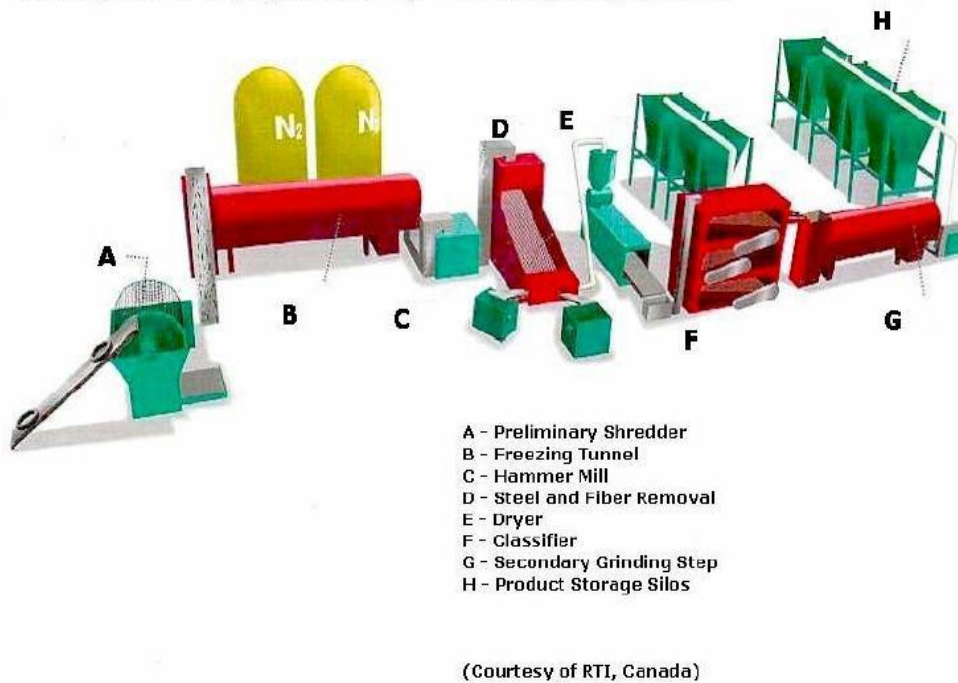


Figure 2.5 Cryogenic scrap tire processing plant schematics (Reschner, 2006)

2.6 Tire Pyrolysis

The pyrolysis method for recycling used tires is a technique which heats whole or shredded tires in a reactor vessel at 400-700°C in the absence of oxygen. In the reactor, the rubber is softened, after which the rubber polymers continuously break down into smaller molecules. These smaller molecules eventually vaporize and exit from the reactor. This vapor contains hydrogen, carbon monoxide and dioxide, aliphatic hydrocarbons, and hydrogen sulphide, which can be burned directly to produce power or condensed into an oily type liquid, generally used as a fuel. Some molecules are too small to condense. They remain as a gas which can be burned as fuel. The minerals that are about 40% by weight of the tire are known as char; char contains zinc, silica, and steel, which are removed as solids. When performed well, a tire pyrolysis process is a very clean operation and has nearly no emissions or waste. With ongoing research into the improvement of existing pyrolysis technologies, and the rising costs of energy and petrochemical raw materials, this method of managing waste tires has promising potential (Sienkiewicz, Kucinska-Lipka, Janik, & Balas, 2012).

2.7 Tire Derived Product

Scrap tires can be reclaimed in many different ways. One way is for a steel mill to use the tires as a carbon source, replacing coal or coke in steel manufacturing. Instead of quarrying coal from the ground and burying tires in landfills, the tires are used directly. In another application, tires are bound together and used as barriers for reducing collision impact, controlling erosion, slowing rainwater runoff, protecting piers and marshes from wave action, and creating sound barriers between roadways and residences.

1. Crumb rubber manufacturing processes have been described in earlier sections. The finished product is mainly used in paving projects and moldable products. The paving projects can be Rubber Modified Asphalt (RMA) or Rubber Modified Concrete.
2. Shredded tires are also known as Tire Derived Aggregate (TDA). To prepare TDA, tires are put into a primary shredder that cuts the tires using knives that rotate at slow speed. TDA has many applications in civil engineering.
3. Chipped and shredded tires are used as Tire Derived Fuel (TDF). To produce TDF-size shreds and chips, whole tires are reduced to nominal 2-inch pieces using one shredder or a series of shredders, screening equipment, and magnetic separation equipment.

2.8 Asphalt

2.8.1 Definition and terminology. Asphalt, Bitumen, Liquid Asphalt, Asphalt Cement, Asphalt Binder, and Binder are interchangeable terms. It is defined as “a dark brown to black cementitious material in which the predominating constituents are bitumens which occur in nature or are obtained in petroleum processing”(ASTM D8, 2014). “Asphalt cement” refers to asphalt that has been made for use in Hot Mix Asphalt and other pavement applications.

2.8.2 History. Asphalt binder has been used as pavement material for more than a century. A lake in Trinidad was documented to be the first source of asphalt used in the U.S. The earliest use of asphalt in the U.S. was recorded to be about 1870 when the first asphalt pavement was laid in Newark, New Jersey. Washington, DC, had its first asphalt pavement laid in 1876. In the late 1800’s, demand for paved roads exceeded the supply of lake asphalts, which led to the use of petroleum asphalts (National Asphalt Pavement Association, 2014).

2.8.3 Uses. Refineries produce asphalt with specific characteristics for different end uses such as paving asphalt, roofing asphalt, or other special uses (waterproofing, sealing). According

to the U.S. Energy and Information Agency, Figure 2.6 represents national asphalt and road oil production; as it can be there overall production has been reduced by 32% from 2005 to 2012. This is when roads and highways constitute the majority of asphalt pavements in the United States. Accordingly, 87% of the annual liquid asphalt production is consumed on road applications while roofing application accounts for approximately 11% percent, and bitumen-based paints and waterproofing account for the remaining 2% (Rasoulzadeha, Mortazavib, Yousefi, & Khavanin, 2011). U.S. crude oil sources are the Gulf coast, mid-continent, Rocky Mountains, west coast, and Alaska. The largest international producers are countries like Mexico, Venezuela, Canada, and the Middle East(Way et al., 2011).

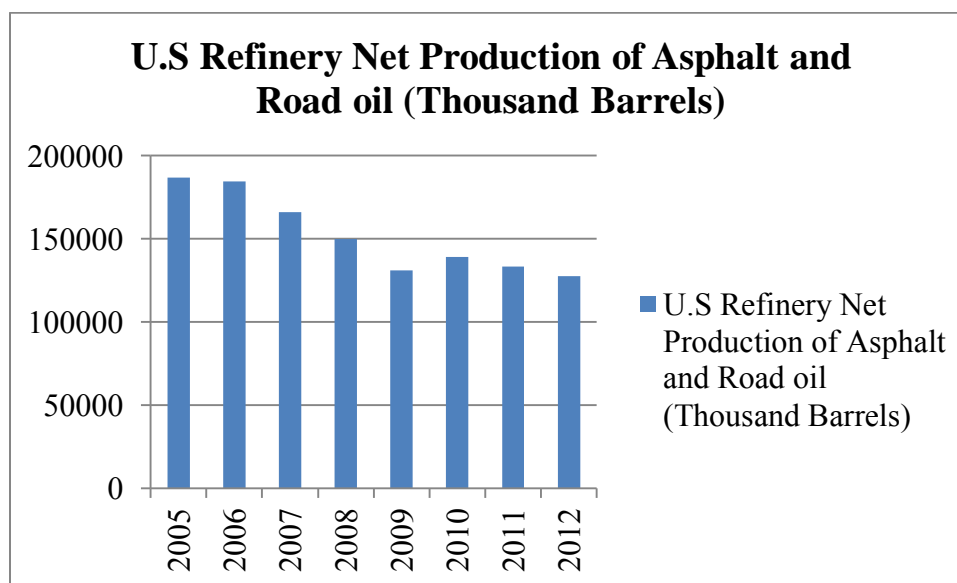


Figure 2.6 National asphalt road and oil production (US energy information agency, 2014)

2.8.4 Refining asphalt is one of the products of the petroleum industry. It is considered to be a waste product from refinery processing. Typical barrels of crude oil have the following fractions, classified from lightest to heaviest as show in Figure2.7:

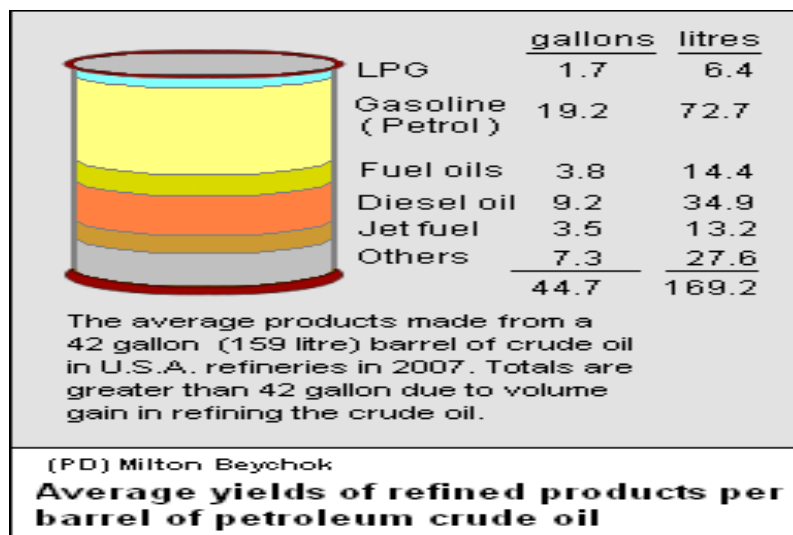


Figure 2.7 Typical barrel of crude oil

The simplest process of separating crude oil components is straight distillation. In this method, crude oil is separated into different products based on their respective boiling point temperature interval, from 300°C up to 900°C. The crude oil is first heated in a large furnace to 340°C (650°F) and partially vaporized. The boiling oil is then fed into a distillation unit where the lightest fractions are distilled (e.g. gasoline, kerosene, light gas oil). The residue from this process is known as steam refined asphalt binder; it is fed into a vacuum distillation unit for further processing, where heavier gas oil is separated (Roberts et al., 2009).

A chemical method of splitting crude oil components for additional analysis is the SARA technique, and four fractions are obtained by this method. Based on their solubility in organic solvents, they are called saturates, aromatics, resins, and asphaltenes (Panda, Jan T., & Wolfgang, 2007). The acronym SARA stands for the cited four components. An algorithm of the approach is illustrated in Figure 2.8.

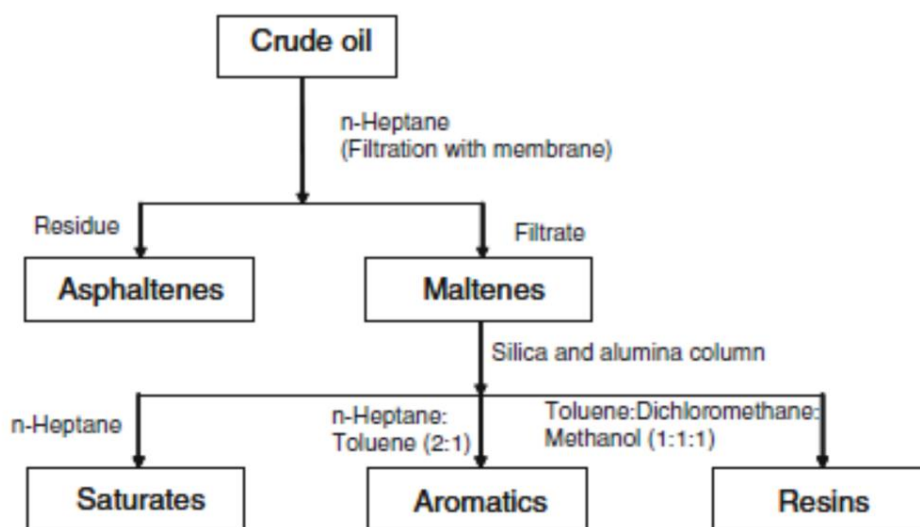


Figure 2.8 A commonly used fractionation scheme for crude oil (SARA)(Barman, Cebolla, & Membrado, 2000)







Asphalt properties depend on refinery operations and crude oil composition, which are source dependent. Asphalt binder grade depends on the amount of heavy gas oil extracted.(Way et al., 2011)

2.8.5 Asphalt cement behavior. It is documented that asphalt is a thermoplastic material that softens as it is heated and hardens when cooled. It has viscoelastic properties. Furthermore, it is a complex chemical substance with the following components: asphaltenes are a large discrete fraction solid with high viscosity; resins are a solid or semisolid fraction at room temperature that is fluid when heated and brittle when cold, and oils are a fraction with low viscosity. The composition influences binder behavior and performance under the effect of temperature (low, medium, or high), time of loading, and aging.

The current method to evaluate the properties of asphalt binder in the U.S. is the Performance Graded (PG) system initiated by the Strategic Highway Research Program (SHRP), also known as Superpave Binder Specifications. The performance graded (PG) system provides a

temperature range throughout which the binder must meet certain physical properties to resist rutting and cracking. High temperature performance is related to rutting, intermediate temperature performance is related to fatigue cracking, and low temperature performance is related to thermal cracking. The PG system also includes conditioning procedures to simulate changes in asphalt properties due to aging in the field. The Superpave asphalt binder specification uses the grading system PGXX-YY, where PG is the performance, XX represent an average seven-day maximum pavement design temperature, and YY is a minimum design temperature. Table 2.4 shows common performance grading and the Superpave test equipment used to define asphalt binder properties. (U.S. Department of Transportation Federal Highway Administration, 1994).

Table 2.4
Performance graded asphalt binder specification (from AASHTO, MPI)

Avg 7-day Max, °C	PG 46	PG 52						PG 58						PG 64						PG 70						PG-76						PG 82														
1-day Min, °C	34	40	46	-10	-16	-22	-28	-34	-40	-46	-16	-22	-28	-34	-40	-46	-10	-16	-22	-28	-34	-40	-46	-16	-22	-28	-34	-40	-46	-10	-16	-22	-28	-34	-40	-46	-16	-22	-28	-34	-40	-46				
ORIGINAL																																														
 ≥ 230 °C	(Flash Point) FP																																													
 ≤ 3 Pa·s @ 135 °C	(Rotational Viscosity) RV																																													
 ≥ 1.00 kPa	(Dynamic Shear Rheometer) DSR G*/sin \square																																													
	46	52						58						64						70						76						82														
(ROLLING THIN FILM OVEN) RTFO Mass Loss ≤ 1.00 %																																														
 ≥ 2.20 kPa	(Dynamic Shear Rheometer) DSR G*/sin \square																																													
	46	52						58						64						70						76						82														
(PRESSURE AGING VESSEL) PAV																																														
20 Hours, 2.07 MPa	90	90						100						100						100 (110)						100 (110)						110 (110)														
 ≤ 5000 kPa	(Dynamic Shear Rheometer) DSR G* sin \square																																													
	10	7	4	25	22	19	16	13	10	7	25	22	19	16	13	10	25	22	19	16	13	10	25	22	19	16	13	10	25	22	19	16	13	10	25	22	19	16	13	10	25	22	19	16	13	10
$S \leq 300$ MPa, $m \geq 0.300$	(Bending Beam Rheometer) BBR "S" Stiffness & "m"-value																																													
	-2	-3	-4	0	-6	-12	-18	-24	-30	-36	-6	-12	-18	-24	-30	0	-6	-12	-18	-24	-30	0	-6	-12	-18	-24	-30	0	-6	-12	-18	-24	-30	0	-6	-12	-18	-24	0	-6	-12	-18	-24			
Report Value	(Bending Beam Rheometer) BBR Physical Hardening																																													
≥ 1.00 %	(Direct Tension) DT																																													
	-2	-3	-4	0	-6	-12	-18	-24	-30	-36	-6	-12	-18	-24	-30	0	-6	-12	-18	-24	-30	0	-6	-12	-18	-24	-30	0	-6	-12	-18	-24	-30	0	-6	-12	-18	-24	0	-6	-12	-18	-24			

2.8.6. Asphalt-rubber cement and asphalt-rubber mixture - application and

performance. The application of scrap tire with asphalt as pavement construction material started in the 1950s (Hanson & Foo, 1994) . Incorporating natural rubber with bitumen was initiated in the 1840s (Heitzman, 1992a) . The objective was to use the flexible nature of rubber to create a more durable paving surface; unfortunately, early asphalt-rubber formulations were inferior compared to conventional asphalt (Carlson & Zhu, 1999). In the 1960s, a successful formulation was developed by Charles H. MacDonald that he called asphalt rubber. The product has gone from a seal coat material to a hot mix asphalt binder usable with modern paving equipment. Additionally, it developed beneficial engineering characteristics of both asphalt and

tire rubber. A mix of recycled ground tire rubber with asphalt cement at elevated temperature has been subject to many uses as binder in different types of bituminous construction, rehabilitation, and maintenance. This blend is called “asphalt-rubber” defined by ASTM D 8 as “A blend of asphalt cement, reclaimed tire rubber and certain additives in which the rubber component is at least 15% by weight of the total blend and has reacted in the hot asphalt cement sufficiently to cause swelling of the rubber particles” (ASTM D8, Vol. 4.03, “Road and Paving Materials” of the Annual Book of ASTM standards 2001). The blend can consist of 18 to 26 percent ground tire rubber by total weight of the blend (Roberts et al., 1989). The elevated temperature of the mix ensures chemical and physical bonding of the two constituents.

Recycled ground tire rubber has been used for various applications: asphalt-rubber seal coat (ARSC), asphalt-rubber stress-absorbing membrane (SAM) (Figure 2.9), asphalt-rubber stress-absorbing membrane interlayer (SAMI) (Figure 2.8), asphalt-rubber concrete (ARC), asphalt concrete rubber filled (ACRF) or rubber-modified asphalt hot mix, and asphalt-rubber crack sealer. Some common abbreviations used in Arizona, California, and other sources such as Greenbook are given below in Table 2.5.

Table 2.5

Common abbreviations for forms of asphalt rubber (from white paper, 2011)

Strategy	Arizona	Current Caltrans	Greenbook and Others
Chip Seals	SAM	ARSC	ARAM
Interlayers	SAMI	SAMI-R	ARAMI
Open Graded		RHMA-O	ARHM-OG
Open Graded High Binder	ARFC	RHMA-O-HB	
Gap Graded	ARAC	RHMA-G	ARHM-GG
Dense Graded		RHMA-D	ARHM-DG

ACRF differs from the rest by using a simple mixture of asphalt cement with granulated ground tire rubber as a partial replacement for an aggregate component. The rest use the asphalt-rubber cement blended at elevated temperatures (Roberts et al., 1989).

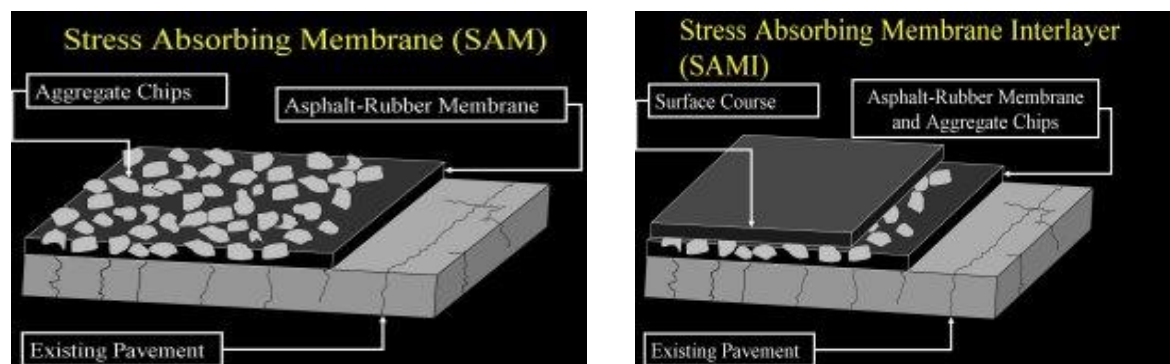


Figure 2.9 Two asphalt-rubber applications (<http://www.clemson.edu/ces/arts/samsami.html>, 2002)

2.8.7. Asphalt-rubber manufacturing processes. Two main processes have been documented for incorporating reclaimed ground tire rubber in hot mix asphalt (HMA); they are

known as the wet process and the dry process. In 1991, the Federal Highway Administration (FHWA) introduced standard terminology to improve the ability to communicate the experience of agencies when evaluating CRM processes. Figure 2.10 summarizes different processes and terminology.

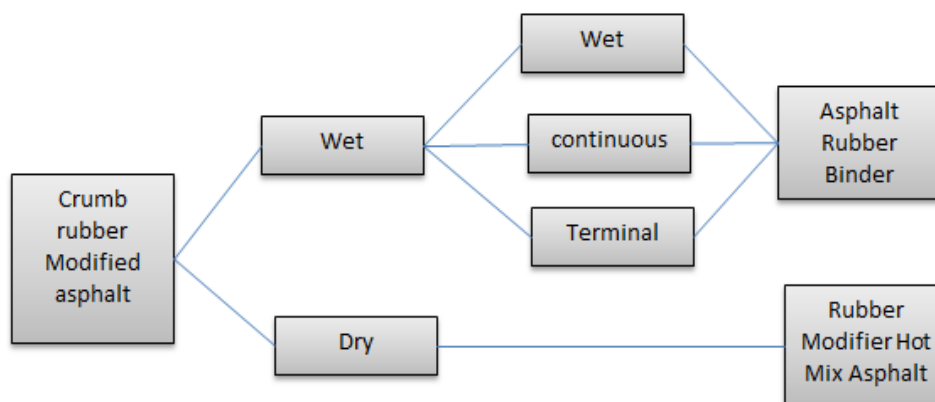


Figure 2.10 Crumb rubber modified asphalt type processes (FHWA, 19941)

In the wet process, 18 to 25% of tire rubber is reacted with asphalt cement before the binder is added to the aggregate. Typically the crumb rubber weight is 18%, and the two base products are blended at temperatures from 330°F to 400°F (166°C to 204°C), for a reaction time ranging from 10 – 15 minutes up to two hours or more (United States Department of Transportation. Federal Highway Administration, 1997). The mixing temperature can range from 375°F to 435°F (190°C to 224°C), and the resulting blend should be kept at an elevated temperature of 375°F to 425°F (190°C to 218°C) for an indicated minimum period of time, usually 45 minutes (Caltrans, 2006 Asphalt-Rubber-Usage-Guide). The reaction is affected by crumb rubber type and size, temperature, aromatic type of asphalt binder, and the type and amount of mechanical mixing (United States Department of Transportation. Federal Highway Administration, 1997)

When reclaimed tire rubber is mixed with asphalt in the wet process, the end products are referred to as asphalt-rubber binders, which are used in chip-seal coats as well as hot mix asphalt paving. Asphalt-rubber application in chip-seal coat has become known as stress absorbing membranes (SAM) (United States Department of Transportation. Federal Highway Administration, 1997). As shown in Figure 2.7, SAM covered with hot mix asphalt is known as stress-absorbing membranes interlayer (SAMI). The two common mixes using the process are asphalt-rubber hot mix gap graded (ARHM-GG) and asphalt-rubber hot mix dense graded (ARHM-DG) (MOD-076-Performance of asphalt rubber as thin overlays).

The wet process is used to produce a large variety of crumb rubber modified binders with different physical properties. The most important differences among the various blends appear to be related to rotational viscosity of the resulting CRM-asphalt cement blend at elevated temperature (threshold is 1500 centipoises (cps) or 1.5 Pa.sec at 375°F (190°C)). The size of crumb rubber particles and tire rubber content strongly affect the viscosity of the CRM-modified blend. CRM-modified binders with viscosities ≥ 1500 cps at 375°F are assumed to require agitation (Caltrans, 2003).

The dry process is known as rubber-modified mixes, and is currently marketed in the U.S. under trademark PlusRide. In this process, granulated rubber accounting for about 3% to 5% of the aggregate weight is added before incorporating asphalt, and mixing takes place (Roberts et al., 1989). The resulting product is referred to as rubber modified asphalt concrete (RUMAC). Hot mix asphalt paving in dense-graded or open-graded can be made by using the dry process. The dry process is not usable in asphalt paving applications such as cold mix and chip seals or surface treatments (United States Department of Transportation. Federal Highway Administration, 1997).

Asphalt-rubber binders can enhance thermal cracking and high temperature properties. It has been reported that asphalt-rubber mixes such as chip seals (SAM and SAMI) are effective in reducing reflective cracking in warmer climates. Open-graded asphalt-rubber friction courses showed improved durability in warmer climates compared to conventional friction courses. Furthermore, a dense-graded asphalt-rubber layer may be effective at reducing thickness.

Terminal blends are classified as wet processes. In these processes, asphalt cement and crumb rubber modified can be blended and stored for long periods of time (United States Department of Transportation. Federal Highway Administration, 1997). The processes use a fine gradation of crumb rubber extracted from 100% tire rubber, and currently use the PG grading specification system similar to polymer modified binders, with variety grading such as PG64-28TR, or PG70-22TR. These processes have been used since the 1980s in Florida, Texas, California, Colorado, Louisiana, Arizona, and Nevada (Shatnawi, 2011b).

2.8.8 Performance record. Performance results from the texts show that adding rubber to hot mix asphalt construction can reduce rutting and increase fatigue life. Asphalt-rubber approval systems have been primarily regional, depending on the beneficial experience gained during trial stages of use (Roberts et al., 1989). Several states had experienced the use of crumb rubber, some with the wet process. The use of CRM in hot-mix asphalt increased significantly in the 1990s as a result of a mandate imposed in ISTEA; a 1992 statement indicated that 21 states used CRM in hot mixes (Hicks & Epps). According to the EPA, state departments of transportation are using larger quantities of asphalt-rubber, led by Arizona, Florida, and California. Texas and Nebraska are presently using larger amounts of asphalt-rubber. South Carolina is also using asphalt-rubber in state highway and county roads. States such as New

York and New Mexico are also using and studying rubberized asphalt (EPA, 2013). Some selected states' experiences are discussed in the remainder of this section.

Arizona is a leading state in the use of asphalt-rubber. Over fourteen million scrap tires have been used by the Arizona Department of Transportation (ADOT) on asphalt-rubber paving construction. It is currently estimated that three-fourths of Arizona's five million annually generated scrap tires are reclaimed in asphalt-rubber pavement construction. The number of asphalt-rubber projects has increased from one in 1988 to fifty-four in 2000. More than 3,000 lane-miles of streets in Phoenix, Arizona, received seal coat using asphalt-rubber technology over a 20-year period, starting in the 1970's (United States Department of Transportation, Federal Highway Administration, 1997). Use of one-inch thick asphalt-rubber hot mix overlays replaced the practice of chip seal in the 1990's. Good performance has been reported, such as reducing shrinkage cracks less than $\frac{1}{4}$ inch and reflection alligator cracks (FHWA, 1997). Both wet and dry processes have been used in Arizona. The common process used in Arizona is the wet process, also called the McDonald Process.

In 1975, California started using asphalt-rubber as chip seals in laboratory experiments and small test patches, and results were promising (Caltrans, 2003). The first California dry process rubber-modified asphalt concrete pavement included one percent ground rubber by mass added to the aggregate. The wet process has been extensively used; it was first implemented in pavement in California in 1980 (Caltrans, 2003). Caltrans has built 17 wet process coat installations (FHWA, 1997) and has reported that rubberized asphalt concrete (RAC) outperformed conventional thicker dense-graded asphalt concrete (Caltrans, 2003) by showing less distress, standing greater deflections, and needing less maintenance (FHWA, 1997).

In Texas, crumb rubber was first implemented in asphalt in 1976; from 1976 to 1981, 850 miles of asphalt-rubber seal coat were placed (Estakhri, Fernando, Button, & Teetes, 1990). More than 2,000 miles of asphalt-rubber chip seals (SAM's) have been built. Based on many years of experience using asphalt-rubber, the Texas DOT has stated that chip seal improved resistance to alligator cracking and raveling, but resistance to shrinkage cracking is not improved (United States Department of Transportation. Federal Highway Administration, 1997)

In 1988-1989, the Florida Department of Transportation began the use of crumb rubber modifier hot mix asphalt (CRM-HMA). Their first trial included 5% by weight of binder in dense-graded friction courses of 25 mm (1in) thickness to enhance the resistance to shoving and rutting (U.S. Department of Transportation Federal Highway Administration, 1995)The state developed the concept of using finer CRM in the wet process, and it doesn't use the dry process (U.S. Department of Transportation Federal Highway Administration, 1995)

2.9 Ongoing Research on High Temperature Properties

It has been well documented that asphalt-rubber shows better resistance to rutting. Rutting is one of the common pavement distresses that occurs due to traffic loading, especially under hot climatic conditions. In a Superpave binder testing procedure, a dynamic shear rheometer (DSR) is used to calculate the complex modulus and phase angle at intermediate temperatures to characterize the rheological properties of asphalt binders. Using complex modulus and phase angle, one can calculate the parameter, $G^*/\sin\delta$, and use it as a measure of rutting resistance. Superpave uses the parameter $G^*/\sin\delta$ to grade asphalt binders according to their resistance to rutting at high pavement temperatures. The asphalt binder with the highest $G^*/\sin\delta$ should have the most resistance to rutting. It has been reported that the rutting resistance parameters of CRM binders improve as the CRM percentage increases. Compared with

cryogenic CRM binders, ambient CRM was found to be a better modifier in producing the CRM binder, which has less sensitivity to rutting at high pavement temperature (Lee, Akisetty, & Amirghanian, 2008). Golzin and his coworker used polyphosphoric acid (PPA) and Vestenamer to evaluate the effect of CR on the performance of unmodified asphalt binder at different temperatures. It was shown that by increasing the PPA content, the value of the softening point was increased, while the penetration grade was decreased. Furthermore, it has been reported that increasing the PPA content from 1.5% to 2% could improve the binder performance at high temperature (Golzin & Hamid Sabbagh, 2011). According to the Superpave specifications, the rutting factor $G^*/\sin\delta$ must be higher than 1.0 kPa for un-aged asphalt and 2.2 kPa for RTFO-aged asphalt. In asphalt samples modified with 10%, 12%, or 15% crumb rubber, the $G^*/\sin\delta$ values were found to be higher than 2.2 kPa at 84.3°C, 82.1°C, and 82°C, respectively. Nejad et al. investigated the effect of crumb rubber produced in Iran on the physical and rheological properties of 60/70 and VB (vacuum bottom) bitumen. Test results showed that adding crumb rubber reduced penetration temperature susceptibility, ductility, and the Fraas breaking point, and increased the softening point, elastic recovery, and adhesion. For un-aged and aged specimens at higher temperature, the increase in crumb rubber content increased the parameters such as G^* , $G^*/\sin\delta$, and $G^*\sin\delta$. However, it was reported that for un-aged specimens at high temperature, adding CR had detrimental effects on the fatigue behavior of modified asphalts (Nejad, Aghajani, Modarres, & Firoozifar, 2012) .

Wang et al. measured the viscosity of asphalt-rubber at different temperatures using a rotational viscometer. It was found that the addition of crumb rubber can greatly increase the binder viscosity. As a result, to meet the Superpave maximum viscosity threshold of 3.00Pa.s, CR asphalt has to be heated to a higher temperature. In addition, it was found that to maintain the

same viscosity reading, the temperature needs to keep increasing as the percentage of rubber increases. As such, when 15%, 20% or 25% crumb rubber was introduced to base asphalt (viscosity > 3.0 Pa.s at 135 °C), in order to maintain viscosity below the 3 Pa.s threshold, the temperature had to be increased from the original 135 °C to 147 °C, 162 °C or 174 °C, respectively (Wang et al., 2012). Therefore, the mixing temperatures and compaction temperatures of rubberized asphalt binders were much higher than those of non-modified asphalt mixtures. This in turn can cause further challenges in the construction schedule, as well as increase the fuel consumption used for heating purposes (Wang et al., 2012). More importantly, it can damage the rubber structure and cause disintegration of rubber particles (Abdelrahman, 2011). At temperatures above 190 °C to 220 °C, rubber dissolves into the asphalt, which leads to the release of different components of rubber, including carbon black and filler components that can negatively impact asphalt binder properties. In this paper, certain amine-based liquid additives are used to facilitate asphalt-rubber interaction so that the dramatic increase in viscosity due to introduction of rubber is prevented. Amine compounds facilitate the release of rubber polymer into asphalt, softening the overall asphalt-rubber matrix. As a result, the viscosity threshold could be met at a relatively lower temperature. This not only prevents disintegration of rubber particles due to reduction in mixing high temperature, but also facilitates pumpability, allowing for application of higher rubber percentages into asphalt.

Certain warm mix additives such as Evotherm and Rediset, as well as bio-binder, include significant amounts of amides. Therefore, introduction of such additives can produce rubberized asphalt mixtures with good properties at lower mixing temperatures. This paper will conduct selected Superpave binder tests to evaluate the effects of three specific amine-based additives on high-temperature properties of CRM asphalt.

2.10 Bio-Binder

2.10.1. Problems with swine manure. According to the EPA, pork is the most commonly consumed meat in the world, estimated to be 43% of world meat consumption. In addition to the meat, several valuable products or by-products come from swine, such as insulin for the regulation of diabetes, valves for human heart surgery, and gelatin for many food and non-food uses (U.S. Environmental Protection Agency., 2012). On the other hand, it is documented that more than 335 million tons of manure are generated annually in the U.S.; North Carolina produces 40 million tons (12% of the total), making the state the second largest producer of manure after Iowa (Fini, et al., 2012). Swine manure management can be cumbersome; disposal of manure is usually handled by storing it in lagoons (see Figure 2.11). This method has negative environmental consequences, such as leachate that can contaminate surface and ground water, and nauseous odors and gaseous emissions which degrade air quality. The originated gases hydrogen sulfide (H₂S), carbon dioxide (CO₂), ammonia (NH₃), and methane (CH₄) produced at higher amounts can cause consequences such as irritation or death (Fini, et al, 2012) . To address these problems, Dr. Fini performed extensive research on swine manure to repurpose the generated waste into useful pavement material. To do so, thermochemical liquefaction of swine manure is used to produce bio oil, which undergoes some further processes to get the final bio-binder product. The production of bio-binder is described in the next section.



Figure 2.11 Lagoon at NCA&T Farm (Swine Unit)

2.10.2. Production. The bio-binder used in this study is produced from thermochemical conversion of swine manure under relatively high temperature (T), high pressure (P), for specific residence times (RT) ($T=340^{\circ}\text{C}$ or 644°F , $P=17.92\text{Mpa}$ or 2600Psi , and $\text{RT}=120\text{mn}$); the process yields bio-oil. The process starts by mixing swine manure with water to make a slurry,. Different percentages of water and manure been investigated by the North Carolina A&T SIM LAB research group; the optimum mixing ratio that gives the maximum yield of bio-oil was determined to be 50% manure plus 50% water for a total weight of 2900 g. A sample of mixed manure and water is shown in Figure 2.12. The aforementioned mix is transferred to the canister (part 1) of the reactor, an air pressure lift is used to lift the canister to be connected to the upper part (part 2), the two parts are tightened together using a torque wrench set at 30Nm. Two heating sleeves, 1000 watts and 2000 watts (part 3), are mounted to the canister (Figure 2.13). The temperature is then set to 340°C at the controller (part 4), and water is circulated through the reactor to maintain a moisture level at 20%. The reactor is heated to the set temperature (340°C), which is maintained at a constant level for 15 minutes. After the reaction is completed, the

reactor is rapidly cooled to room temperature. The gas is then released from the canister, reducing the pressure in the canister to atmospheric pressure. The sticky residue is then collected from the aqueous solutions, and undergoes vacuum filtration to obtain the final product, bio-binder. An algorithm of the process is depicted in Figure 2.15.



Figure 2.12 A Sample of mixed manure with water

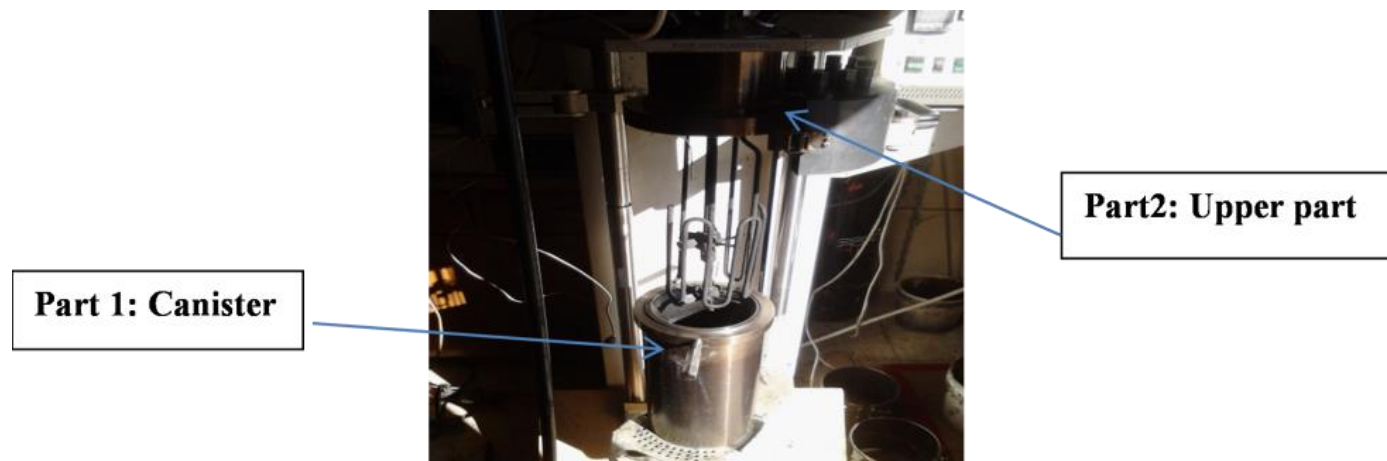


Figure 2.13 Canister

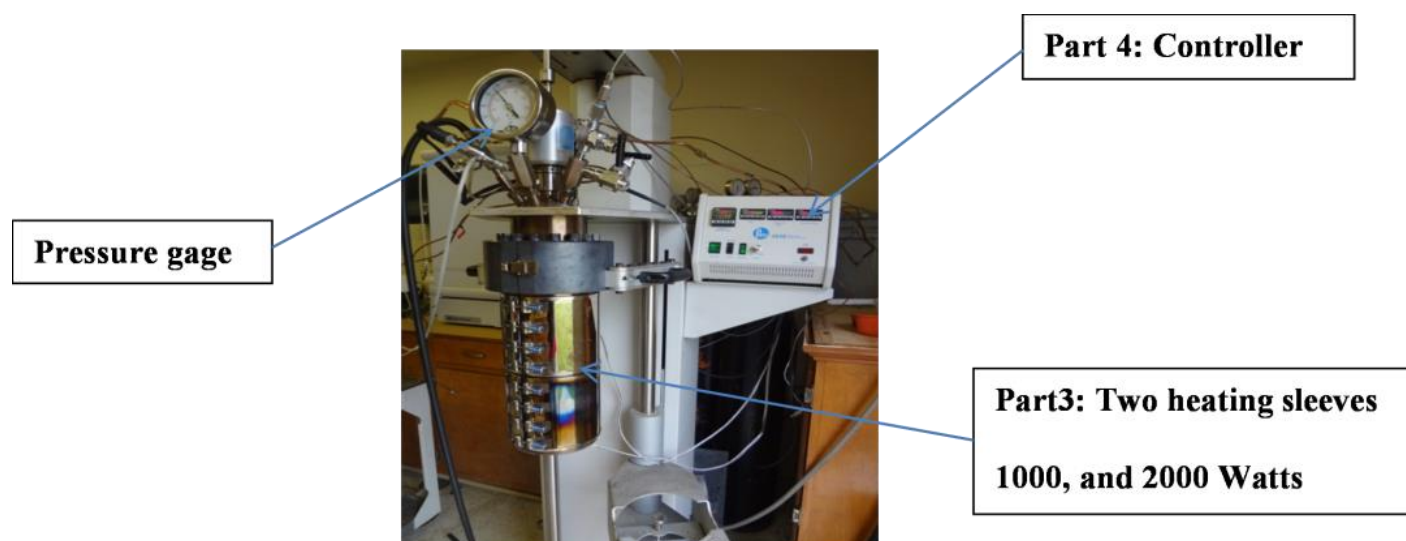


Figure 2.14 Running reactor producing bio-oil

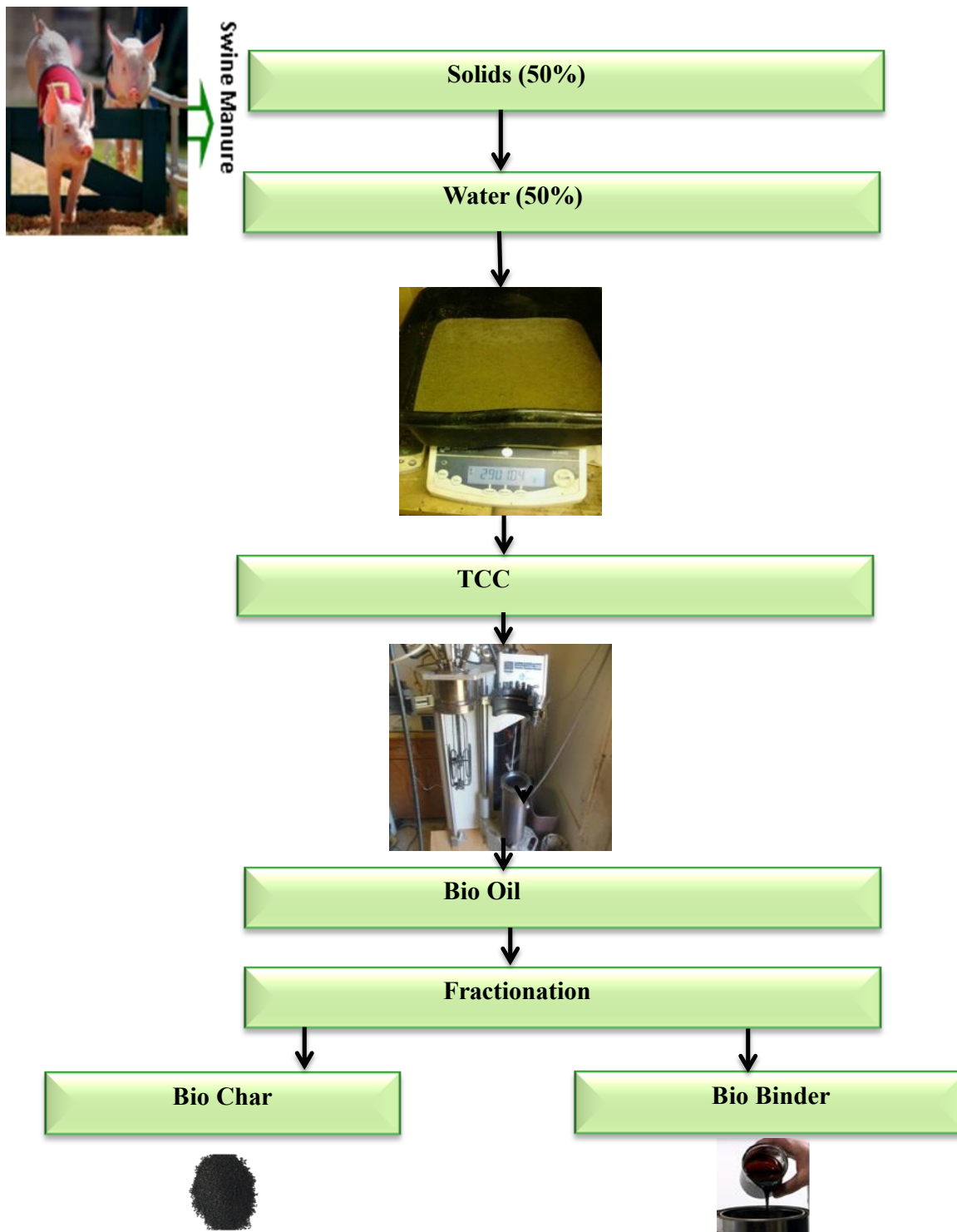


Figure 2.15 Algorithm of bio-binder production.

2.10.3. Chemical characterization of bio-binder. Bio-binder is a newly developed product on which there is extensive ongoing research. A preliminary study conducted by Dr. Fini and her team focused on evaluating the compatibility of bio-binder with petroleum-asphalt binder, using elemental analysis and a determination of saturates, aromatics, resins, and asphaltenes (SARA) fractions (Fini et al., 2011). The comparison of elemental analysis of bio-binder with a petroleum-asphalt binder used in the Federal Highway Administration (FHWA) funded SHRP-1 program (AAD-1) is shown in Table 2.6. Chemical composition of bio-binder compared to AAD-1 is shown in Table 2.7.

Table 2.6

Comparison of SARA components of bio-binder and bituminous binder (Fini et al., 2011)

Adhesive Type	<u>S</u> aturate (aliphatic) Percentage by weight (wt%)	Naphthene <u>A</u> romatics Percentage by weight (wt%)	Polar aromatic (<u>R</u> esin) Percentage by weight (wt%)	<u>A</u> sphaltenes Percentage by weight
Bio-binder From swine manure	2.48	1.67	45.87	43.39
AAD-1 The softest asphalt binder	8.6	41.3	25.1	20.5

Table 2.7

Chemical composition of bio-binder and bituminous binder (Fini, et al., 2011)

Component Percent by weight	Bio-binder	AAD-1
Carbon (C)	72.58	81.6
Hydrogen (H)	9.76	10.8
Nitrogen (N)	4.47	0.77
Oxygen (O)	13.19	0.9

CHAPTER 3

Materials Preparation and Test Procedures

This chapter contains detailed descriptions of the materials used and the tests conducted on different bio-modified asphalt-rubber binder samples. Ten types of binders were produced using a base binder asphalt PG64-22, provided by Asphalt Associates, and one type of ambient ground tire rubber), provided by Crumb Rubber Manufacturers of Mesa, Arizona, at 15% and 20% by weight of base binder. For the case of 15% CRM, the percentage of bio-binder was 5%, 10%, 15%, or 20%. For the case of 20% CRM, the percentage of bio-binder was 5%, 10%, 15%, 20%, 30%, or 50%. Table 3.3 shows the different modified binders developed and tested.

3.1 Materials Description.

3.1.1 Base binder asphalt. PG64-22, a Performance Grade (PG) of asphalt cement, was the base binder used in this study. It is the most commonly used virgin binder in North Carolina, South Carolina, and Texas, as well as other warmer geographical areas. It is used in low volume secondary, primary and interstate pavement construction and rehabilitation (Horan, 2003, Superpave-PG Binder Grading). According to the material safety data sheet from the PG64-22 provider (Asphalt Associates), the melting temperature ranges from 110°F to 130°F, this is different from the heating point. Some state specifications require a maximum heating temperature of 350°F (177°C) at hot mix asphalt plants for PG64-22, and a desired storage temperature range from 285°F to 335°F (140°C to 168°C) (U.S. OIL & REFINING CO.). The physical data of the base binder is presented in Table 3.1.

Table 3.1
Physical data of PG64-22 (from Asphalt Associates)

Product Name	PG 64-22
Chemical Name	Petroleum Asphalt
Chemical Family	Petroleum Hydrocarbon
Boiling Point	> 900 °F
Specific Gravity	1.0-1.10
Vapor Pressure (mm hg)	Not Determined
Melting Point	110-130 °F
Solubility in water	Negligible
Vapor Density (air=10)	Not Determined
Evaporation Rate(N-Butyl) Acetate=1)	Not Determined
PH	Neutral
Appearance and Odor	Black Viscous Semisolid. Asphalt Odor
Flash Point and Method	> 550 °F

3.1.2 Crumb rubber modifier (CRM). Crumb rubber modifier is produced by mechanical shredding at ambient temperature; the process is described in Chapter 2. Crumb Rubber Manufacturers of Mesa, Arizona, provided the crumb rubber with mesh 200-80. Table 3.2 shows the grading and characteristics of the crumb rubber particles. Figure 3.1 shows the CRM used. Throughout the study, crumb rubber was added to binder at two different levels: 15%CRM according to the ASTM D8 definition, and 20%CRM based on the Caltrans procedure.

Table 3.2
Grading and Characteristics of Crumb Rubber Particles by Mesh Size

Sieve No	mm	Weight Retained	Individual % Retained	Cumulative %Passing
80	0.177	42	41.50%	58.50%
100	0.149	13.7	13.60%	44.9%
120	0.125	16.5	16.3%	28.6%
140	0.105	13.9	13.7%	14.8%
170	0.088	7.2	7.1%	7.7%
200	0.074	7.8	7.7%	0.00%
Pan		3.1	0.00%	
Total		104.2	100.0%	



Figure 3.1 Crumb Rubber Mesh Size 80-200 from Rubber Manufacturers

3.1.3 Bio-binder. The bio-binder used in the study was physically produced by the author with a three-gallon reactor using a thermochemical liquefaction process at the NCA&T farm. It was derived from swine manure; an extensive explanation of the production is given in Chapter 2. A sample is shown in Figure 3.2.



Figure 3.2 Bio-binder produced at NCA&T Farm

3.2 Modified Binder Preparation

The same procedure was used to produce all specimens. These are the steps followed in the laboratory production of bio-modified rubber:

- The control binder PG64-22 was preheated at 180°C (356 °F) using a traditional oven for a short period of time until the material turned into a liquid stage.
- 100 grams of warm liquid binder PG64-22 was poured into a can to be used as a control. Nothing more was added to this can.
- 200 grams of warm liquid binder PG64-22 was poured into a new can, and 15% CRM by weight of PG64-22 was blended with the can's contents. No bio-binder was added to this can.

- 200 grams of warm liquid binder PG64-22 was poured into a new can, and 20% CRM by weight of PG64-22 was blended with the can's contents. No bio-binder was added to this can.
- 350 grams of warm liquid binder PG64-22 was poured into each of four new cans, and 15% CRM by weight of PG64-22 was blended with each can's contents. Then 5%, 10%, 15% and 20% of bio-binder by weight of PG64-22 was blended respectively and separately with each can's contents.
- Another 350 grams of warm liquid binder PG64-22 was poured into each of four new cans, and 20% CRM by weight of PG64-22 was blended with each can's contents. Then 5%, 10%, 15%, and 20% of bio-binder by weight of PG64-22 was blended respectively and separately with each can's contents.
- An additional 250 grams of warm liquid binder PG64-22 was poured into a new can, and the can's contents were blended with 20% CRM by weight of PG64-22. Then 30% of bio-binder by weight of PG64-22 was blended into the can's contents.
- An additional 200 grams of warm liquid binder PG64-22 was poured into a new can, and the can's contents were blended with 20% CRM by weight of PG64-22. Then 50% of bio-binder by weight of PG64-22 was blended into the can's contents.

A total of thirteen specimens were developed. Table 3.3 presents the contents of the thirteen types of binders developed and evaluated. The label BMR-X-Y is given to the different modified binders, where BMR stands for Bio-Modified Rubber, X represents the percentage of crumb rubber modifier by weight of PG64-22, and Y represents the percentage of bio-binder by weight of PG64-22. For example, BMR-15-5 means Bio-Modified Rubberized Binder with 15% CRM and 5% bio-binder by weight of PG64-22. The label X%CRM is

given to specimens modified with rubber only, where X represents the percentage of crumb rubber modifier by weight of PG64-22.

Table 3.3
Content of Binders Developed and Evaluated

Binders ID	PG64-22 (weight in grams)	CRM (percentage by weight of PG64-22)	Bio-binder (Percentage by weight of PG64-22)
Control	100	0	0
15%CRM	200	15	0
20%CRM	200	20	0
BMR-15-5	350	15	5
BMR-15-10	350	15	10
BMR-15-15	350	15	15
BMR-15-20	350	15	20
BMR-20-5	350	20	5
BMR-20-10	350	20	10
BMR-20-15	350	20	15
BMR-20-20	350	20	20
BMR-20-30	250	20	30
BMR-20-50	200	20	50

3.3 Blending Process

The asphalt-rubber was produced in the laboratory, incorporating an ambient CRM source provided by Crumb Rubber Manufacturers of Mesa, Arizona, at percentages of 15% and 20% by weight of asphalt binder into PG64-22. The blending of the CRM with the base asphalt binder (PG64-22) was done mechanically using a 3000rpm drill equipped with an open mixing blade as shown in Figure 3.3. The CRM 200-80 mesh was gradually poured into the base binder PG64-22, as the shear was conducted at 180°C by the usage of a hot plate for 60 min, and the drill speed was maintained at constant speed of 3000 rpm. This mixing condition matches the practices used in California to produce field mixtures (Caltrans, 2003). The twelve modified specimens were prepared using the same procedure.



Figure 3.3 Sample Blending

3.4 Test Procedure.

3.4.1 Viscosity testing. To study the effects of rubber and bio-binder on rheological properties of bio-rubberized modified asphalt binder, as well as its pumpability, each modified

specimen and each non-modified specimen was tested using a Brookfield viscometer following the ASTM D4402 (ASTM Standard D4402, 2013) specification to evaluate its viscosity and high temperature properties. The simple rotational viscometer (RV) test measures the torque required to maintain a constant rotational speed of a cylindrical spindle while submerged in an asphalt binder at a constant temperature, and the torque is converted to a viscosity and displayed automatically by the RV (Pavement interactive, 2011). Viscosity was measured at four different temperatures (105°C, 120°C, 135°C, and 150°C) and six different speeds (rpm) (5, 10, 20, 25, 50, and 100). A smooth spindle SC4-27 was used for measurements. The testing specimen was prepared by pouring 10.5g of each material into an aluminum chamber. The specimens were preheated for twenty minutes, then placed into the thermosel set at the selected temperature for twenty minutes. Three readings of viscosity and the corresponding temperature and speed (rpm) were taken, with an interval of three minutes between readings. The average of the three viscosity readings was recorded as the specimen's viscosity. Figure 3.4 shows the actual RV instrument used for this study.



Figure 3.4 Brookfield viscometer (RV-DVIII Ultra)

3.4.2 Temperature susceptibility. Temperature susceptibility is a measure of variation of asphalt binder viscosity with temperature change (Claudy P.M., Martin D., & Planche J. P., 1998). Equation 3.1 has been commonly used to calculate the viscosity-temperature susceptibility (VTS) (Rasmussen R., Lytton R., & Chang G., 2002).

$$VTS = \frac{\log[\log(\eta_{T2})] - \log[\log(\eta_{T1})]}{\log(T2) - \log(T1)} \quad \text{Equation 3.1}$$

Where T1 and T2 are the temperature of the binder at two known points, and η_{T1} and η_{T2} are the viscosity of the binder at the same two points.

The value of the VTS is directly proportional to the temperature susceptibility of the binder.

3.4.3 Shear susceptibility. The rate of change in viscosity with the shear rate is called shear susceptibility (Roberts, Kandhal, Brown, Lee, & Kennedy, 1996). Shear susceptibility, also known as the shear index, is determined by calculating the slope of the line on a graph of the log of viscosity versus the log of rotational speed, or by using Equation 3.2 (Raouf & Williams, 2010).

$$SS = \frac{\log(\text{viscosity})}{\log(\text{speed})} \quad \text{Equation 3.2}$$

Where speed is the rate at which shear is applied to the material.

3.4.4 Dynamic shear rheometer (DSR). All laboratory-produced binders were tested using a dynamic shear rheometer shown in Figure 3.5. The DSR is used to characterize asphalt binder viscoelastic behavior at medium to high temperatures. The standard dynamic shear rheometer test is AASHTO T315. All un-aged specimens and RTFO aged materials were tested following this standard. The test procedure consists of using a thin asphalt binder sample inserted

between two circular parallel metal plates: the upper plate oscillates at 10rad/sec (1.59Hz) back and forth across the sample loaded on the fixed lower plate. The indicated oscillation rate of 10radians/second is intended to simulate the shearing action corresponding to a traffic speed of about 55 mph (90km/hr) (Pavement interactive, 2011). The samples are prepared by pouring the preheated modified and non-modified binders into a circular silicone mold as shown in Figure 3.6. The mold in Figure 3.5 is 25 mm (1inch) in diameter (specimen diameter), its use is specified for un-aged and RTFO aged materials, and the test gap or specimen thickness is 1mm (0.04inch), in accordance with the test standard. Furthermore, test temperatures higher than 115°F (46°C) also use a specimen 1mm (0.04 inches) thick and 25mm (1 inch) in diameter. Two parameters are measured by the DSR, the complex shear modulus (G^*), and the phase angle (δ). The complex shear modulus is defined as a measure of total resistance of a material (asphalt binder) to deform under repeated load, and the phase angle is the angle in degrees between a sinusoidally applied strain and the resultant sinusoidal stress in a controlled strain testing mode. Values for G^* can range from 500Pa to 6000Pa. Restrictive values of phase angle are between 0° and 90°. The larger the value of the phase angle, the more viscous the material; the lower the value of the phase angle, the more elastic the material (Pavement interactive, 2011). Parameters G^* and δ are used as predictors of hot mix asphalt (HMA) rutting and fatigue cracking. Pavement faces two major problems: rutting, a concern in early stages of pavement life, and cracking, a concern in later stages. The factor $G^*/\sin\delta$ is specified to be the rutting parameter; therefore, a larger value of $G^*/\sin\delta$ is required when rutting is a main concern during an HMA pavement's early and mid-life. The performance graded asphalt binder specification uses G^* and δ to determine the performance grade of the binders. $G^*/\sin\delta$ determines the maximum design temperature, with a minimum value of 1 kPa at 10 rad/s (1.59Hz) frequency for un-aged

materials, and 2.2 kPa at 10rad/s frequency for RTFO aged materials, according to the performance graded asphalt binder specification.



Figure 3.5 Dynamic shear rheometer



Figure 3.6 DSR Sample (25mm in Diameter)

3.4.5 Specimens' master curves. Master curves of all binders have been constructed, after performing a frequency sweep method of testing in the DSR. The frequency sweep method uses different testing temperature and frequency; their values are summarized in Table 3.4. All specimens, un-aged and RTFO aged, were tested using a silicone mold with the following geometry: 25 mm in diameter and 1mm gap as shown in Figure 3.6. Seven testing temperatures and eight frequencies were used to test the specimens.

Table 3.4
Factors Used for Frequency Sweeps

Factor	Values
Testing Temperature in °C	40, 46, 52, 58, 64, 70, and 76
Frequency, in Hz	0.00159, 0.0157, 0.017, 0.156, 0.169, 0.819, 1.67, 3.98

3.4.6 Rolling thin film oven (RTFO). The Rolling Thin-Film Oven (RTFO) (Figure 3.7) technique provides simulated short-term aged asphalt binder for physical property testing. The effect of heat and air on a moving film of semi-solid asphaltic materials is measured. The RTFO procedure consists of feeding un-aged binder specimens into cylindrical glass bottles and placing these bottles in a rotating carriage within an oven. The oven is heated to 163°C (325°F) for at least four hours, and the carriage is rotated at a speed of 15 RPM for 85 minutes. The carriage rotation continuously exposes un-aged binder to the heat and air flow, and blends each sample (ASTM Standards D2872, 2012). The RTFO aged specimens were obtained using this technique.



Figure 3.7 Rolling thin film oven (RTFO).

CHAPTER 4

Results and Discussion

This chapter will present and discuss the results obtained from the testing that was carried out following the experiment plan described in Chapter 1. The following sections will report the bio-modified rubber (BMR) and non-modified specimens binder testing results, which include viscosity, rheology, shear susceptibility, temperature susceptibility, master curves, high temperature properties, and the effect of temperature on $\tan(\delta)$ of un-aged specimens and RTFO specimens.

4.1 Bio Modified Rubber and Non-Modified Binders Viscosity Testing

The viscosities of laboratory-prepared bio-modified rubber, and non-modified binders were estimated by means of Brookfield rotational viscometer using the ASTM.D4402 test procedure. The average viscosities for each specimen at each testing temperature are shown in Table 4.1 through Table 4.3.

Table 4.1
Specimens' Average Viscosity at 120°C

Average Viscosity (Pa.s)							
Test Temp.(°C)	Specimens	5 RPM	10 RPM	20 RPM	25 RPM	50 RPM	100 RPM
120	Control	1.15	1.02	0.95	0.94	0.92	0.91
	15%CRM	8.63	7.74	7.03	6.79	N/A	N/A
	20%CRM	10.48	9.22	8.07	7.72	N/A	N/A
	BMR-15-5	5.06	4.89	4.67	4.68	4.51	N/A
	BMR-15-10	2.48	2.40	2.32	2.28	2.22	2.14
	BMR-15-15	2.10	2.09	2.06	2.06	2.01	1.94
	BMR-15-20	2.06	2.02	1.95	1.93	1.86	1.73
	BMR-20-5	6.85	6.48	6.13	5.98	N/A	N/A
	BMR-20-10	4.70	4.20	3.93	3.86	3.65	N/A
	BMR-20-15	4.31	4.11	3.94	3.88	3.69	N/A
	BMR-20-20	4.36	4.12	3.91	3.85	3.61	N/A
	BMR-20-30	4.31	4.00	3.7	3.62	3.36	N/A
BMR-20-50	2.40	2.15	1.97	1.92	1.80	1.68	

Table 4.2
Specimens' Average Viscosity at 135°C

Test Temp.(°C)	Specimens	Average Viscosity (Pa.s) at Velocity					
		5 RPM	10 RPM	20 RPM	25 RPM	50 RPM	100 RPM
135	Control	0.50	0.50	0.46	0.45	0.41	0.41
	15%CRM	4.33	3.90	3.42	3.47	3.14	N/A
	20%CRM	4.05	3.65	3.57	3.34	3.12	N/A
	BMR-15-5	2.56	2.52	2.44	2.44	2.29	2.13
	BMR-15-10	1.15	1.12	1.10	1.09	1.07	1.05
	BMR-15-15	1.183	1.18	1.17	1.19	1.16	1.10
	BMR-15-20	1.16	1.12	1.09	1.10	1.08	1.03
	BMR-20-5	3.20	3.10	2.95	2.94	2.77	N/A
	BMR-20-10	2.45	2.13	1.95	1.90	1.79	1.70
	BMR-20-15	2.31	2.23	2.14	2.13	2.01	1.86
	BMR-20-20	2.31	2.25	2.17	2.15	1.98	1.81
	BMR-20-30	2.40	2.27	2.13	2.10	1.92	1.72
BMR-20-50	1.48	1.32	1.16	1.13	1.04	0.96	

Table 4.3
Specimens' Average Viscosity at 150°C

Test Temp.(°C)	Specimens	Average Viscosity (Pa.s) at Velocity					
		5 RPM	10 RPM	20 RPM	25 RPM	50 RPM	100 RPM
150	Control	0.20	0.22	0.21	0.22	0.21	0.20
	15%CRM	2.95	2.57	2.30	2.24	2.00	1.77
	20%CRM	2.15	1.95	1.75	1.70	1.59	1.50
	BMR-15-5	1.73	1.71	1.65	1.64	1.50	1.34
	BMR-15-10	0.65	0.65	0.63	0.62	0.60	0.59
	BMR-15-15	0.75	0.741	0.77	0.80	0.78	0.73
	BMR-15-20	0.80	0.80	0.80	0.83	0.80	0.73
	BMR-20-5	2.05	1.95	1.87	1.86	1.74	1.59
	BMR-20-10	1.48	1.29	1.12	1.09	1.02	0.97
	BMR-20-15	1.60	1.53	1.46	1.45	1.34	1.21
	BMR-20-20	1.76	1.66	1.56	1.54	1.38	1.21
	BMR-20-30	1.55	1.45	1.36	1.34	1.23	1.10
BMR-20-50	1.15	0.99	0.87	0.83	0.72	0.65	

It is reported that at high temperature, the viscosity of asphalt binder is a significant property because it represents the binder's capability to be pumped through an asphalt plant, coating aggregate in asphalt concrete mix, and be elaborated in a new pavement surface (Akisetty, Lee, & Amirghanian, 2009). The influence of bio-binder concentration, amine base additives, rubber concentration, temperature, and shear rate on viscosity of non-modified and modified asphalt-rubber was evaluated. Figures 4.1 and 4.2 represent the viscosity values at the two rubber concentrations and four testing temperatures, for control, rubberized and bio-rubberized asphalt binders. Two general trends can be seen from these results: the viscosity of all specimens decreased with an increase in temperature, and the addition of bio-binder into rubberized binder decreased the rubberized binder's viscosity compared to the control rubberized binder. Introduction of 5% up to 20% of bio-binder at the two rubber concentrations (15% and 20%CRM) decreased the viscosity, which in turn reduced the stiffening effect of the rubber. For the case of the 20%CRM concentration, we increased the number of tested specimens by adding two more bio-binder percentages: 30% and 50%. As Figure 4.2 shows, the viscosity was in the same range for 10%, 15%, 20%, and 30% bio-binder; no significant change was recorded in viscosity values. This can be attributed to the swelling effect of rubber particles absorbing bio-binder. It has been reported that because of its cross-links, crumb rubber never dissolves completely in asphalt (Ghavibazoo, Abdelrahman, & Ragab, 2013). Moreover, it has been proven that light-molecular-weight components of asphalt are absorbed by CRM, causing it to swell up to three to five times its original volume at low temperatures (Heitzman, 1992b). The lack of significant decrease in viscosity values for some comparisons in Figure 4.2 could be attributed to the non-saturation of rubber particles. It is documented that an increase in the crumb rubber modifier binder viscosity is a result of oily fraction reduction of the binder, so a constant

value of binder viscosity may indicate reaction completion; the rubber may be dissolved, disintegrated, or reduced molecular weight due to devulcanization and depolymerization processes. Increasing the bio-binder percentage to 50% showed a significant decrease in viscosity in Figure 4.2. At all temperatures (105°C to 150°C), the viscosity was below the Superpave specification threshold (maximum asphalt binder viscosity no greater than 3 pa.s at 135 °C) designated to ensure mixture workability.

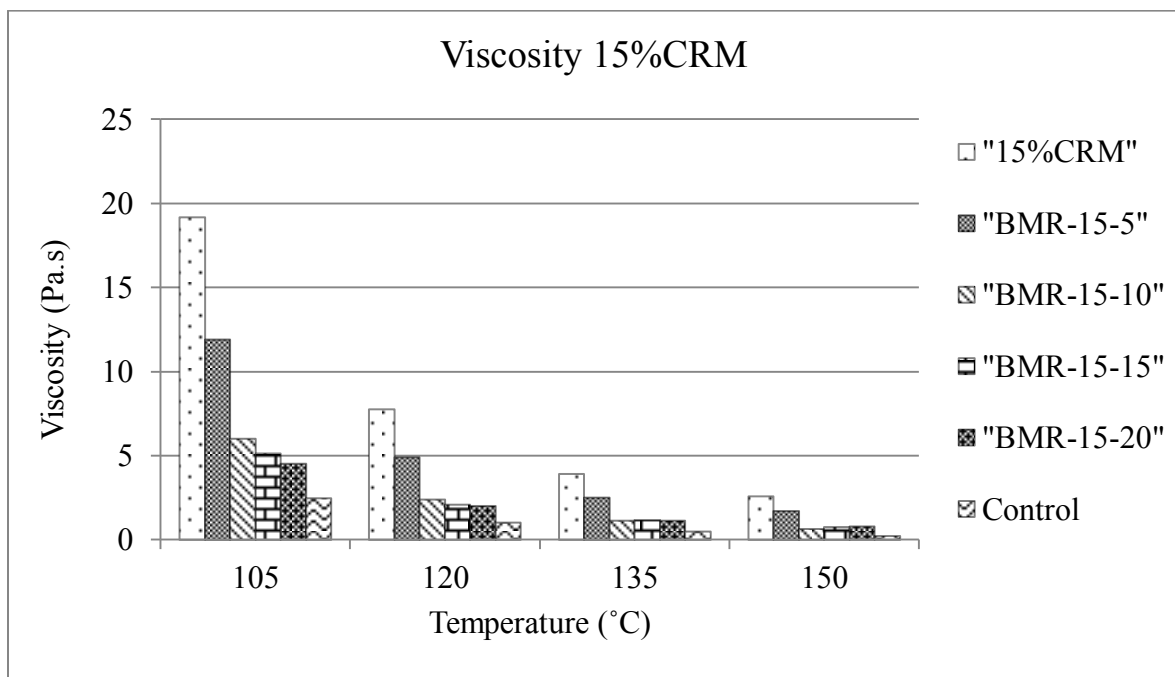


Figure 4.1 Viscosity vs temperature for control, 15% CRM, with Bio-binder at 10 rpm

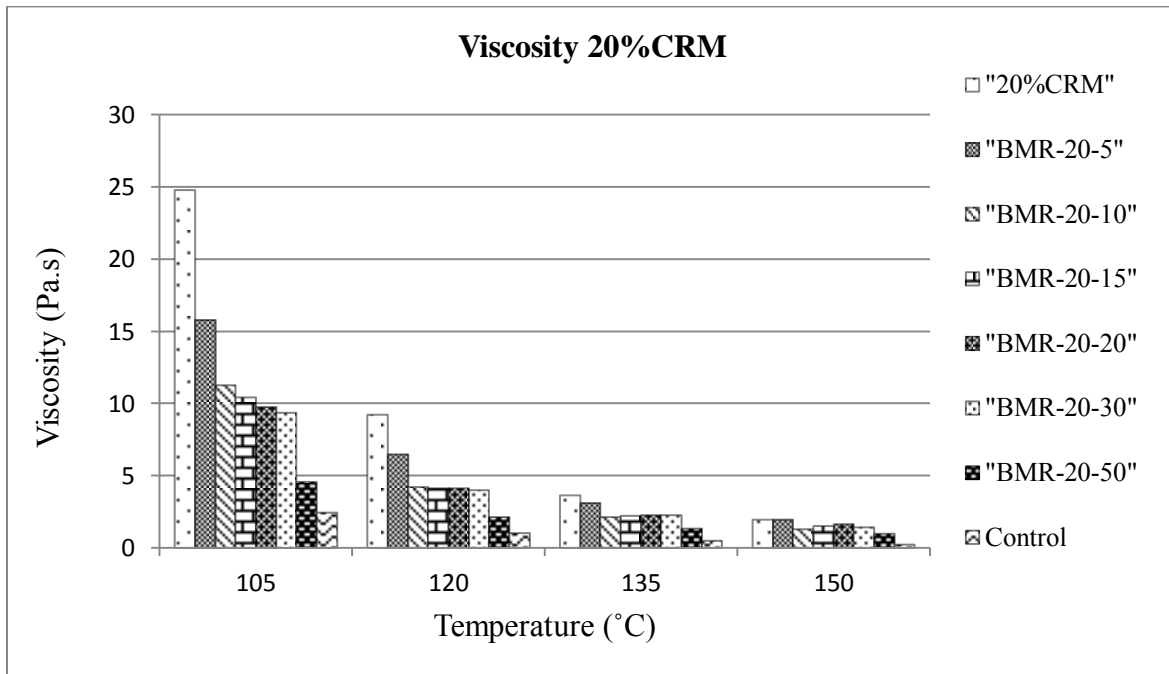


Figure 4.2 Viscosity vs Temperature for control, 20% CRM, with Bio-binder at 10 rpm

Figure 4.3 shows the viscosity of all specimens at a standard test temperature of 135°C following the superpave binder specifications. It can be seen in this figure that specimen 15%CRM and 20%CRM are above the maximum value required by superpave specifications which is 3Pa.s. In the other hand, all bio-modified rubber sample viscosity is below the 3Pa.s, therefore passed the criteria. Introduction of bio-binder to asphalt rubber can help one achieve higher percentage of crumb rubber.

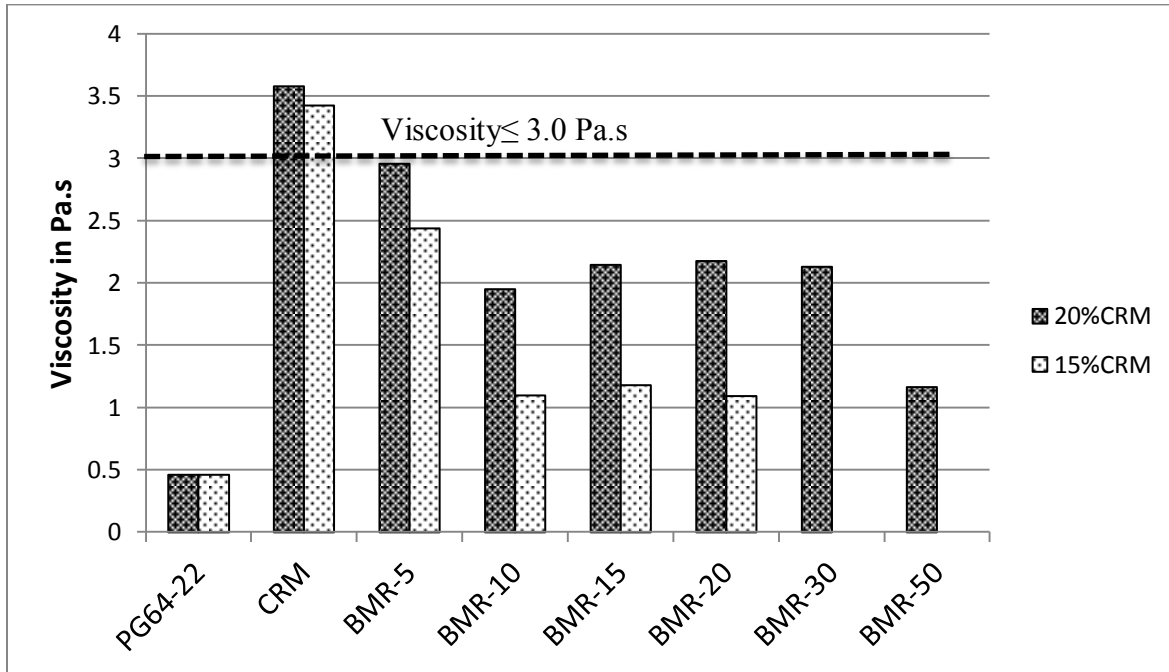


Figure 4.3 Viscosity of all specimens at test temperature 135°C

4.2 Viscosity Temperature Susceptibility

Figure 4.4 is a graphical plot of $\text{Log}(\log(\text{viscosity}))$ versus $\text{Log}(\text{temperature})$ for the control binder, 15%CRM binder non-modified, and the bio-binder-modified specimens with 15% CRM binder. Figure 4.5 is a similar plot for the specimens with 20%CRM binder. In both figures, it can be observed that the control binder has a slope that is higher in magnitude (steeper slope) than all the CRM binders at different rubber concentration levels, modified or non-modified. The slope is equal to the viscosity temperature susceptibility ($\text{VTS}=\text{slope}$); the higher the magnitude (steeper slope) of the VTS, the more susceptible the specimen is to changes in viscosity with changes in temperature (Rasmussen et al., 2002). Based on that concept, the results showed the temperature susceptibility of control binder was reduced by incorporating the bio-binder. From Figure 4.4, the specimens “BMR-15-15” and “BMR-15-20” have the same slope with an insignificant difference; this can be attributed to the interaction of rubber particles

swelling and absorbing light-molecular-weight components of both asphalt and bio-binder, since both materials are very similar in composition. In Figure 4.5, the same scenario is happening for the cases of “BMR-20-15”, “BMR-20-20”, and “BMR-20-30”, and the same explanation could be given as for the 15%CRM concentration cases. To confirm the previous statement, we can see by increasing the bio-binder percentage to fifty percent, a significant increase in the magnitude of the VTS value occurred, which can be attributed to the effect of bio-binder helping rubber particles to dissolve into the binder matrix following the devulcanization process. Furthermore, the VTS value of “BMR-20-50” is close to the VTS value of the control, which shows that by increasing the bio-binder percentage, one can partially or totally replace the virgin asphalt content and still have similar properties to the control, while adding useful rubber properties. Further tests are needed to confirm the results.

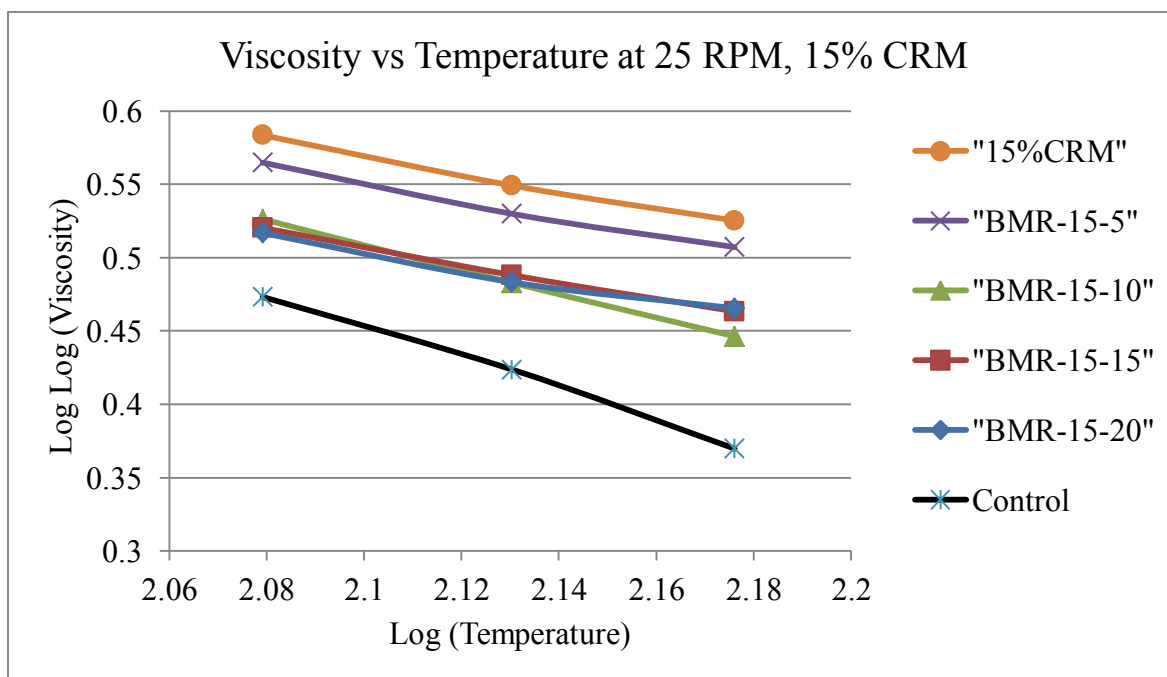


Figure 4.4 Viscosity temperature susceptibility (VTS) for 15% concentration of CRM

Table 4.4
Slope for Different Specimens with 15%CRM (VTS)

Specimens	Slope
Control	-1.065
15%CRM	-0.601
BMR-15-5	-0.596
BMR-15-10	-0.824
BMR-15-15	-0.588
BMR-15-20	-0.531

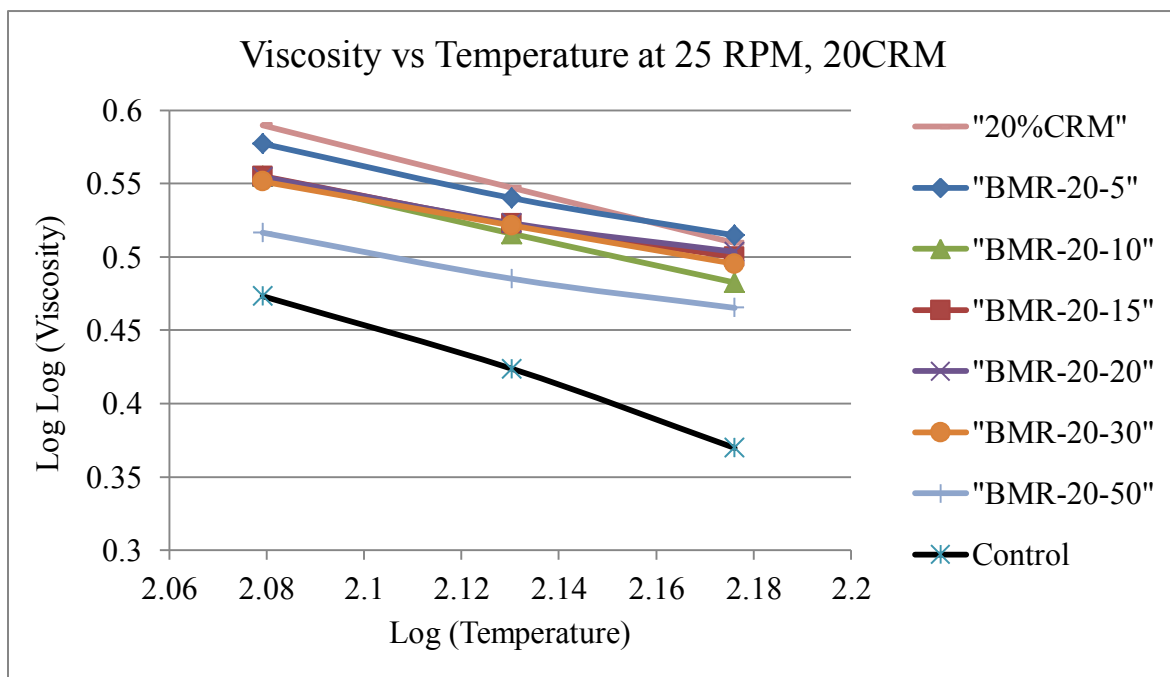


Figure 4.5 Viscosity Temperature susceptibility (VTS) for 20% concentration of CRM.

Table 4.5
Slope for Different Specimens with 20%CRM (VTS)

Specimens	Slope
Control	-1.065
20%CRM	-0.827
BMR-20-5	-0.646
BMR-20-10	-0.745
BMR-20-15	-0.577
BMR-20-20	-0.529
BMR-20-30	-0.578
BMR-20-50	-0.53

4.3 Shear susceptibility

Shear susceptibility is illustrated in Figures 4.6 and 4.7, which show a plot of Log(viscosity) versus Log(shear rate) at 150°C temperature. From the analysis of Figure 4.6, it can be seen that the shear susceptibility of the control binder is considerably reduced by modifying it with rubber. A comparison of Figures 4.6 and 4.7 shows that the higher the rubber concentration, the lower the shear susceptibility. This can be due to the chemical interaction of bio-binder and rubber particles with the control binder. No trend was found for bio modified rubber specimen in term of increasing or decreasing shear susceptibility.

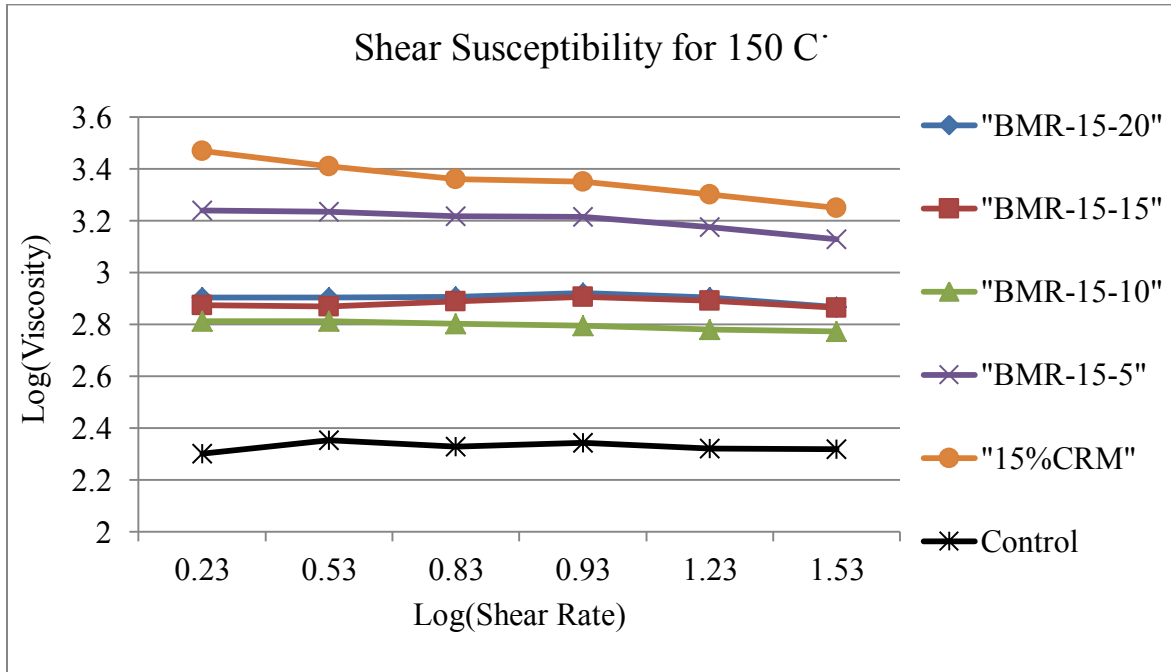


Figure 4.6 Shear Susceptibility (SS) for 15%CRM with different percentages of Bio-binder at 150°C.

Table 4.6

Slope for Different Specimens with 15%CRM (SS)

Specimens	Slope or SS
Control	0.0004
15%CRM	-0.0049
BMR-15-5	-0.0208
BMR-15-10	-0.0086
BMR-15-15	0.0008
BMR-15-20	0.0044

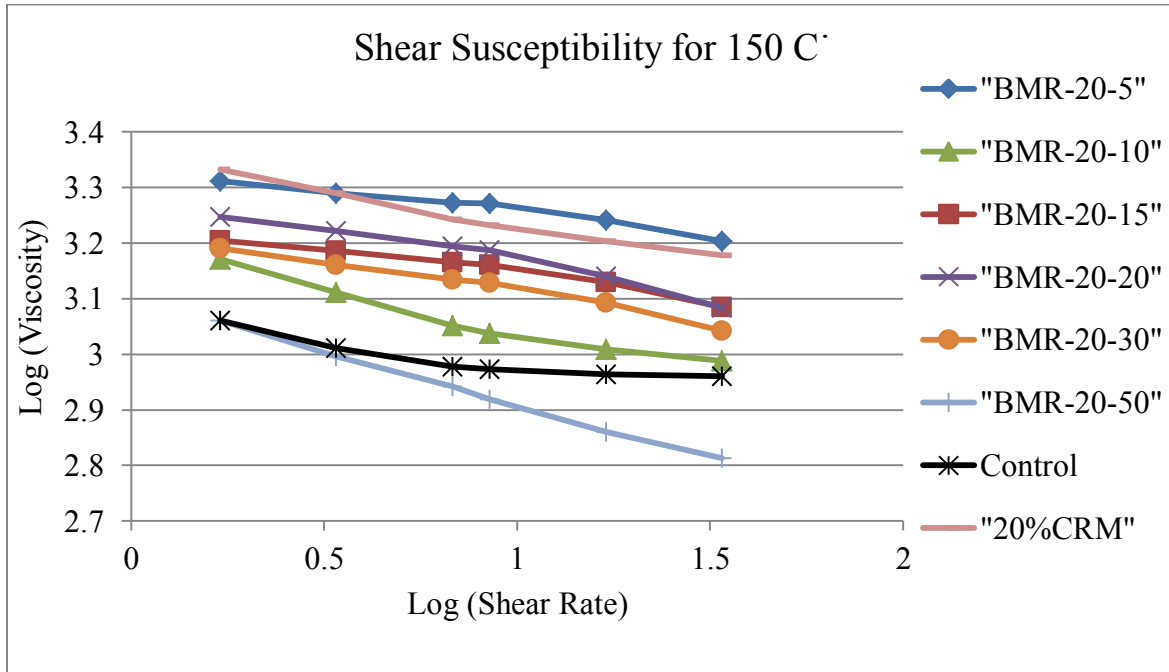


Figure 4.7 Shear susceptibility (SS) for 20%CRM with different percentages of Bio-binder at 150°C.

Table 4.7

Slope for Different Specimens with 20%CRM (SS)

Specimens	Slope or SS
Control	-0.0748
20%CRM	-0.1196
BMR-20-5	-0.0796
BMR-20-10	-0.142
BMR-20-15	-0.0892
BMR-20-20	-0.142
BMR-20-30	-0.1102
BMR-20-50	-0.1912

4.4 Dynamic Shear Rheometer (DSR) Results Before and After RTFO

In the Superpave specification, high temperature grade has been defined as the temperature at which $G^*/\sin\delta$ of the asphalt binder has a minimum value of 1 kPa before aging and 2.2 kPa after aging. All specimens passed those criteria.

The Dynamic Shear Rheometer (DSR) following ASTM D7175 (ASTM Standard D7175-08, 2008) was used to characterize the viscoelastic behavior of the non-modified and the bio-modified rubberized binder asphalts. A temperature sweep method was used to characterize all specimens. Master curves of un-aged and aged RTFO samples are presented in Figures 4.8 to 4.11. The effect of temperature on DSR parameters $G^*/\sin\delta$ and δ is shown in Figures 4.12 to 4.15. It can be seen from the master curves in Figures 4.8 to 4.11 of un-aged and RTFO-aged specimens that G^* increases as the amount of bio-binder increases at lower frequency, and a converse trend is observed for G^* values at higher frequency. This trend holds true for all bio-modified rubberized asphalt binder at the two rubber concentration levels of 15% and 20%. It also can be seen that the master curves of all modified specimens extend a little more over in the frequency span than the control, which means some reduction of temperature susceptibility occurred on modified samples. Comparison between un-aged and RTFO aged specimens shows that at the same crumb rubber and bio-binder content, aged specimens had higher stiffness (higher G^*), rutting ($G^*/\sin\delta$), and (δ) than un-aged specimens.

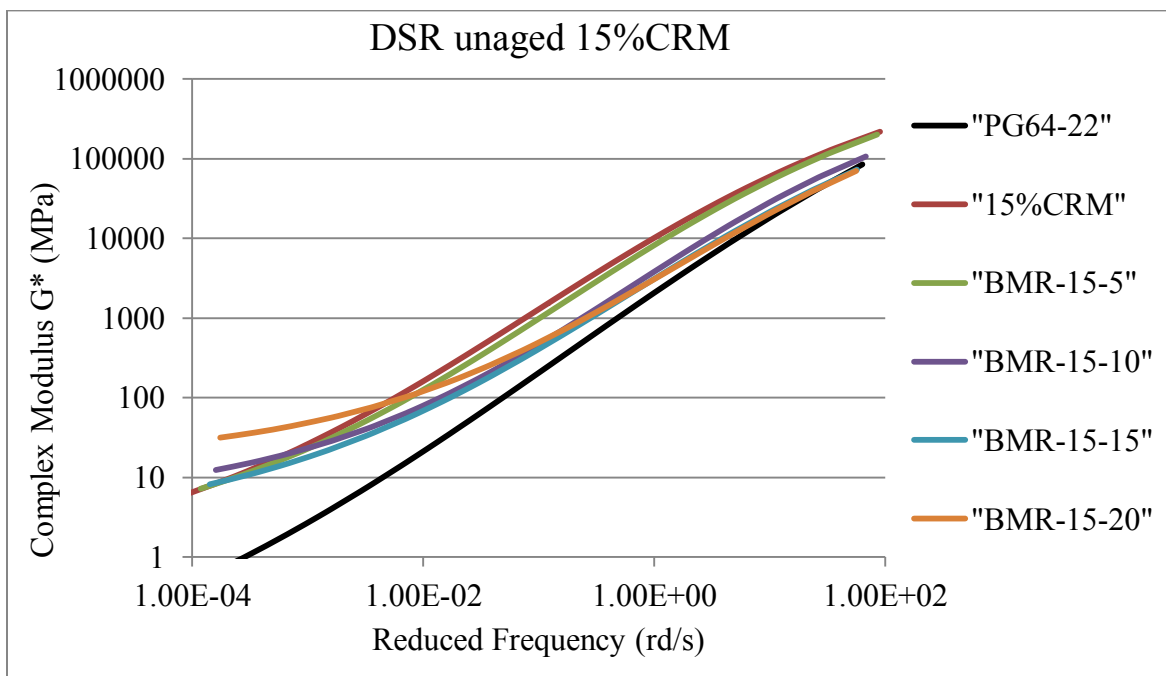


Figure 4.8 Master curves for PG64-22, 15%CRM, un-aged specimens

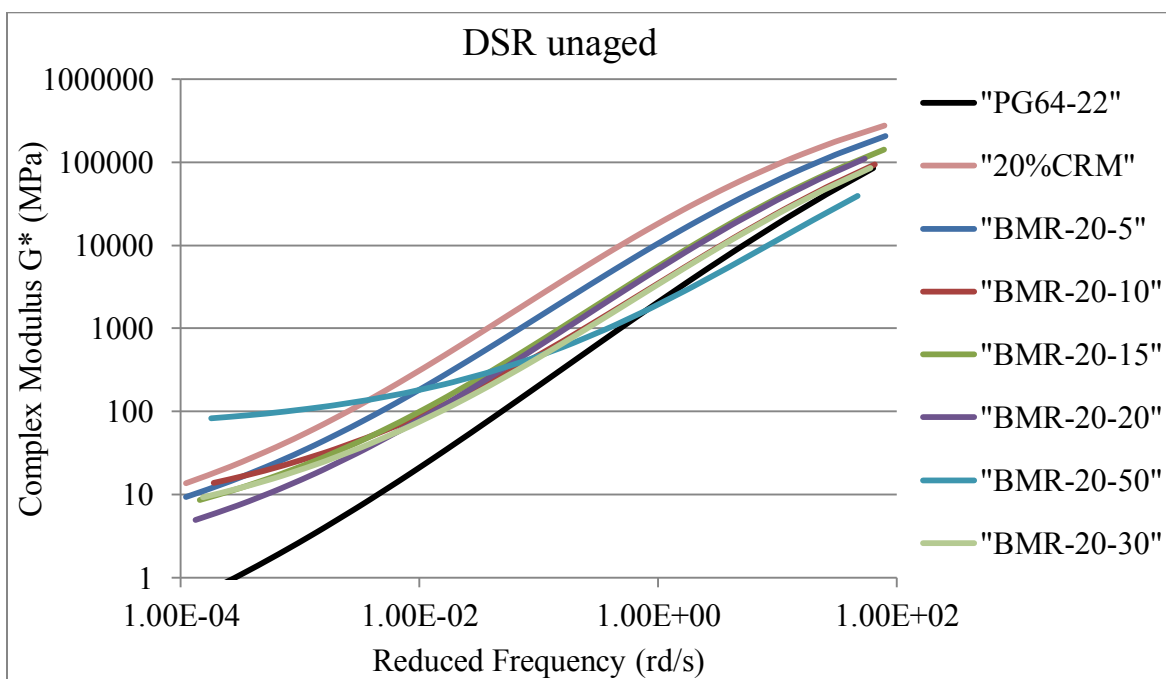


Figure 4.9 Master curves for PG64-22, 20%CRM, un-aged specimens

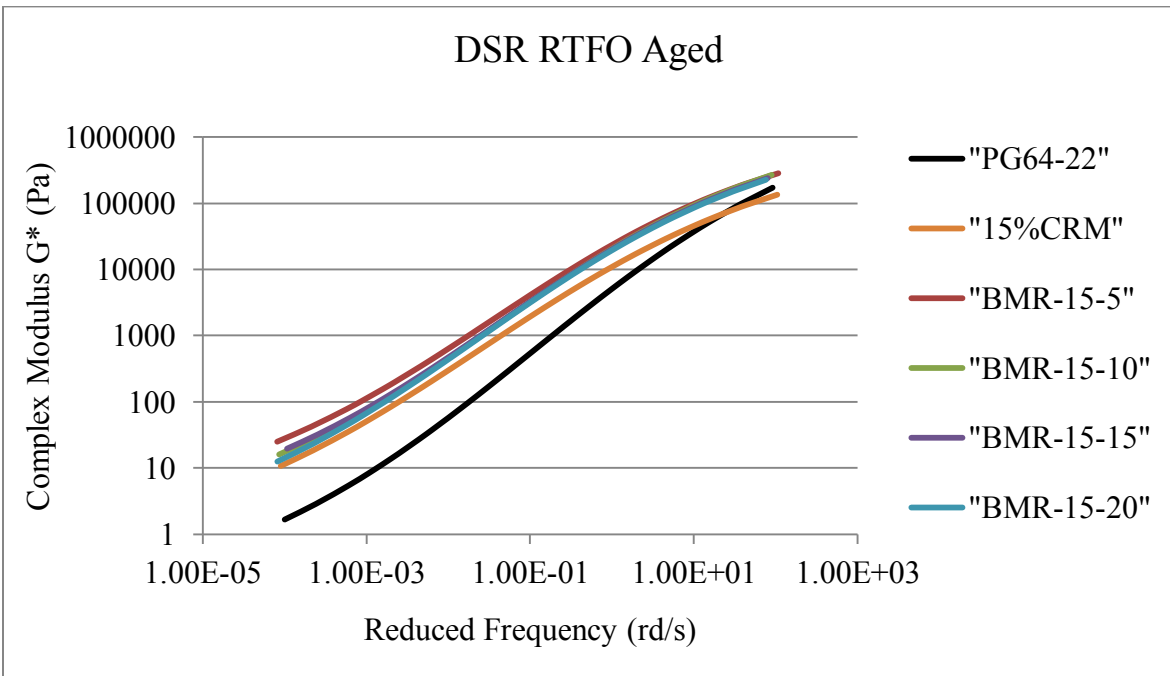


Figure 4.10 Master curves for PG64-22, 15%CRM, aged specimens

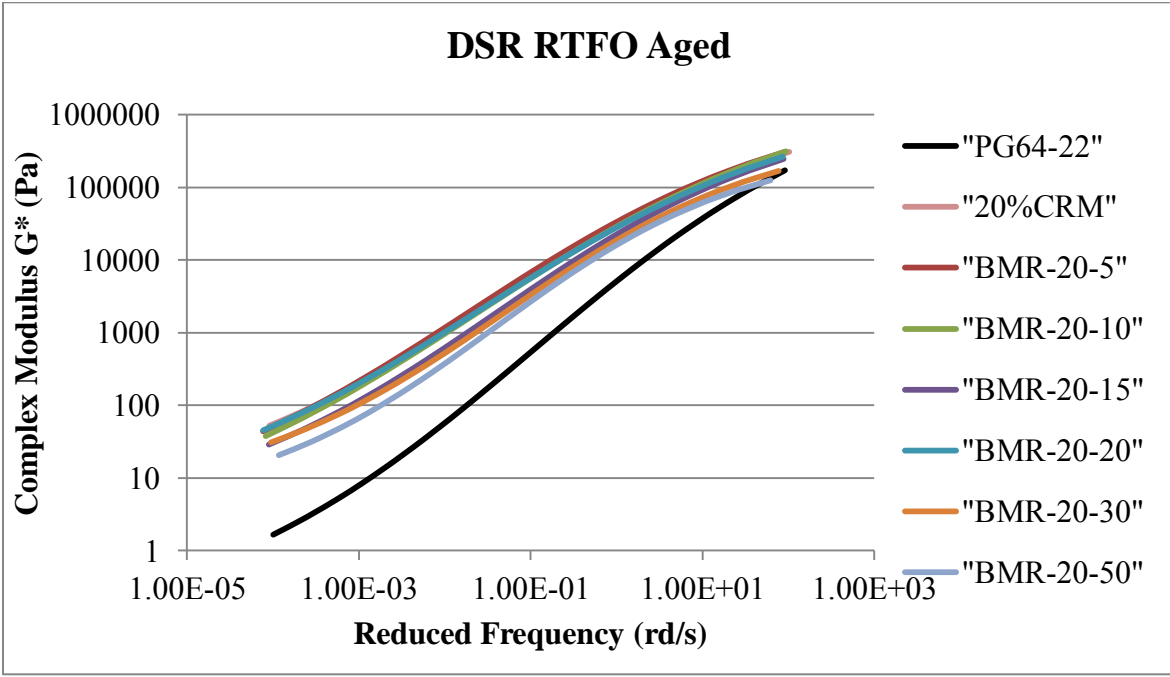


Figure 4.11 Master Curves for PG64-22, 20%CRM, Aged Specimens

4.5 Effect of Temperature on Parameter $G^*/\sin(\delta)$ Un-Aged and Aged Specimens

The effect of temperature on $G^*/\sin\delta$ for un-aged and aged specimens is shown in Figures 4.12 to 4.15. The Superpave specification classifies the parameter $G^*/\sin\delta$ as an indicator for evaluating the rutting resistance of both unmodified and modified polymer binders (Wong et al., 2004). Rutting is defined as the progressive accumulation of permanent deformation of pavement layers, generally in the asphalt layers under recurring loads (Li, Ni, Gao, Yuan, & Xia, 2014). Results indicate that for un-aged specimens, the rutting parameter considerably increased by increasing the rubber content, comparing Figure 4.12 and Figure 4.13. Conversely, introduction of bio-binder at the two rubber concentration level decreases $G^*/\sin\delta$ values for all specimens. Also, it can be seen that rutting parameter values decrease as the temperature increases; this trend holds true for all specimens. Comparison of the results in Figures 4.12 to 4.15 indicates that at constant crumb rubber and bio-binder content, RTFO aged specimens had higher stiffness and rutting resistance (higher G^* and $G^*/\sin\delta$) than un-aged specimens. It can be observed from Figure 4.12 through 4.14 that all specimens at temperature of 64°C pass the Superpave binder specification which 1.1 kPa for unaged specimen and 2.2 kPa for aged specimen.

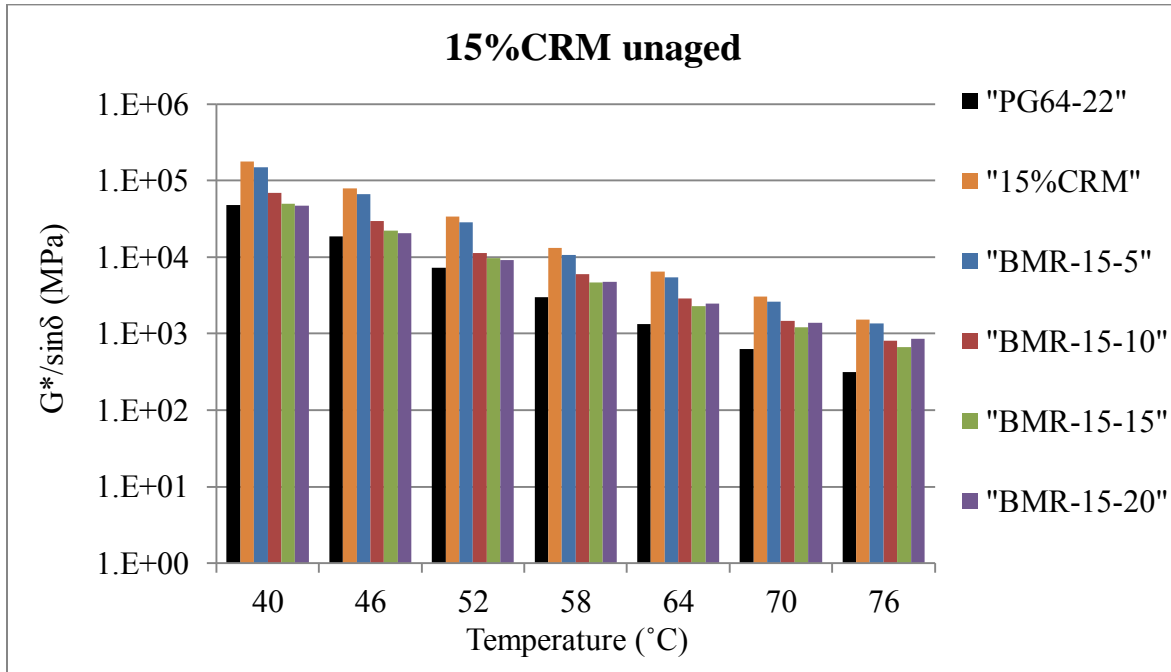


Figure 4.12 Effect of temperature on $G^*/\sin\delta$, 15%CRM, un-aged specimens

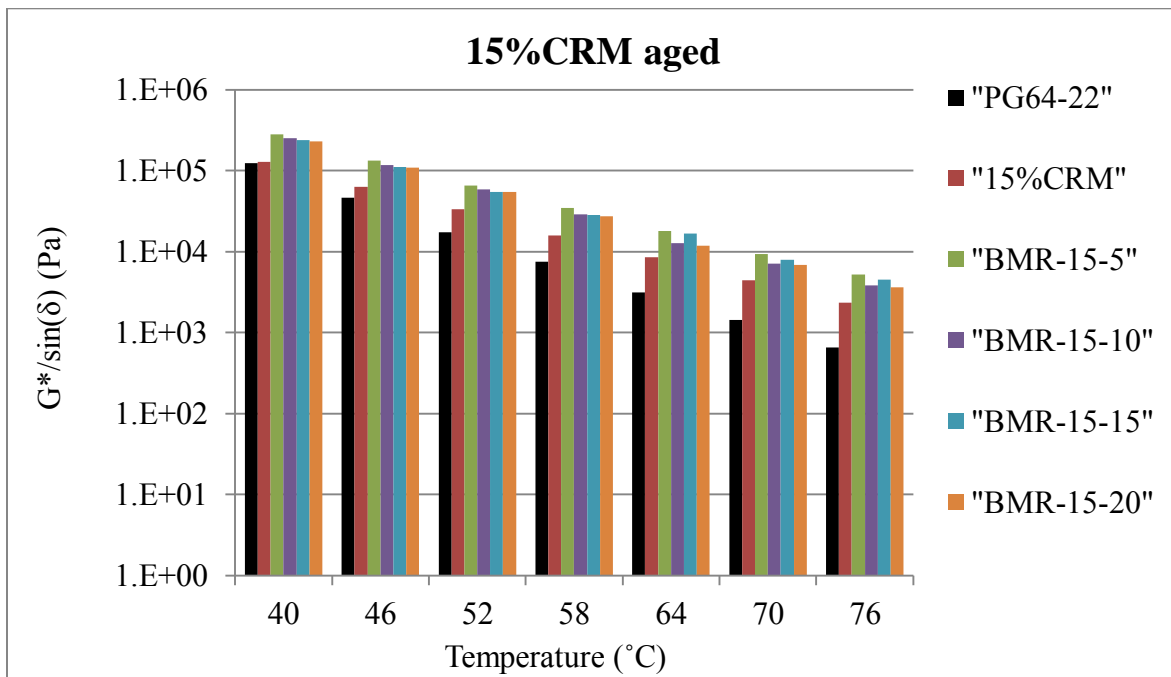


Figure 4.13 Effect of temperature on $G^*/\sin\delta$, 15%CRM, aged specimens

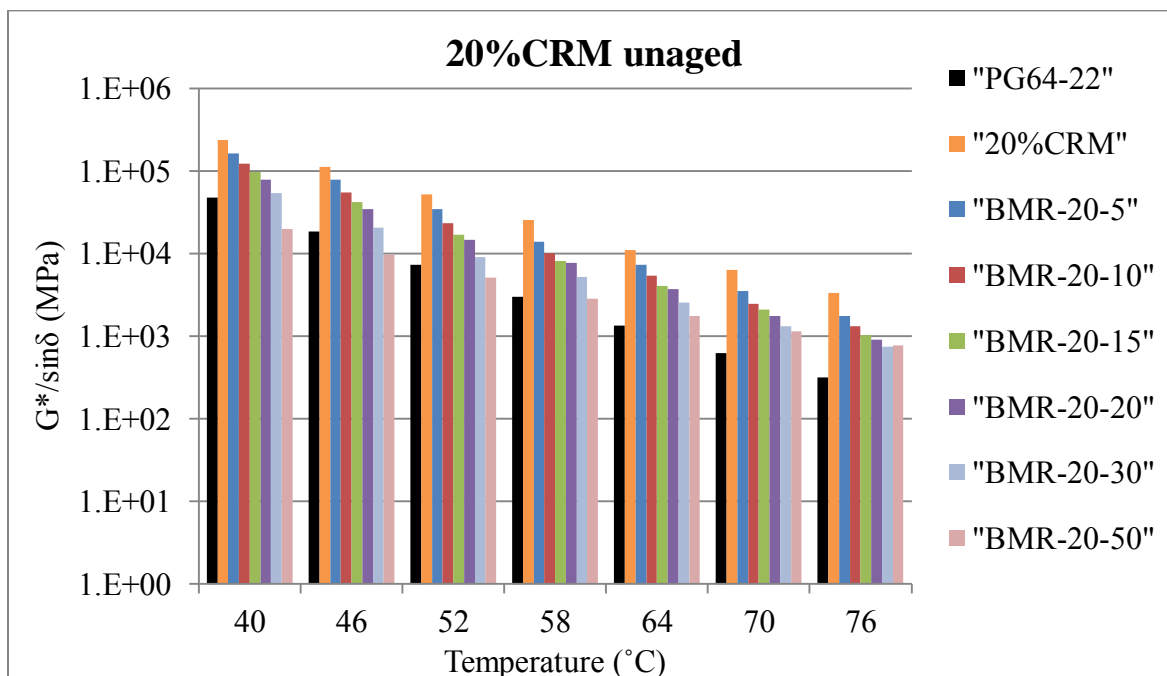


Figure 4.14 Effect of temperature on $G^*/\sin\delta$, 20%CRM, un-aged specimens

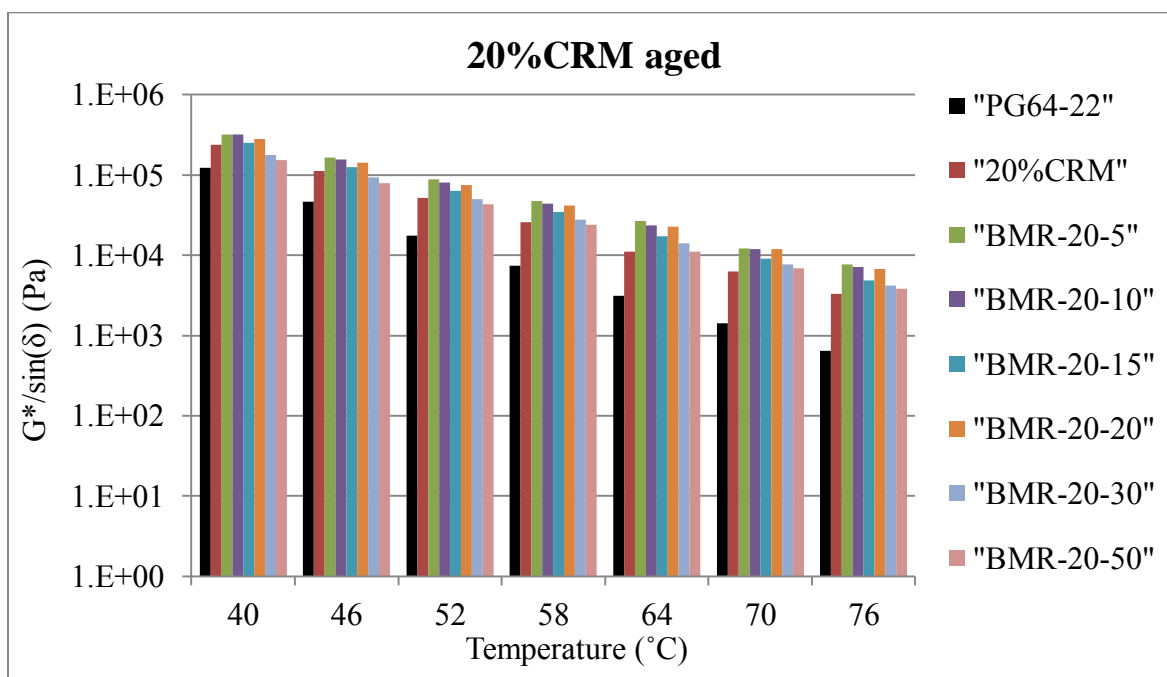


Figure 4.15 Effect of temperature on $G^*/\sin\delta$, 20%CRM, aged specimens

4.6 Effect of Temperature on Parameter (δ) Un-Age and Aged Specimens

Figures 4.16 and 4.17 have graphical plots of the phase angle versus temperature. The phase angle (δ) is the interval between the applied shear stress and the resulting shear strain (pavement interactive, 2011). As seen in Figures 4.16 and 4.17, the phase angle (δ) for the control binder (PG64-22) has the highest phase angle at low and high temperature for both unaged and aged case. The introduction of 15%CRM and 20%CRM into the control binder decreased the phase angle value at both low and high temperature for unaged specimens. The reduction of phase angle is proportional to the rubber percentage, 20%CRM concentration has more reduction effect of phase angle than 15%CRM. The phase angle (δ) is an indicator of the viscoelastic properties of a material; limiting values for phase angle are 0° and 90° . The lower the phase angle is (closer to zero), the more elastic the material; a larger value of the phase angle (closer to 90°), means the material is more viscous (pavement interactive, 2011). Introduction of bio binder further decreased the phase angle value for all bio modified rubber (BMR) specimens at the two rubber concentration level. The phase angle reduction is proportional to the bio binder content. Binders with a high G^* value and lower δ value are more rut resistant. A decrease in (δ) values is an improvement of the elastic property of a material. It can be seen from Figures 4.16 and 4.17 that phase angle for all bio modified rubber specimen decreases as the temperature increases. For specimens with 15%CRM concentration, the more the bio-binder content, the lower the phase angle. This means a 15%CRM specimen with higher bio-binder content (e.g. 20% bio-binder) is less rut resistant. For the case of 20%CRM specimens, a similar trend is observed: the phase angle decreases as the temperature increases proportionally to the bio binder content for specimens BMR-20-15, BMR-20-30 and BMR-20-50. This observation is significant for the case of BMR-20-50 specimen. This means for specimens with 20%CRM, increasing bio-

binder content up to 30% one can obtain a binder with improved elastic properties, more rutting resistant and less temperature susceptibility. For the case of the BMR-20-50 specimen, the phase angle decreases significantly as the temperature increases, this means better rutting resistance properties and better temperature susceptibility.

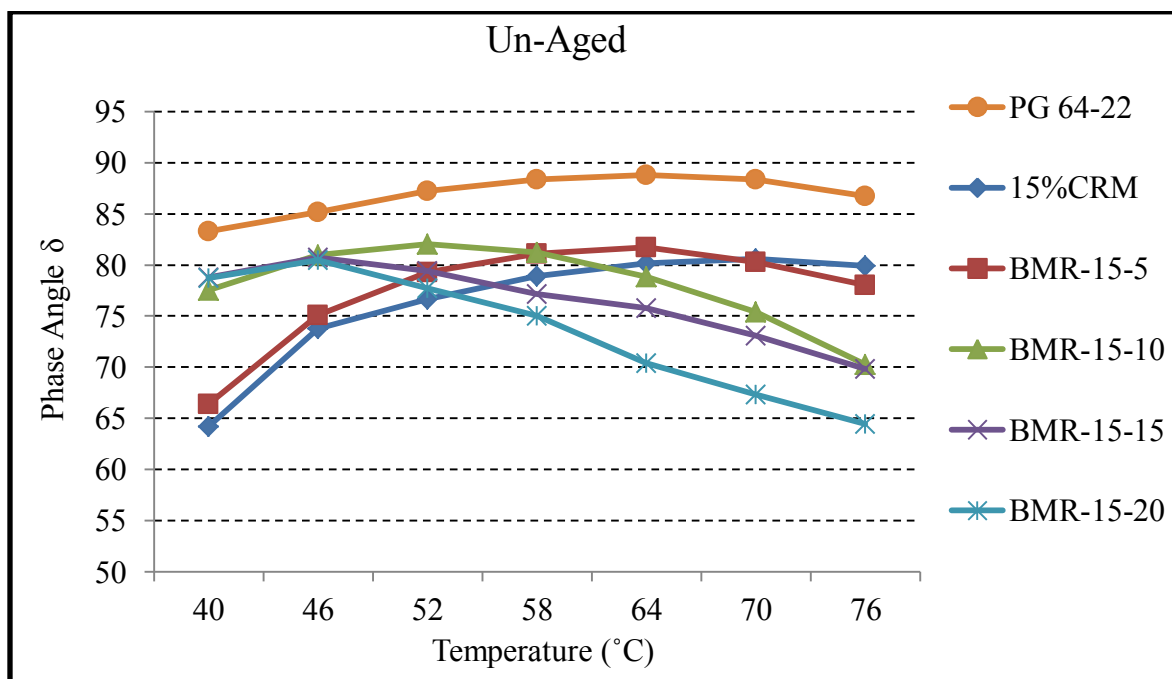


Figure 4.16 Effect of temperature on phase angle (δ), un-aged 15%CRM

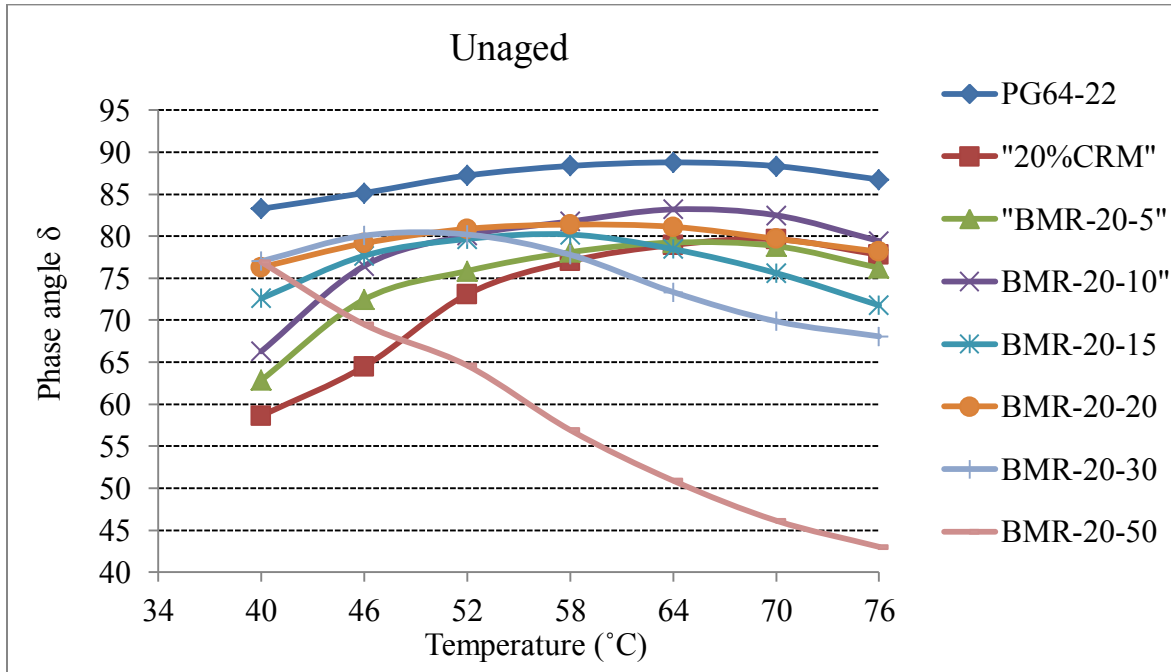


Figure 4.17 Effect of temperature on phase angle (δ), un-aged 20% CRM

For RTFO aged specimens, it can be observed from Figures 4.18 and 4.19 that bio modified rubber (BMR) showed to have higher phase angle than the control crumb rubber, and lower than the base binder (PG64-22). Therefore rutting parameter decreases for aged specimen compared to un-aged specimens at both rubber concentration level 15%CRM and 20%CRM with different percentages of bio-binder. Also, temperature susceptibility decrease compared to un-aged specimens. Further tests are needed to confirm the results

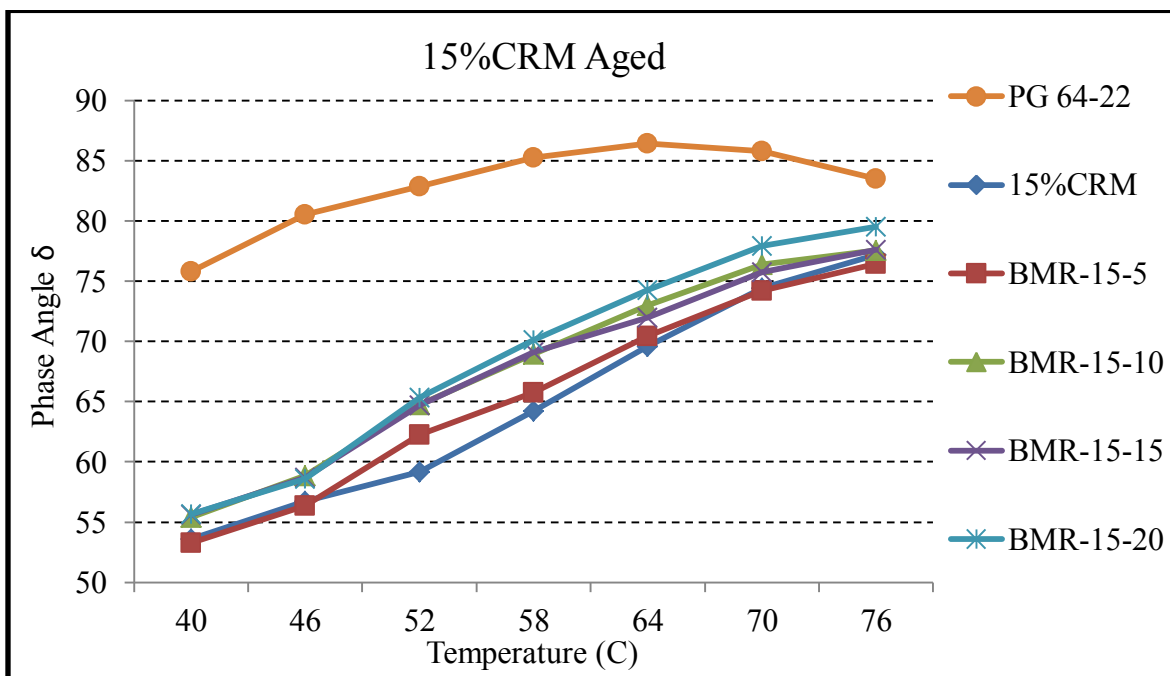


Figure 4.18 Effect of temperature on parameter (δ), RTFO 15%CRM

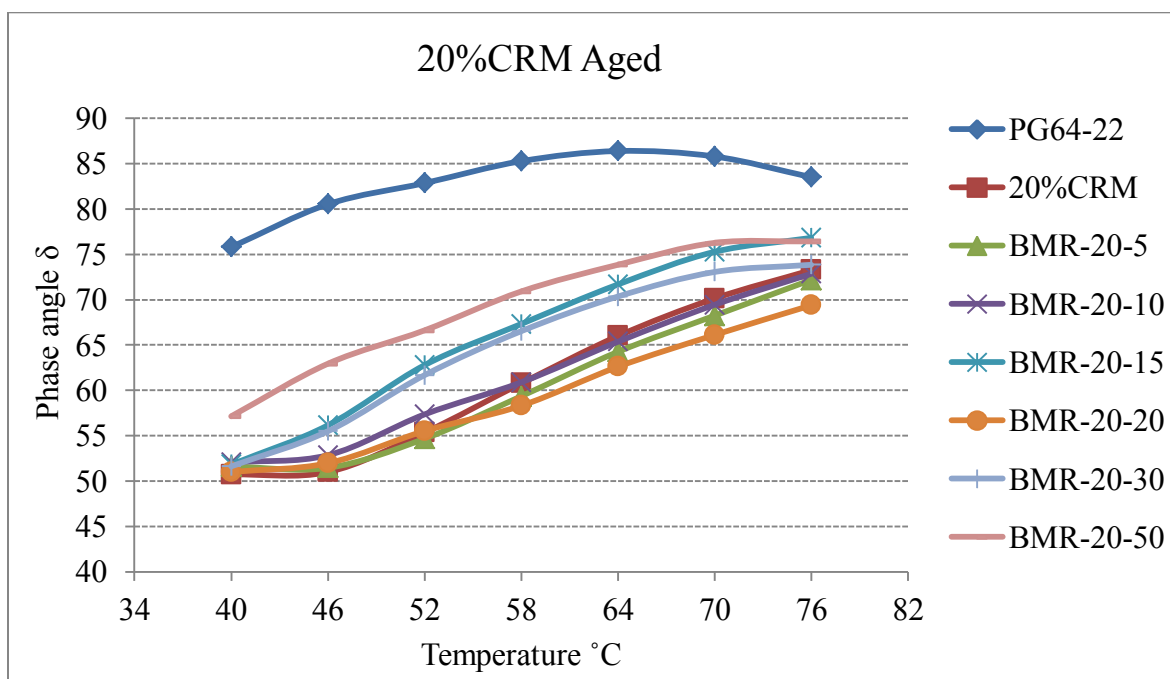


Figure 4.19 Effect of temperature on phase angle (δ) aged 20%CRM

Figure 4.20 and 4.21 shows plots of the phase angle at of all binders at a temperature of 64°C and a frequency of 1.67E+00 for the two rubber concentration 15%CRM and 20%CRM, according to the superpave binders specification. Phase is reduced after oxidation aging resulting in more brittle materials. However, addition of certain percentage of bio binder found to be effective in restoring the phase angle. From observation of Figure 4.20 it can be seen that the phase angle of all unaged bio modified rubber (BMR) specimen is higher than the aged specimen phase angle, except for the case of BMR-15-20, in that case a converse trend is observed. From that perspective it can be stated that when 15%CRM was used, the minimum percentage of bio binder to restore the phase angle was 20%. By a similar observation of the Figure 4.21 it can be seen that all unaged bio modified rubber (BMR) specimen up to 15% bio binder content has higher phase angle than aged the aged specimen phase angle. For the case of BMR-20-30 and BMR-20-50 the trend is conversed. Therefore when 20%CRM was used, the minimum percentage of bio binder used to restore the phase angle was 30%.

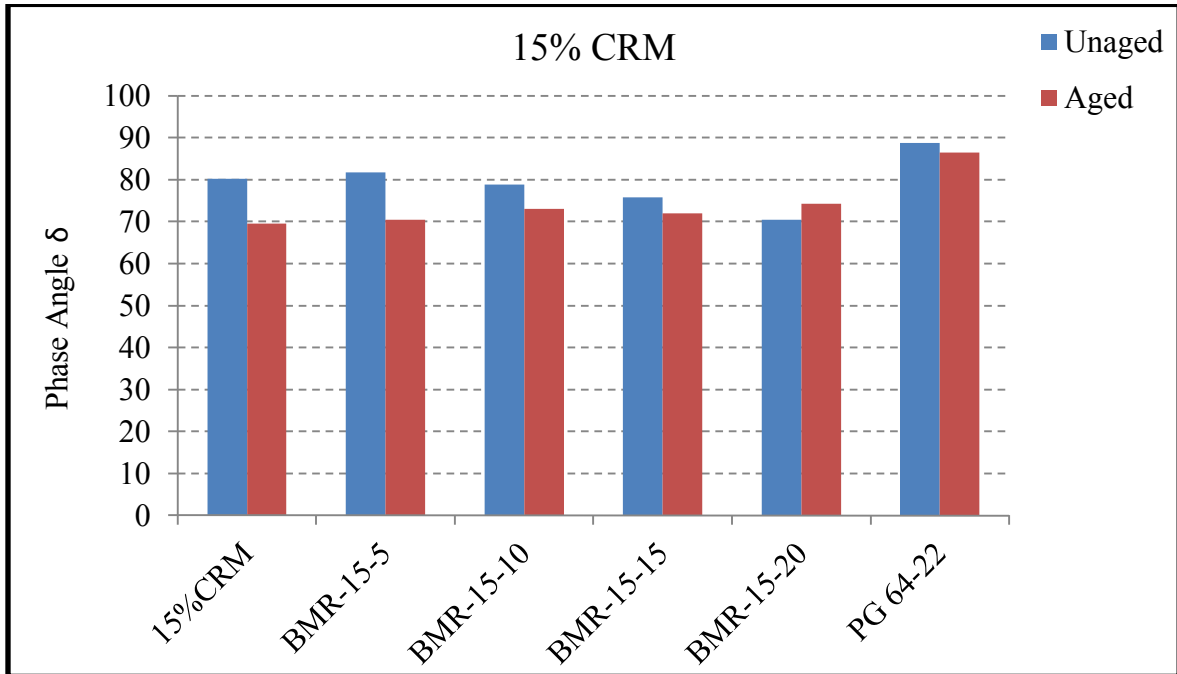


Figure 4.20 Phase angle of binders at 64°C and a frequency of 1.67E+00, 15%CRM

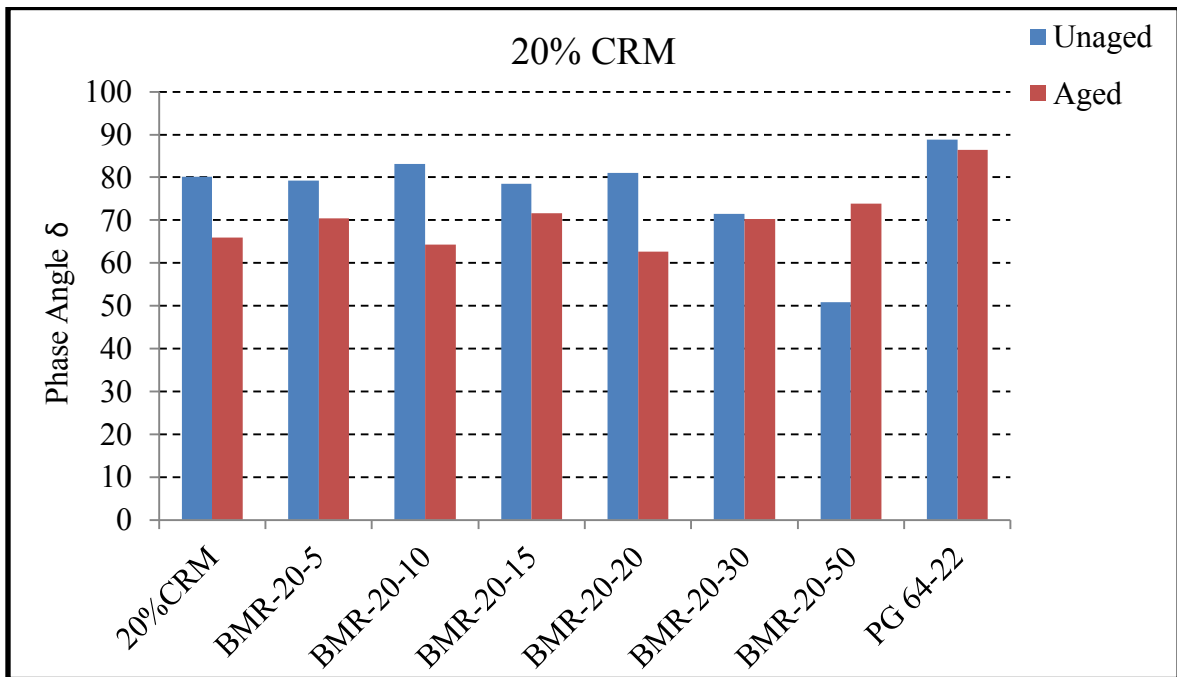


Figure 4.21 Phase angle of binders at 64°C and a frequency of 1.67E+00, 20%CRM

CHAPTER 5

Summary and Conclusions

This research has determined the rheological characteristics of newly-developed bio-modified rubber (BMR) asphalt binder, prepared by the addition of various percentages of bio-binder to rubberized asphalt binder at two concentration levels of rubber (15%CRM and 20%CRM). One specimen of virgin binder PG64-22 and twelve laboratory-produced specimens were tested: 15%CRM, 20%CRM, BMR-15-5, BMR-15-10, BMR-15-15, BMR-15-20, BMR-20-5, BMR-20-10, BMR-20-15, BMR-20-20, BMR-20-30, and BMR-20-50. The viscosity of each of these specimens was evaluated by means of a Brookfield rotational viscometer using a SC-27 spindle at four different temperatures and six velocities, following the ASTM.D 4402 test procedure.

Data from the viscosity tests was used to evaluate the temperature susceptibility and shear susceptibility of Bio-modified rubber (BMR) asphalt, Crumb rubber modified (CRM) asphalt, and virgin asphalt. Comparison between specimens was made based on viscosity, temperature susceptibility, and shear susceptibility. In addition, the complex shear modulus (G^*) and phase angle (δ) of all specimens were evaluated using Dynamic Shear Rheometer (DSR) after specimens were exposed to oxidative aging. To do the oxidative aging, the RTFO samples were prepared following the ASTM standard D2872.

It was found that the introduction of bio-binder to asphalt binder at concentrations up to 50% bio-binder improves asphalt rheological and high-temperature properties. When bio-binder is added to asphalt-rubber, the bio-binder components (mainly amine-based compounds) react with the rubber facilitating the de-association of the rubber polymer so called “devulcanization”. This in turn, help rubber polymer be released into the asphalt matrix enhancing asphalt

rheological properties. It was shown in this study that additions of 5%, 10%, or 15% bio-binder to asphalt-rubber decrease the mixture viscosity significantly facilitating its workability and pumpability. Addition of higher percentages above 15% up to 30% rubber did affect the viscosity to some extent; however the impact appeared to be reaching a plateau. The lack of significant changes from 15% to 30% can be attributed to the non-saturation of additional rubber particles to the extent that rubber polymer could not be released to affect the rheology of asphalt matrix. This was further evidenced when percentages of bio-binder increased to 50% at which point a significant decrease in the viscosity of the binder was observed; the percentage drop in viscosity compared to base asphalt was 47% at a test temperature of 120°C, 45.21% at a test temperature of 135°C, and 35.66% at test temperature of 150°C. Furthermore, it was found that the viscosity value of the BMR-20-50 was close to the control binder's viscosity at all test temperatures; indicating that at a specific ratio of crumb rubber/bio-binder (ex. 20/50), a bio-modified rubber with viscosity similar to that of control asphalt could be obtained. Considering that reduced viscosity is one of the main factors affecting the pumping and workability of asphalt, bio-modified rubber could be a promising material to address workability issues with conventional rubber asphalt. It should be noted that BMR is a newly-developed hybrid material with good high-temperature properties and enhanced workability and pumpability.

Accordingly, the BMR-20-30, and BMR-15-20, appeared to have improved rheological properties and enhanced pumpability. As such it is recommended that when using 15%CRM the minimum percentage of bio binder to ensure enhanced rheological properties and workability be 20%. For the case of 20%CRM the minimum percentage of bio binder should be 30%.

The outcome of this research was the development of a new paving material, bio-modified rubber (BMR), which uses additives made from two waste materials: swine manure and

scrap tires. Use of BMR will add value to the management of those two waste materials, providing social and environmental benefits: eliminating the need for manure disposal will reduce the environmental pollution caused by manure odors and spillage in manure storage lagoons, and adding a major use for recycled tire rubber will help alleviate the problems caused by tire stockpiles around the country.

Future Research

Additional testing is needed to investigate the interaction mechanisms of bio-binder, rubber, and asphalt. Furthermore, further study is recommend to examine applicability of bio-binder at concentrations above recommended saturation point to understand its effect of long term aging and possible rejuvenation of asphalt matrix.

References

- Abdelrahman, M. (2011). Monitoring the interaction of asphalt with crumb rubber modifier (CRM). *Engineering Research and Innovation Conference 2011: Atlanta, GA*.
- Akisetty, C. K., Lee, S.-J., & Amirkhanian, S. N. (2009). High temperature properties of rubberized binders containing warm asphalt additives. *Construction and Building Materials, 23*(1), 565-573. doi: <http://dx.doi.org/10.1016/j.conbuildmat.2007.10.010>
- ASTM D8. (2014). Standard Terminology Relating to Materials for Roads and Pavements American Society for Testing Materials: ASTM International Standards Worldwide Road and Paving Materials vehicle Pavement Systems.
- ASTM Standard D4402. (2013). Standard Test Method for Viscosity Determination of Asphalt at Elevated Temperatures Using a Rotational Viscometer. West Conshohocken, PA.
- ASTM Standard D7175-08. (2008). Standard Test Method for Determining the Rheological Properties of Asphalt Binder Using a Dynamic Shear Rheometer. West Conshohocken, PA: ASTM International.
- ASTM Standards D2872. (2012). Effect of Heat and Air on a Moving Film of Asphalt (Rolling Thin-Film Oven Test). West Conshohocken, PA.
- Barla, M. A., Eleazer, W. E., & Whittle, D. J. (1993). POTENTIAL TO USE WASTE TIRES AS SUPPLEMENTAL FUEL IN PULP AND PAPER MILL BOILERS, CEMENT KILNS AND IN ROAD PAVEMENT
- Barman, B. N., Cebolla, V. L., & Membrado, L. (2000). *Crit Rev Anal Chemistry 30*:75-120.
- Caltrans. (2003). *ASPHALT RUBBER USAGE GUIDE*. Sacramento, CA: State of California Department of Transportation.
- Carlson, D. D., & Zhu, H. (1999). Asphalt-Rubber An Anchor to Crumb Rubber Markets

- Claudy P.M., Martin D., & Planche J. P. (1998). The thermal behavior of asphalt cement. *Thermochimica Acta*, Vol.324(pp-203-213).
- Cong, P., Xun, P., Xing, M., & Chen, S. (2013). Investigation of asphalt binder containing various crumb rubbers and asphalts. *journal Construction and Building Materials*, 40 pp 632-641.
- Daryl, M., Susanna, H., Ryan, W., & Ludo, Z. (2007). Study of crumb rubber materials as paving asphalt modifiers. . *Can. J. Civil Eng*, 34:1276–1288.
- Dong, R., Li, J., & Wang, S. (2011). Laboratory Evaluation of Pre-Devulcanized Crumb Rubber-Modified Asphalt as a Binder in Hot-Mix Asphalt
- Encyclopaedia Britannica. (2014). Rubber. from <http://www.britannica.com/EBchecked/topic/511800/rubber>
- Estakhri, C. K., Fernando, E. G., Button, J. W., & Teetes, G. R. (1990). USE. AVAILABILITY AND COST-EFFECTIVENESS OF ASPHALT RUBBER IN TEXAS College Station, Texas Texas Transportation Institute, The Texas A&M University System.
- Fan, L.-t., & Shafie, S. R. (2013). USA Patent No. US 8,445,553 B2.
- Fini, E. H., W., K. E., Abolghasem, S., Mufeed, B., Zhanping, Y., Hasan, O., & Qazi, A. (2011). Chemical Characterization of Biobinder from Swine Manure: Sustainable Modifier for Asphalt Binder
- Ghavibazoo, A., Abdelrahman, M., & Ragab, M. (2013). Mechanism of Crumb Rubber Modifier Dissolution Into Asphalt Matrix and Its Effect on Final Physical Properties of Crumb Rubber-Modified Binder. *Journal of the Transportatio Research Board NO 2371*, pp. 92-101. doi: 10.3141/2370-12

- Golzin, Y., & Hamid Sabbagh, M. (2011). Improving the performance of Crumb Rubber bitumen by means of Poly Phosphoric Acid (PPA) and Vestenamer additives *Journal of Construction and Building Materials*, 2008 (22), 1368-1376.
- Hanson, D. I., & Foo, K. (1994). Evaluation and Characterization of a Rubber Modified Hot Mix Asphalt Pavement, National Center for Asphalt Technology
- Heitzman, M. A. (1992a). State of the Practice-Design and Construction of Asphalt Paving Materials with Crumb Rubber Modifier *Research Report No. FHWA-SA-92-022*. Washington, DC: Federal Highway Administration.
- Heitzman, M. A. (1992b). State of the Practice – Design and Construction of Asphalt Paving Materials With Crumb Rubber Modifier, Report FHWA A-SA-92-022. FHWA.
- Hicks, R. G., & Epps, J. A. Life cycle costs for asphalt-rubber paving materials.
- Isayev, A. I. (2005). Recycling of rubbers. In: Mark JE, Erman B, Eirich FR. *editors Science and technology of rubber. 3rd ed Elsevier Inc*, p. 663e701.
- Kandhal, P. S. (1992). WASTE MATERIALS INHOT MIX ASPHALT -AN OVERVIEW. In National Center for Asphalt Technology (Ed.). Auburn Alabama: Auburn University.
- Lee, S.-J., Akisetty, C. K., & Amirkhanian, S. N. (2008). The effect of crumb rubber modifier (CRM) on the performance properties of rubberized binders in HMA pavements. *Journal of Construction and Building Materials*, 2008 (22): pp.1368–1376.
- Li, Q., Ni, F., Gao, L., Yuan, Q., & Xia, Y. (2014). Evaluating the rutting resistance of asphalt mixtures using an advanced repeated load permanent deformation test under field conditions. *Construction and Building Materials*, 61, pp. 241-251.

- Liu, S., Cao, W., Fang, J., & Shang, S. (2009). Variance analysis and performance evaluation of different crumb rubber modified (CRM) asphalt. *Construction and Building Materials* 23 (2009) 2701–2708.
- National Asphalt Pavement Association. (2014). History of Asphalt. Retrieved June 10 2014, 2014, from <http://www.asphaltpavement.org>
- Nehdi, M., & Khan, A. (2001). Cementitious Composites Containing Recycled Tire Rubber: An Overview of Engineering Properties and Potential Applications. *Cement Concrete and Aggregates CCAGDP, Vol. 23 No. 1*, pp.3-10.
- Nejad, F. M., Aghajani, P., Modarres, A., & Firoozifar, H. (2012). Investigating the properties of crumb rubber modified bitumen using classic and SHRP testing methods. *Construction and Building Materials*, 26(1), 481-489. doi: 10.1016/j.conbuildmat.2011.06.048
- Panda, S. K., Jan T., A., & Wolfgang, S. (2007). Mass-spectrometric analysis of complex volatile and nonvolatile crude oil components: a challenge
- Pavement interactive. (2011). Dynamic Shear Rheometer. Retrieved May, 2014
<http://www.pavementinteractive.org/article/dynamic-shear-rheometer/>
- Rahman, M. M. (2004). *Characterisation of Dry Process Crumb Rubber Modified Asphalt Mixtures. Thesis submitted to the university of Nottingham for the degree of Doctor of philosophy, University of Nottingham, school of Civil Engineering.*
- Raouf, M. A., & Williams, R. C. (2010). Temperature and shear susceptibility of a nonpetroleum binder as a pavement material. (*Transp. Res. Res.*, 2180(1), 9-18).
- Rasmussen R., Lytton R., & Chang G. (2002). Method to Predict Temperature Susceptibility of an Asphalt Binder. *Journal of Materials in Civil Engineering*, 14(3), pp 246-252.

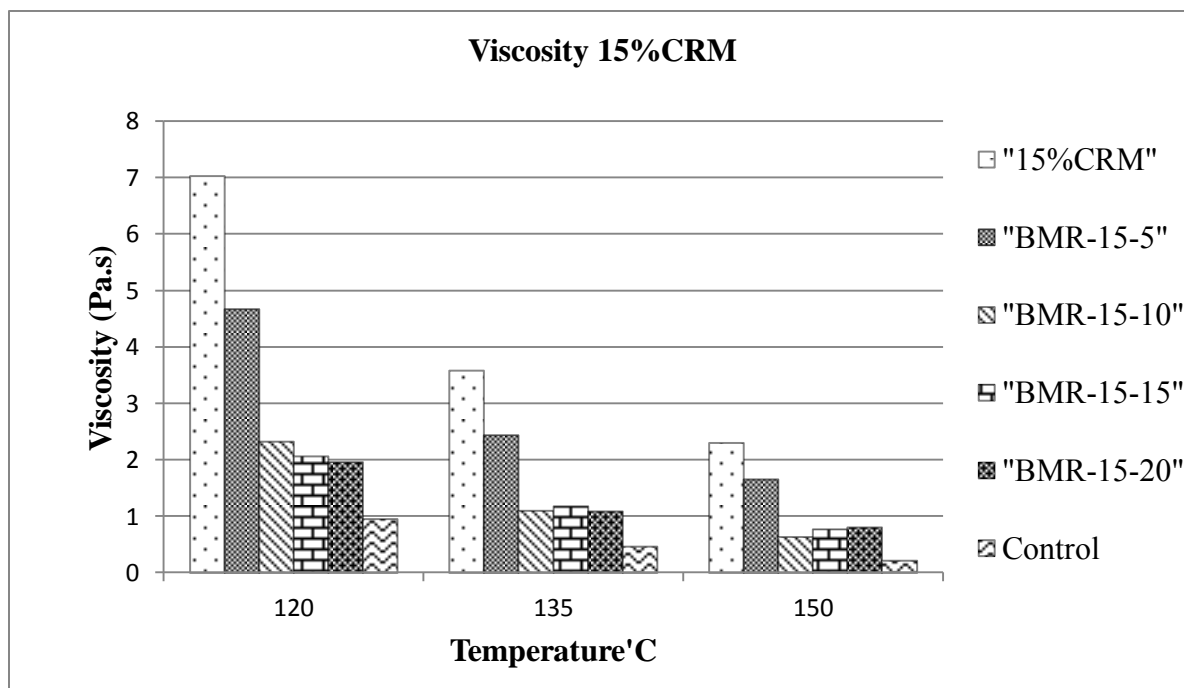
- Rasoulzadeha, Y., Mortazavib, S. B., Yousefi, A. A., & Khavanin, A. (2011). Decreasing polycyclic aromatic hydrocarbons emission from bitumen using alternative bitumen production process
- Reschner, K. (2006). Scrap Tire Recycling-A Summary of prevalent disposal and Recycling Methods. Berlin, 2006
- Roberts, F. L., Kandha, P. S., Brown, E. R., & Dunning, R. L. (1989). Investigation and evaluation of ground tire rubber in hot mix asphalt *NCAT Report No. 89-3*. Auburn, AL: National Center for Asphalt Technology of Auburn University.
- Roberts, F. L., Kandhal, P. S., Brown, E. R., Lee, D. Y., & Kennedy, T. W. (1996). Hot Mix Asphalt Materials, Mixture, Design, and Construction, in National Asphalt Pavement Association Research and Education Foundation: Lanham, Md
- Roberts, F. L., Kandhal, P. S., Brown, E. R., Lee, D. Y., Kennedy, T. W., & (2009). Hot mix asphalt materials, mixture design and construction Lanham, Md Napa Educational Foundation.
- Rubber Manufacturers Association. (2009). Scrap Tire Markets in the United States 9th Biennial Report, Report downloaded from http://www.rma.org/scrap_tires/ March 2014.
- Shatnawi, S. (2011a). Comparisons of Rubberized Asphalt Binders. Asphalt – Rubber and Terminal Blend. *Rubber Pavement Association*.
- Shatnawi, S. (2011b). White Paper on Comparisons of Rubberized Asphalt Binders Asphalt-Rubber and Terminal Blend
- Shulman, V. L. (2000). Tire Recycling After 2000:Status and Options. European Tire Recycling Association, Paris, France.

- Sienkiewicz, M., Kucinska-Lipka, J., Janik, H., & Balas, A. (2012). Progress in used tyres management in the European Union: A review.
- U.S. Department of Transportation Federal Highway Administration. (1994). Superpave Fundamentals Reference Manual Course #131053 NATIONAL HIGHWAY INSTITUTE.
- U.S. Department of Transportation Federal Highway Administration. (1995). *Crumb Rubber Modifier (CRM) in Asphalt Pavement - Summary Practices in Arizona, California and Florida*. (FHWA-SA-95-056). Corvallis, OR.
- U.S. Environmental Protection Agency. (2006). Scrap Tire Cleanup Guidebook. EPA-905-B-06-001.
- U.S. Environmental Protection Agency. (2012). *Pork production Ag 101*. Retrieved from <http://www.epa.gov/agriculture/ag101/printpork.html>.
- U.S. Environmental Protection Agency. (2013, 3/28/2013). Scrap tires. Retrieved June 9, 2014, from <http://www.epa.gov/wastes/conservation/materials/tires/>
- U.S. OIL & REFINING CO. PAVING GRADE ASPHALT, PG64-22. Retrieved April 2014, from <http://www.usor.com/>
- Unapumnuk, K. (2006). *A study of the pyrolysis of tire derived fuels and an analysis of derived chars and oils*. (PhD), University of Cincinnati, Cincinnati, OH.
- United States Department of Transportation. Federal Highway Administration. (1997). *User Guidelines for Waste and Byproduct Materials in Pavement Construction*. Washington, DC: Retrieved from <http://www.fhwa.dot.gov/publications/research/infrastructure/structures/97148/st2.cfm>.

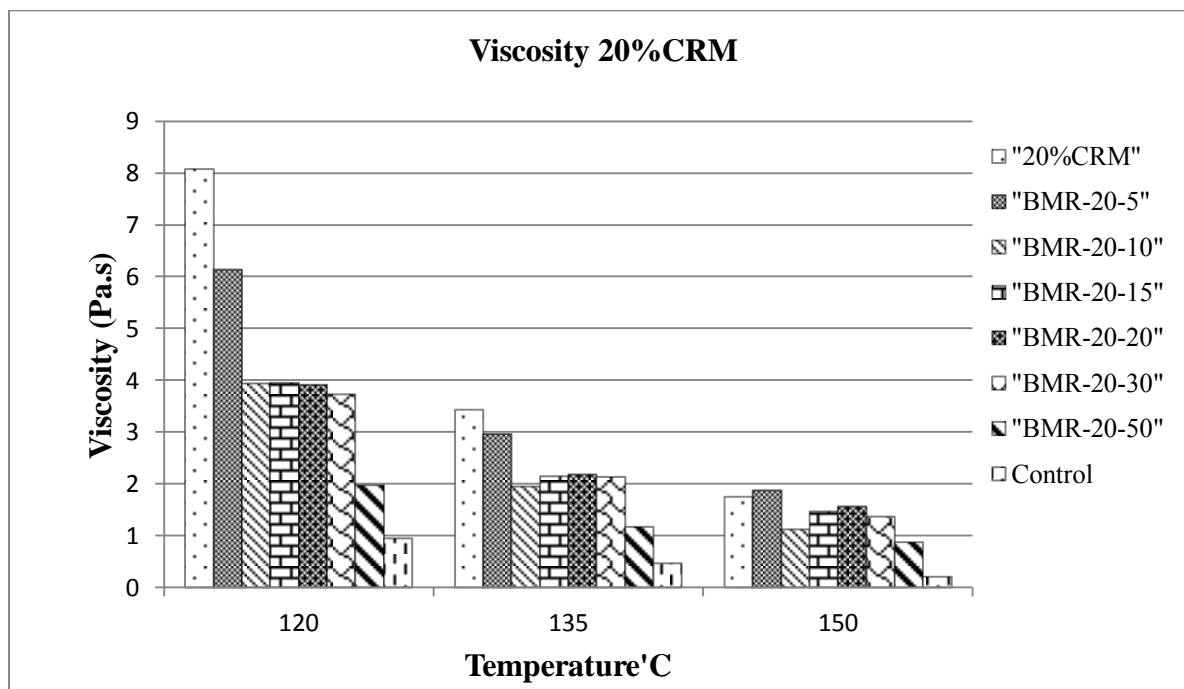
Wang, H., Dang, Z., You, Z., & Cao, D. (2012). Effect of warm mixture asphalt (WMA) additives on high failure temperature properties for crumb rubber modified (CRM) binders. *Construction and Building Materials*, 35, 281-288. doi: 10.1016/j.conbuildmat.2012.04.004

Way, G. B., Kaloush, K. E., & Biligiri, K. P. (2011). *Asphalt-Rubber Standard Practice Guide* (First Edition ed.). Tempe, AZ.

Appendix



Viscosity vs temperature for control, 15% CRM, with Bio-binder at 20 rpm



Viscosity vs temperature for control, 20% CRM, with Bio-binder at 20 rpm

DSR result PG64-22

Temperature[1]
: 40
Temp Run[1] :
Last Data Point
: 7
Start Test Time
: 536.9857

Header[1]	:	Time	Temperature	Frequency	Phase Angle	Complex Modulus
Header[2]	:	(s)	(°C)	(Hz)	(°)	(Pa)
Data Pt[1]	:	630	40.07	1.59E-03	89.59	6.51E+01
Data Pt[2]	:	695.642	40	1.57E-02	87.47	6.38E+02
Data Pt[3]	:	756.497	40	1.70E-02	87.16	6.91E+02
Data Pt[4]	:	765.028	40	1.56E-01	84.17	5.75E+03
Data Pt[5]	:	773.121	40	1.69E-01	83.26	6.13E+03
Data Pt[6]	:	776.462	40	8.19E-01	86	2.64E+04
Data Pt[7]	:	779.824	40.01	1.67E+00	79.31	4.69E+04
Data Pt[8]	:	783.01	40.01	3.98E+00	75.99	1.03E+05

Test Run[1] :
Temperature[2]
: 46
Temp Run[1] :
Last Data Point
: 7
Start Test Time
: 1676.507

Header[1]	:	Time	Temperature	Frequency	Phase Angle	Complex Modulus
Header[2]	:	(s)	(°C)	(Hz)	(°)	(Pa)
Data Pt[1]	:	629.999	45.93	1.59E-03	89.54	2.21E+01
Data Pt[2]	:	695.638	46	1.57E-02	88.71	2.16E+02
Data Pt[3]	:	756.421	46	1.70E-02	88.57	2.33E+02
Data Pt[4]	:	764.972	46	1.56E-01	85.52	2.00E+03
Data Pt[5]	:	773.052	46	1.69E-01	85.14	2.16E+03
Data Pt[6]	:	776.406	46	8.19E-01	83.51	9.24E+03
Data Pt[7]	:	779.778	46	1.67E+00	80.96	1.83E+04
Data Pt[8]	:	782.971	46	3.98E+00	79.4	3.94E+04

Test Run[1] :
 Temperature[3]
 : 52
 Temp Run[1] :
 Last Data Point
 : 7
 Start Test Time
 : 2831.222

Header[1]	:	Time	Temperature	Frequency	Phase	Complex
Header[2]	:	(s)	(°C)	(Hz)	Angle	Modulus
					(°)	(Pa)
Data Pt[1]	:	629.998	51.93	1.59E-03	89.65	7.92E+00
Data Pt[2]	:	695.636	52	1.57E-02	89.37	7.76E+01
Data Pt[3]	:	756.423	52.01	1.70E-02	89.3	8.40E+01
Data Pt[4]	:	764.984	52	1.56E-01	87.42	7.56E+02
Data Pt[5]	:	773.063	52	1.69E-01	87.22	8.13E+02
Data Pt[6]	:	776.421	52	8.19E-01	85.22	3.72E+03
Data Pt[7]	:	779.796	52	1.67E+00	83.51	7.28E+03
Data Pt[8]	:	782.991	52.01	3.98E+00	82.03	1.62E+04

Test Run[1] :
 Temperature[4]
 : 58
 Temp Run[1] :
 Last Data Point
 : 7
 Start Test Time
 : 3979.744

Header[1]	:	Time	Temperature	Frequency	Phase	Complex
Header[2]	:	(s)	(°C)	(Hz)	Angle	Modulus
					(°)	(Pa)
Data Pt[1]	:	629.996	57.92	1.59E-03	86.47	3.23E+00
Data Pt[2]	:	695.711	58	1.57E-02	89.4	3.03E+01
Data Pt[3]	:	756.493	58	1.70E-02	89.37	3.27E+01
Data Pt[4]	:	765.067	58	1.56E-01	88.41	2.99E+02
Data Pt[5]	:	773.138	58	1.69E-01	88.36	3.23E+02
Data Pt[6]	:	776.492	58	8.19E-01	86.23	1.52E+03
Data Pt[7]	:	779.877	58	1.67E+00	85.64	2.99E+03
Data Pt[8]	:	783.057	58.01	3.98E+00	84.14	6.82E+03

Test Run[1] :
 Temperature[5]
 : 64
 Temp Run[1] :
 Last Data Point
 : 7
 Start Test Time
 : 5146.665

Header[1]	:	Time	Temperature	Frequency	Phase	Complex
Header[2]	:	(s)	(°C)	(Hz)	Angle	Modulus
					(°)	(Pa)
Data Pt[1]	:	629.996	63.92	1.59E-03	82.73	1.34E+00
Data Pt[2]	:	695.711	64	1.57E-02	88.48	1.31E+01
Data Pt[3]	:	756.494	64	1.70E-02	87.8	1.44E+01
Data Pt[4]	:	765.056	64	1.56E-01	88.73	1.29E+02
Data Pt[5]	:	773.148	64	1.69E-01	88.78	1.39E+02
Data Pt[6]	:	776.484	64	8.19E-01	87.67	6.66E+02
Data Pt[7]	:	779.845	64	1.67E+00	86.87	1.34E+03
Data Pt[8]	:	782.996	63.99	3.98E+00	85.7	3.09E+03

Test Run[1] :
 Temperature[6]
 : 70
 Temp Run[1] :
 Last Data Point
 : 7
 Start Test Time
 : 6303.384

Header[1]	:	Time	Temperature	Frequency	Phase	Complex
Header[2]	:	(s)	(°C)	(Hz)	Angle	Modulus
					(°)	(Pa)
Data Pt[1]	:	629.998	69.93	1.59E-03	60.73	6.91E-01
Data Pt[2]	:	695.708	70	1.57E-02	87.3	6.12E+00
Data Pt[3]	:	756.495	70.01	1.70E-02	89.04	6.68E+00
Data Pt[4]	:	765.068	69.99	1.56E-01	88.45	6.04E+01
Data Pt[5]	:	773.137	70.01	1.69E-01	88.34	6.50E+01
Data Pt[6]	:	776.494	70.01	8.19E-01	88.33	3.10E+02
Data Pt[7]	:	779.875	70	1.67E+00	87.82	6.27E+02
Data Pt[8]	:	783.06	70	3.98E+00	86.94	1.46E+03

Test Run[1] :
 Temperature[7]
 : 76
 Temp Run[1] :
 Last Data Point
 : 7
 Start Test Time
 : 7476.503

Header[1]	:	Time	Temperature	Frequency	Phase Angle	Complex Modulus
Header[2]	:	(s)	(°C)	(Hz)	(°)	(Pa)
Data Pt[1]	:	629.997	75.94	1.59E-03	62.43	6.92E-01
Data Pt[2]	:	695.636	76.01	1.57E-02	82.51	3.39E+00
Data Pt[3]	:	756.423	76	1.70E-02	86.5	4.02E+00
Data Pt[4]	:	764.983	76.01	1.56E-01	86.95	3.12E+01
Data Pt[5]	:	773.074	76	1.69E-01	86.74	3.31E+01
Data Pt[6]	:	776.42	75.99	8.19E-01	87.85	1.57E+02
Data Pt[7]	:	779.786	75.99	1.67E+00	87.94	3.16E+02
Data Pt[8]	:	782.981	75.99	3.98E+00	87.52	7.43E+02

DSR result 15%CRM

Test Run[1] :
 Temperature[1]
 : 40
 Temp Run[1] :
 Last Data Point
 : 7
 Start Test Time 858.318
 : 7

Header[1]	:	Time	Temperature	Frequency	Phase Angle	Complex Modulus
Header[2]	:	(s)	(°C)	(Hz)	(°)	(Pa)
Data Pt[1]	:	630.001	39.94	1.59E-03	80.19	6.14E+02
Data Pt[2]	:	695.716	40.02	1.57E-02	76.91	4.45E+03

Data Pt[3]	:	756.5	40	1.70E-02	75.85	4.91E+03
Data Pt[4]	:	765.083	40	1.56E-01	62.43	3.08E+04
Data Pt[5]	:	773.15	40	1.69E-01	64.19	2.57E+04
Data Pt[6]	:	776.521	40.02	8.19E-01	61.97	9.11E+04
Data Pt[7]	:	779.887	40	1.67E+00	58.32	1.50E+05
Data Pt[8]	:	783.06	39.98	3.98E+00	55.67	2.60E+05

Test Run[1] :
 Temperature[2] :
 : 46
 Temp Run[1] :
 Last Data Point :
 : 7
 Start Test Time 1997.43
 : 9

Header[1]	:	Time	Temperature	Frequency	Phase Angle	Complex Modulus
Header[2]	:	(s)	(°C)	(Hz)	(°)	(Pa)
Data Pt[1]	:	629.998	45.92	1.59E-03	81.52	2.11E+02
Data Pt[2]	:	695.708	46	1.57E-02	79.26	1.57E+03
Data Pt[3]	:	756.493	46	1.70E-02	78.58	1.71E+03
Data Pt[4]	:	765.069	46	1.56E-01	76.62	1.11E+04
Data Pt[5]	:	773.135	46	1.69E-01	73.8	1.26E+04
Data Pt[6]	:	776.499	46	8.19E-01	72.04	3.66E+04
Data Pt[7]	:	779.874	46	1.67E+00	61.56	7.00E+04
Data Pt[8]	:	783.064	46	3.98E+00	60.05	1.25E+05

Test Run[1] :
 Temperature[3] :
 : 52
 Temp Run[1] :
 Last Data Point :
 : 7
 Start Test Time 3157.75
 : 6

Header[1]	:	Time	Temperature	Frequency	Phase Angle	Complex Modulus
Header[2]	:	(s)	(°C)	(Hz)	(°)	(Pa)
Data Pt[1]	:	629.996	51.94	1.59E-03	82.04	7.61E+01
Data Pt[2]	:	695.64	51.98	1.57E-02	80.79	5.85E+02

Data Pt[3]	:	756.493	52	1.70E-02	80.28	6.34E+02
Data Pt[4]	:	765.043	52.01	1.56E-01	77.27	4.52E+03
Data Pt[5]	:	773.112	52	1.69E-01	76.68	4.78E+03
Data Pt[6]	:	776.47	52	8.19E-01	79.84	2.35E+04
Data Pt[7]	:	779.835	51.99	1.67E+00	67.64	3.11E+04
Data Pt[8]	:	783.039	52	3.98E+00	64.81	5.96E+04

Test Run[1] :
 Temperature[4]
 : 58
 Temp Run[1] :
 Last Data Point
 : 7
 Start Test Time 4300.67
 : 6

Header[1]	:	Time	Temperature	Frequency	Phase Angle	Complex Modulus
Header[2]	:	(s)	(°C)	(Hz)	(°)	(Pa)
Data Pt[1]	:	629.996	57.92	1.59E-03	82.34	3.04E+01
Data Pt[2]	:	695.636	58	1.57E-02	81.75	2.30E+02
Data Pt[3]	:	756.492	58	1.70E-02	81.56	2.48E+02
Data Pt[4]	:	765.03	58	1.56E-01	79.31	1.78E+03
Data Pt[5]	:	773.098	58	1.69E-01	78.93	1.92E+03
Data Pt[6]	:	776.473	58	8.19E-01	78.71	7.26E+03
Data Pt[7]	:	779.844	58	1.67E+00	80.25	1.29E+04
Data Pt[8]	:	783.028	58	3.98E+00	69.47	2.76E+04

Test Run[1] :
 Temperature[5]
 : 64
 Temp Run[1] :
 Last Data Point
 : 7
 Start Test Time 5474.99
 : 7

Header[1]	:	Time	Temperature	Frequency	Phase Angle	Complex Modulus
Header[2]	:	(s)	(°C)	(Hz)	(°)	(Pa)
Data Pt[1]	:	629.996	63.93	1.59E-03	76.07	1.41E+01
Data Pt[2]	:	695.711	64	1.57E-02	81.52	9.68E+01

Data Pt[3]	:	756.492	63.99	1.70E-02	81.41	1.06E+02
Data Pt[4]	:	765.069	64	1.56E-01	80.58	7.72E+02
Data Pt[5]	:	773.136	64	1.69E-01	80.16	8.23E+02
Data Pt[6]	:	776.5	63.99	8.19E-01	79.45	3.44E+03
Data Pt[7]	:	779.855	64	1.67E+00	77.02	6.35E+03
Data Pt[8]	:	783.042	63.99	3.98E+00	73.94	1.33E+04

Test Run[1] :
 Temperature[6]
 : 70
 Temp Run[1] :
 Last Data Point
 : 7
 Start Test Time 6628.71
 : 6

Header[1]	:	Time	Temperature	Frequency	Phase Angle	Complex Modulus
Header[2]	:	(s)	(°C)	(Hz)	(°)	(Pa)
Data Pt[1]	:	629.998	69.92	1.59E-03	79.78	8.06E+00
Data Pt[2]	:	695.711	70.01	1.57E-02	77.38	4.60E+01
Data Pt[3]	:	756.494	70.01	1.70E-02	78.6	4.95E+01
Data Pt[4]	:	765.082	69.99	1.56E-01	80.84	3.58E+02
Data Pt[5]	:	773.151	70	1.69E-01	80.57	3.83E+02
Data Pt[6]	:	776.505	70.01	8.19E-01	79.28	1.59E+03
Data Pt[7]	:	779.861	70	1.67E+00	79.44	3.02E+03
Data Pt[8]	:	783.059	70	3.98E+00	77.37	6.53E+03

Test Run[1] :
 Temperature[7]
 : 76
 Temp Run[1] :
 Last Data Point
 : 7
 Start Test Time 7804.03
 : 4

Header[1]	:	Time	Temperature	Frequency	Phase Angle	Complex Modulus
Header[2]	:	(s)	(°C)	(Hz)	(°)	(Pa)
Data Pt[1]	:	630.004	75.94	1.59E-03	60.9	7.82E+00
Data Pt[2]	:	695.642	76	1.57E-02	82.72	2.54E+01

Data Pt[3]	:	756.499	76.01	1.70E-02	75.13	2.67E+01
Data Pt[4]	:	765.049	75.97	1.56E-01	79.94	1.80E+02
Data Pt[5]	:	773.119	75.99	1.69E-01	79.93	1.91E+02
Data Pt[6]	:	776.486	76.01	8.19E-01	80.85	7.79E+02
Data Pt[7]	:	779.843	76	1.67E+00	80.84	1.51E+03
Data Pt[8]	:	783.03	76	3.98E+00	79.65	3.32E+03

DSR result BMR-15-5

Test Run[1] :
 Temperature[1]
 : 40
 Temp Run[1] :
 Last Data Point
 : 7
 Start Test Time
 : 861.7344

Header[1]	:	Time	Temperature	Frequency	Phase Angle	Complex Modulus
Header[2]	:	(s)	(°C)	(Hz)	(°)	(Pa)
Data Pt[1]	:	630.004	39.99	1.59E-03	81.71	4.50E+02
Data Pt[2]	:	695.715	40	1.57E-02	79.36	3.46E+03
Data Pt[3]	:	756.569	40.02	1.70E-02	78.54	3.80E+03
Data Pt[4]	:	765.182	40	1.56E-01	67.71	2.39E+04
Data Pt[5]	:	773.258	40.01	1.69E-01	66.41	1.85E+04
Data Pt[6]	:	776.685	40	8.19E-01	65.81	7.58E+04
Data Pt[7]	:	780.027	40.01	1.67E+00	59.83	1.30E+05
Data Pt[8]	:	783.242	40.01	3.98E+00	56.94	2.28E+05

Test Run[1] :
 Temperature[2]
 : 46
 Temp Run[1] :
 Last Data Point
 : 7

Start Test Time
: 2003.654

Header[1]	:	Time	Temperature	Frequency	Phase Angle	Complex Modulus
Header[2]	:	(s)	(°C)	(Hz)	(°)	(Pa)
Data Pt[1]	:	629.997	45.93	1.59E-03	82.23	1.49E+02
Data Pt[2]	:	695.71	46	1.57E-02	81.84	1.19E+03
Data Pt[3]	:	756.566	46	1.70E-02	81.33	1.30E+03
Data Pt[4]	:	765.185	45.99	1.56E-01	79.24	9.20E+03
Data Pt[5]	:	773.313	46	1.69E-01	75.1	1.02E+04
Data Pt[6]	:	776.74	46.01	8.19E-01	83.67	4.28E+04
Data Pt[7]	:	780.081	46.01	1.67E+00	64.34	5.95E+04
Data Pt[8]	:	783.278	46	3.98E+00	61.69	1.09E+05

Test Run[1] :
Temperature[3]
: 52
Temp Run[1] :
Last Data Point
: 7
Start Test Time
: 3765.333

Header[1]	:	Time	Temperature	Frequency	Phase Angle	Complex Modulus
Header[2]	:	(s)	(°C)	(Hz)	(°)	(Pa)
Data Pt[1]	:	630.003	52.07	1.59E-03	81.32	5.45E+01
Data Pt[2]	:	695.715	51.99	1.57E-02	81.8	4.36E+02
Data Pt[3]	:	756.57	51.99	1.70E-02	81.63	4.70E+02
Data Pt[4]	:	765.148	52	1.56E-01	78.97	3.48E+03
Data Pt[5]	:	773.227	52.01	1.69E-01	79.28	3.76E+03
Data Pt[6]	:	776.644	51.99	8.19E-01	68.77	1.64E+04
Data Pt[7]	:	779.999	51.99	1.67E+00	69.5	2.68E+04
Data Pt[8]	:	783.198	52.01	3.98E+00	66.45	4.97E+04

Test Run[1] :
Temperature[4]
: 58
Temp Run[1] :
Last Data Point
: 7

Start Test Time
: 4920.446

Header[1]	:	Time	Temperature	Frequency	Phase Angle	Complex Modulus
Header[2]	:	(s)	(°C)	(Hz)	(°)	(Pa)
Data Pt[1]	:	629.999	57.92	1.59E-03	74.54	2.51E+01
Data Pt[2]	:	695.71	58.01	1.57E-02	80.05	1.78E+02
Data Pt[3]	:	756.563	58	1.70E-02	80.37	1.90E+02
Data Pt[4]	:	765.127	58	1.56E-01	81.5	1.40E+03
Data Pt[5]	:	773.209	58	1.69E-01	81.1	1.51E+03
Data Pt[6]	:	776.632	58.01	8.19E-01	82.46	6.00E+03
Data Pt[7]	:	779.981	57.99	1.67E+00	81.73	1.05E+04
Data Pt[8]	:	783.181	58	3.98E+00	71.6	2.35E+04

Test Run[1] :
Temperature[5]
: 64
Temp Run[1] :
Last Data Point
: 7
Start Test Time
: 6091.169

Header[1]	:	Time	Temperature	Frequency	Phase Angle	Complex Modulus
Header[2]	:	(s)	(°C)	(Hz)	(°)	(Pa)
Data Pt[1]	:	629.997	63.93	1.59E-03	69.45	1.31E+01
Data Pt[2]	:	695.709	63.99	1.57E-02	77.01	8.25E+01
Data Pt[3]	:	756.565	63.99	1.70E-02	76.26	8.79E+01
Data Pt[4]	:	765.129	63.99	1.56E-01	81.55	6.24E+02
Data Pt[5]	:	773.206	64.01	1.69E-01	81.74	6.59E+02
Data Pt[6]	:	776.582	64.01	8.19E-01	80.33	2.89E+03
Data Pt[7]	:	779.979	64.01	1.67E+00	79.14	5.33E+03
Data Pt[8]	:	783.178	64	3.98E+00	76.02	1.13E+04

Test Run[1] :
Temperature[6]
: 70
Temp Run[1] :
Last Data Point
: 7

Start Test Time
: 7249.688

Header[1]	:	Time	Temperature	Frequency	Phase	Complex
Header[2]	:	(s)	(°C)	(Hz)	Angle	Modulus
	:				(°)	(Pa)
Data Pt[1]	:	629.999	69.92	1.59E-03	61.41	8.05E+00
Data Pt[2]	:	695.708	69.99	1.57E-02	71.01	4.49E+01
Data Pt[3]	:	756.566	70.01	1.70E-02	71.3	4.77E+01
Data Pt[4]	:	765.161	70.01	1.56E-01	80.18	3.02E+02
Data Pt[5]	:	773.23	70	1.69E-01	80.28	3.18E+02
Data Pt[6]	:	776.654	70.01	8.19E-01	81.51	1.32E+03
Data Pt[7]	:	779.999	69.99	1.67E+00	81.12	2.58E+03
Data Pt[8]	:	783.192	69.99	3.98E+00	79.07	5.69E+03

Test Run[1] :
Temperature[7]
: 76
Temp Run[1] :
Last Data Point
: 7
Start Test Time
: 8430.405

Header[1]	:	Time	Temperature	Frequency	Phase	Complex
Header[2]	:	(s)	(°C)	(Hz)	Angle	Modulus
	:				(°)	(Pa)
Data Pt[1]	:	629.996	75.93	1.59E-03	75.11	5.83E+00
Data Pt[2]	:	695.709	76.02	1.57E-02	65.7	2.57E+01
Data Pt[3]	:	756.565	75.98	1.70E-02	65.89	2.76E+01
Data Pt[4]	:	765.162	75.99	1.56E-01	77.2	1.60E+02
Data Pt[5]	:	773.228	76.01	1.69E-01	78.02	1.68E+02
Data Pt[6]	:	776.608	76	8.19E-01	81.87	7.05E+02
Data Pt[7]	:	780.01	76.01	1.67E+00	81.93	1.33E+03
Data Pt[8]	:	783.218	75.99	3.98E+00	81.03	2.94E+03

DSR result BMR-15-10

Test Run[1] :
 Temperature[1]
 : 40
 Temp Run[1] :
 Last Data Point
 : 7
 Start Test Time
 : 1349.379

Header[1]	:	Time	Temperature	Frequency	Phase	Complex
Header[2]	:	(s)	(°C)	(Hz)	(°)	(Pa)
Data Pt[1]	:	630.003	40.07	1.59E-03	77.37	1.72E+02
Data Pt[2]	:	695.643	39.99	1.57E-02	81.11	1.24E+03
Data Pt[3]	:	756.426	40.01	1.70E-02	80.98	1.34E+03
Data Pt[4]	:	764.992	40	1.56E-01	80.46	9.33E+03
Data Pt[5]	:	773.071	40	1.69E-01	77.51	1.02E+04
Data Pt[6]	:	776.429	40	8.19E-01	85.37	4.26E+04
Data Pt[7]	:	779.796	40	1.67E+00	66.67	6.32E+04
Data Pt[8]	:	782.985	39.99	3.98E+00	63.95	1.18E+05

Test Run[1] :
 Temperature[2]
 : 46
 Temp Run[1] :
 Last Data Point
 : 7
 Start Test Time
 : 2490.897

Header[1]	:	Time	Temperature	Frequency	Phase	Complex
Header[2]	:	(s)	(°C)	(Hz)	(°)	(Pa)
Data Pt[1]	:	629.997	45.93	1.59E-03	67.72	7.32E+01
Data Pt[2]	:	695.71	46	1.57E-02	80.19	4.43E+02
Data Pt[3]	:	756.493	46	1.70E-02	80.56	4.76E+02
Data Pt[4]	:	765.082	46	1.56E-01	80.64	3.58E+03
Data Pt[5]	:	773.15	46	1.69E-01	81	3.85E+03
Data Pt[6]	:	776.5	46	8.19E-01	75.43	1.93E+04
Data Pt[7]	:	779.862	46	1.67E+00	72.06	2.81E+04

Data Pt[8] : 783.014 46 3.98E+00 69.27 5.53E+04

Test Run[1] :
 Temperature[3] : 52
 Temp Run[1] :
 Last Data Point : 7
 Start Test Time : 3661.417

Header[1]	:	Time	Temperature	Frequency	Phase Angle	Complex Modulus
Header[2]	:	(s)	(°C)	(Hz)	(°)	(Pa)
Data Pt[1]	:	629.998	51.93	1.59E-03	62.25	4.14E+01
Data Pt[2]	:	695.639	52.01	1.57E-02	74.33	1.98E+02
Data Pt[3]	:	756.493	52	1.70E-02	75.46	2.07E+02
Data Pt[4]	:	765.032	52.01	1.56E-01	82.21	1.47E+03
Data Pt[5]	:	773.11	52	1.69E-01	82.06	1.58E+03
Data Pt[6]	:	776.465	52.01	8.19E-01	82.88	6.36E+03
Data Pt[7]	:	779.827	52	1.67E+00	83.53	1.13E+04
Data Pt[8]	:	783.033	52	3.98E+00	73.59	2.52E+04

Test Run[1] :
 Temperature[4] : 58
 Temp Run[1] :
 Last Data Point : 7
 Start Test Time : 4811.536

Header[1]	:	Time	Temperature	Frequency	Phase Angle	Complex Modulus
Header[2]	:	(s)	(°C)	(Hz)	(°)	(Pa)
Data Pt[1]	:	629.998	57.94	1.59E-03	59.6	2.60E+01
Data Pt[2]	:	695.711	58	1.57E-02	68.48	1.07E+02
Data Pt[3]	:	756.495	58	1.70E-02	69.66	1.09E+02
Data Pt[4]	:	765.077	58	1.56E-01	80.77	6.85E+02
Data Pt[5]	:	773.157	58.01	1.69E-01	81.21	7.24E+02
Data Pt[6]	:	776.509	58	8.19E-01	81.51	3.10E+03
Data Pt[7]	:	779.867	58.01	1.67E+00	80.08	5.89E+03

Data Pt[8] : 783.007 58.01 3.98E+00 77.29 1.23E+04

Test Run[1] :

Temperature[5]

: 64

Temp Run[1] :

Last Data Point

: 7

Start Test Time

: 5975.656

Header[1]	:	Time	Temperature	Frequency	Phase Angle	Complex Modulus
Header[2]	:	(s)	(°C)	(Hz)	(°)	(Pa)
Data Pt[1]	:	629.997	63.92	1.59E-03	70.49	1.72E+01
Data Pt[2]	:	695.708	64.02	1.57E-02	63.15	6.11E+01
Data Pt[3]	:	756.495	64	1.70E-02	63.13	6.30E+01
Data Pt[4]	:	765.056	64	1.56E-01	78.07	3.42E+02
Data Pt[5]	:	773.124	64	1.69E-01	78.86	3.64E+02
Data Pt[6]	:	776.48	63.99	8.19E-01	81.94	1.41E+03
Data Pt[7]	:	779.861	63.99	1.67E+00	81.59	2.83E+03
Data Pt[8]	:	783.044	63.99	3.98E+00	79.89	6.17E+03

Test Run[1] :

Temperature[6]

: 70

Temp Run[1] :

Last Data Point

: 7

Start Test Time

: 7129.376

Header[1]	:	Time	Temperature	Frequency	Phase Angle	Complex Modulus
Header[2]	:	(s)	(°C)	(Hz)	(°)	(Pa)
Data Pt[1]	:	630.004	69.93	1.59E-03	54.47	1.35E+01
Data Pt[2]	:	695.715	70	1.57E-02	56.38	4.16E+01
Data Pt[3]	:	756.497	69.99	1.70E-02	55.78	4.20E+01
Data Pt[4]	:	765.062	69.99	1.56E-01	73.33	1.88E+02
Data Pt[5]	:	773.143	69.98	1.69E-01	75.38	2.00E+02
Data Pt[6]	:	776.495	70	8.19E-01	81.77	7.22E+02
Data Pt[7]	:	779.868	70	1.67E+00	81.91	1.44E+03

Data Pt[8] : 783.06 70.01 3.98E+00 81.63 3.23E+03

Test Run[1] :

Temperature[7]

: 76

Temp Run[1] :

Last Data Point

: 7

Start Test Time

: 8312.689

Header[1] :	Time	Temperature	Frequency	Phase	Complex
Header[2] :	(s)	(°C)	(Hz)	Angle	Modulus
				(°)	(Pa)
Data Pt[1] :	629.997	75.94	1.59E-03	50.83	1.07E+01
Data Pt[2] :	695.636	76.01	1.57E-02	51.72	2.71E+01
Data Pt[3] :	756.424	76	1.70E-02	52.48	2.99E+01
Data Pt[4] :	764.972	75.99	1.56E-01	69.67	1.12E+02
Data Pt[5] :	773.053	76	1.69E-01	70.29	1.14E+02
Data Pt[6] :	776.411	76	8.19E-01	79.51	4.21E+02
Data Pt[7] :	779.769	76.01	1.67E+00	81.69	8.06E+02
Data Pt[8] :	782.981	76	3.98E+00	81.93	1.71E+03

DSR test result BMR-15-15

Test Run[1] :

Temperature[1]

: 40

Temp Run[1] :

Last Data Point

: 7

Start Test Time

: 1462.654

Header[1] :	Time	Temperature	Frequency	Phase	Complex
Header[2] :	(s)	(°C)	(Hz)	Angle	Modulus
				(°)	(Pa)

Data Pt[1]	:	630.004	40.07	1.59E-03	76.13	3.46E+02
Data Pt[2]	:	695.642	39.99	1.57E-02	81.63	8.09E+02
Data Pt[3]	:	756.429	40	1.70E-02	81.29	8.83E+02
Data Pt[4]	:	764.955	40	1.56E-01	80.93	6.58E+03
Data Pt[5]	:	773.032	40.01	1.69E-01	78.78	6.98E+03
Data Pt[6]	:	776.388	39.99	8.19E-01	36.69	2.13E+04
Data Pt[7]	:	779.763	40	1.67E+00	69.98	4.70E+04
Data Pt[8]	:	782.94	40	3.98E+00	66.36	9.11E+04

Test Run[1] :
 Temperature[2]
 : 46
 Temp Run[1] :
 Last Data Point
 : 7
 Start Test Time
 : 2603.776

Header[1]	:	Time	Temperature	Frequency	Phase Angle	Complex Modulus
Header[2]	:	(s)	(°C)	(Hz)	(°)	(Pa)
Data Pt[1]	:	630.003	45.93	1.59E-03	64.25	5.79E+01
Data Pt[2]	:	695.716	46	1.57E-02	77.03	3.36E+02
Data Pt[3]	:	756.5	46	1.70E-02	77.19	3.60E+02
Data Pt[4]	:	765.062	46	1.56E-01	80.77	2.60E+03
Data Pt[5]	:	773.133	46.01	1.69E-01	80.69	2.77E+03
Data Pt[6]	:	776.492	46	8.19E-01	77.81	1.10E+04
Data Pt[7]	:	779.847	46.01	1.67E+00	74.12	2.12E+04
Data Pt[8]	:	782.997	46	3.98E+00	70.77	4.16E+04

Test Run[1] :
 Temperature[3]
 : 52
 Temp Run[1] :
 Last Data Point
 : 7
 Start Test Time
 : 3765.098

Header[1]	:	Time	Temperature	Frequency	Phase Angle	Complex Modulus
Header[2]	:	(s)	(°C)	(Hz)	(°)	(Pa)

Data Pt[1]	:	629.998	51.9	1.59E-03	61.88	3.62E+01
Data Pt[2]	:	695.637	52	1.57E-02	69.41	1.70E+02
Data Pt[3]	:	756.423	52.02	1.70E-02	70.42	1.81E+02
Data Pt[4]	:	764.974	52.01	1.56E-01	79.58	1.16E+03
Data Pt[5]	:	773.03	52	1.69E-01	79.38	1.21E+03
Data Pt[6]	:	776.406	52.01	8.19E-01	83.15	4.82E+03
Data Pt[7]	:	779.765	52	1.67E+00	78.45	9.43E+03
Data Pt[8]	:	782.893	52	3.98E+00	74.53	1.98E+04

Test Run[1] :
 Temperature[4]
 : 58
 Temp Run[1] :
 Last Data Point
 : 7
 Start Test Time
 : 4916.014

Header[1]	:	Time	Temperature	Frequency	Phase Angle	Complex Modulus
Header[2]	:	(s)	(°C)	(Hz)	(°)	(Pa)
Data Pt[1]	:	629.997	57.93	1.59E-03	56.52	2.48E+01
Data Pt[2]	:	695.638	58	1.57E-02	64.25	1.00E+02
Data Pt[3]	:	756.421	58	1.70E-02	65.26	1.04E+02
Data Pt[4]	:	764.974	58.01	1.56E-01	76.75	5.72E+02
Data Pt[5]	:	773.039	58	1.69E-01	77.13	6.15E+02
Data Pt[6]	:	776.401	58	8.19E-01	79.12	2.42E+03
Data Pt[7]	:	779.769	58	1.67E+00	79.94	4.63E+03
Data Pt[8]	:	782.958	58	3.98E+00	77.8	1.00E+04

Test Run[1] :
 Temperature[5]
 : 64
 Temp Run[1] :
 Last Data Point
 : 7
 Start Test Time
 : 6091.135

Header[1]	:	Time	Temperature	Frequency	Phase Angle	Complex Modulus
Header[2]	:	(s)	(°C)	(Hz)	(°)	(Pa)

Data Pt[1]	:	629.996	63.93	1.59E-03	55.21	1.44E+01
Data Pt[2]	:	695.64	63.99	1.57E-02	61.15	5.25E+01
Data Pt[3]	:	756.423	64	1.70E-02	61.59	5.47E+01
Data Pt[4]	:	764.947	64.02	1.56E-01	75.15	2.78E+02
Data Pt[5]	:	773.019	64	1.69E-01	75.78	3.00E+02
Data Pt[6]	:	776.387	63.99	8.19E-01	80.32	1.11E+03
Data Pt[7]	:	779.742	64	1.67E+00	81.03	2.28E+03
Data Pt[8]	:	782.878	64	3.98E+00	80.29	4.91E+03

Test Run[1] :
 Temperature[6]
 : 70
 Temp Run[1] :
 Last Data Point
 : 7
 Start Test Time
 : 7250.052

Header[1]	:	Time	Temperature	Frequency	Phase	Complex
Header[2]	:	(s)	(°C)	(Hz)	Angle	Modulus
					(°)	(Pa)
Data Pt[1]	:	629.998	69.92	1.59E-03	43.68	8.48E+00
Data Pt[2]	:	695.638	70	1.57E-02	57.13	3.24E+01
Data Pt[3]	:	756.422	70	1.70E-02	56.57	3.44E+01
Data Pt[4]	:	764.935	70.01	1.56E-01	71.14	1.53E+02
Data Pt[5]	:	772.956	70	1.69E-01	73.08	1.63E+02
Data Pt[6]	:	776.309	70	8.19E-01	79.01	6.04E+02
Data Pt[7]	:	779.676	70	1.67E+00	80.85	1.20E+03
Data Pt[8]	:	782.816	70.01	3.98E+00	81.3	2.52E+03

Test Run[1] :
 Temperature[7]
 : 76
 Temp Run[1] :
 Last Data Point
 : 7
 Start Test Time
 : 8434.571

Header[1]	:	Time	Temperature	Frequency	Phase	Complex
Header[2]	:	(s)	(°C)	(Hz)	Angle	Modulus
					(°)	(Pa)

Data Pt[1]	:	629.996	75.92	1.59E-03	71.74	7.00E+00
Data Pt[2]	:	695.637	75.99	1.57E-02	57.54	1.88E+01
Data Pt[3]	:	756.421	76	1.70E-02	57.49	2.01E+01
Data Pt[4]	:	764.119	76	1.56E-01	72.26	9.05E+01
Data Pt[5]	:	772.167	76	1.69E-01	69.85	9.72E+01
Data Pt[6]	:	775.522	76	8.19E-01	77.35	3.50E+02
Data Pt[7]	:	778.885	75.99	1.67E+00	79.4	6.61E+02
Data Pt[8]	:	782.02	75.99	3.98E+00	81.12	1.53E+03

DSR result BMR-15-20

Test Run[1] :
 Temperature[1]
 : 40
 Temp Run[1] :
 Last Data Point
 : 7
 Start Test Time
 : 1492.404

Header[1]	:	Time	Temperature	Frequency	Phase	Complex
Header[2]	:	(s)	(°C)	(Hz)	Angle	Modulus
					(°)	(Pa)
Data Pt[1]	:	630.003	40.06	1.59E-03	67.77	2.23E+02
Data Pt[2]	:	695.643	40.01	1.57E-02	74.56	1.09E+03
Data Pt[3]	:	756.426	40.01	1.70E-02	75.47	1.13E+03
Data Pt[4]	:	764.952	40	1.56E-01	79.63	6.84E+03
Data Pt[5]	:	773.022	40	1.69E-01	78.69	6.67E+03
Data Pt[6]	:	776.386	39.99	8.19E-01	65.26	1.98E+04
Data Pt[7]	:	779.742	40	1.67E+00	68.94	4.36E+04
Data Pt[8]	:	782.881	40.01	3.98E+00	66.67	8.23E+04

Test Run[1] :

Temperature[2]
: 46
Temp Run[1] :
Last Data Point
: 7
Start Test Time
: 2630.328

Header[1]	:	Time	Temperature	Frequency	Phase	Complex
Header[2]	:	(s)	(°C)	(Hz)	Angle	Modulus
	:				(°)	(Pa)
Data Pt[1]	:	629.996	45.93	1.59E-03	55.75	9.12E+01
Data Pt[2]	:	695.637	46	1.57E-02	73.4	3.67E+02
Data Pt[3]	:	756.422	46	1.70E-02	74.54	3.78E+02
Data Pt[4]	:	764.933	46	1.56E-01	80.32	2.51E+03
Data Pt[5]	:	773.014	46	1.69E-01	80.45	2.68E+03
Data Pt[6]	:	776.381	45.99	8.19E-01	77.4	1.04E+04
Data Pt[7]	:	779.741	46	1.67E+00	73.93	1.99E+04
Data Pt[8]	:	782.878	46	3.98E+00	70.26	3.92E+04

Test Run[1] :
Temperature[3]
: 52
Temp Run[1] :
Last Data Point
: 7
Start Test Time
: 4382.607

Header[1]	:	Time	Temperature	Frequency	Phase	Complex
Header[2]	:	(s)	(°C)	(Hz)	Angle	Modulus
	:				(°)	(Pa)
Data Pt[1]	:	630.002	52.07	1.59E-03	54.16	7.64E+01
Data Pt[2]	:	695.714	52.01	1.57E-02	64.64	2.45E+02
Data Pt[3]	:	756.498	52.02	1.70E-02	66.07	2.46E+02
Data Pt[4]	:	765.063	51.99	1.56E-01	77.42	1.30E+03
Data Pt[5]	:	773.142	52	1.69E-01	77.7	1.35E+03
Data Pt[6]	:	776.492	52	8.19E-01	81.01	5.09E+03
Data Pt[7]	:	779.793	52.01	1.67E+00	78.79	8.95E+03
Data Pt[8]	:	782.915	51.98	3.98E+00	74.17	1.91E+04

Test Run[1] :

Temperature[4]
: 58
Temp Run[1] :
Last Data Point
: 7
Start Test Time
: 5536.927

Header[1]	:	Time	Temperature	Frequency	Phase	Complex
Header[2]	:	(s)	(°C)	(Hz)	Angle	Modulus
	:				(°)	(Pa)
Data Pt[1]	:	629.999	57.93	1.59E-03	51.83	5.65E+01
Data Pt[2]	:	695.637	58.01	1.57E-02	58.25	1.63E+02
Data Pt[3]	:	756.426	58.01	1.70E-02	59.36	1.60E+02
Data Pt[4]	:	764.973	58	1.56E-01	74.53	7.09E+02
Data Pt[5]	:	773.042	58	1.69E-01	75.04	7.15E+02
Data Pt[6]	:	776.399	58.01	8.19E-01	78.34	2.63E+03
Data Pt[7]	:	779.768	58	1.67E+00	78.82	4.68E+03
Data Pt[8]	:	782.899	57.99	3.98E+00	77.03	9.67E+03

Test Run[1] :
Temperature[5]
: 64
Temp Run[1] :
Last Data Point
: 7
Start Test Time
: 6715.237

Header[1]	:	Time	Temperature	Frequency	Phase	Complex
Header[2]	:	(s)	(°C)	(Hz)	Angle	Modulus
	:				(°)	(Pa)
Data Pt[1]	:	629.998	63.93	1.59E-03	51.21	4.84E+01
Data Pt[2]	:	695.638	63.99	1.57E-02	55.06	1.20E+02
Data Pt[3]	:	756.42	63.99	1.70E-02	56.5	1.16E+02
Data Pt[4]	:	764.947	64	1.56E-01	70	4.35E+02
Data Pt[5]	:	773.017	64	1.69E-01	70.39	4.29E+02
Data Pt[6]	:	776.387	64.01	8.19E-01	78.54	1.25E+03
Data Pt[7]	:	779.743	64	1.67E+00	79.04	2.43E+03
Data Pt[8]	:	782.879	64	3.98E+00	79.51	4.91E+03

Test Run[1] :

Temperature[6]
 : 70
 Temp Run[1] :
 Last Data Point
 : 7
 Start Test Time
 : 7880.362

Header[1]	:	Time	Temperature	Frequency	Phase	Complex
Header[2]	:	(s)	(°C)	(Hz)	Angle	Modulus
	:				(°)	(Pa)
Data Pt[1]	:	629.999	69.94	1.59E-03	48.74	3.33E+01
Data Pt[2]	:	695.636	70.01	1.57E-02	52.15	7.60E+01
Data Pt[3]	:	756.426	70	1.70E-02	52.44	7.63E+01
Data Pt[4]	:	764.984	69.99	1.56E-01	66.89	2.56E+02
Data Pt[5]	:	773.053	70	1.69E-01	67.3	2.54E+02
Data Pt[6]	:	776.421	70	8.19E-01	77.09	7.18E+02
Data Pt[7]	:	779.783	70.01	1.67E+00	78.46	1.35E+03
Data Pt[8]	:	782.911	70	3.98E+00	79.26	2.79E+03

Test Run[1] :
 Temperature[7]
 : 76
 Temp Run[1] :
 Last Data Point
 : 7
 Start Test Time
 : 9067.08

Header[1]	:	Time	Temperature	Frequency	Phase	Complex
Header[2]	:	(s)	(°C)	(Hz)	Angle	Modulus
	:				(°)	(Pa)
Data Pt[1]	:	629.998	75.92	1.59E-03	50.51	2.54E+01
Data Pt[2]	:	695.637	76.01	1.57E-02	49.08	5.73E+01
Data Pt[3]	:	756.42	75.98	1.70E-02	49.75	5.53E+01
Data Pt[4]	:	764.986	76.01	1.56E-01	63.57	1.68E+02
Data Pt[5]	:	773.004	76	1.69E-01	64.43	1.67E+02
Data Pt[6]	:	776.369	76.01	8.19E-01	74.56	4.63E+02
Data Pt[7]	:	779.726	75.99	1.67E+00	76.76	8.31E+02
Data Pt[8]	:	782.863	75.99	3.98E+00	78.76	1.70E+03

DSR result 20%CRM

Test Run[1] :
 Temperature[1]
 : 40
 Temp Run[1] :
 Last Data Point
 : 7
 Start Test Time
 : 895.27

Header[1]	:	Time	Temperature	Frequency	Phase Angle	Complex Modulus
Header[2]	:	(s)	(°C)	(Hz)	(°)	(Pa)
Data Pt[1]	:	630.003	40.07	1.59E-03	78.47	1.05E+03
Data Pt[2]	:	695.643	39.98	1.57E-02	73.79	7.31E+03
Data Pt[3]	:	756.429	40.01	1.70E-02	72.54	8.10E+03
Data Pt[4]	:	764.979	39.98	1.56E-01	55.41	5.30E+04
Data Pt[5]	:	773.059	40	1.69E-01	58.63	4.17E+04
Data Pt[6]	:	776.417	40	8.19E-01	55.94	1.22E+05
Data Pt[7]	:	779.757	40.01	1.67E+00	52.89	1.89E+05
Data Pt[8]	:	782.906	40.01	3.98E+00	50.66	3.09E+05

Test Run[1] :
 Temperature[2]
 : 46
 Temp Run[1] :
 Last Data Point
 : 7
 Start Test Time 2033.58
 : 6

Header[1]	:	Time	Temperature	Frequency	Phase Angle	Complex Modulus
Header[2]	:	(s)	(°C)	(Hz)	(°)	(Pa)
Data Pt[1]	:	629.998	45.93	1.59E-03	78.07	3.78E+02
Data Pt[2]	:	695.64	46	1.57E-02	77.29	2.70E+03
Data Pt[3]	:	756.421	46	1.70E-02	76.51	2.95E+03
Data Pt[4]	:	764.947	46	1.56E-01	68.62	1.74E+04
Data Pt[5]	:	773.026	46	1.69E-01	64.49	1.71E+04
Data Pt[6]	:	776.393	46	8.19E-01	60.95	5.89E+04
Data Pt[7]	:	779.753	46	1.67E+00	57.27	9.40E+04
Data Pt[8]	:	782.945	46	3.98E+00	54.58	1.60E+05

Test Run[1] :
 Temperature[3]
 : 52
 Temp Run[1] :
 Last Data Point
 : 7
 Start Test Time 3187.30
 : 8

Header[1]	:	Time	Temperature	Frequency	Phase	Complex Modulus
Header[2]	:	(s)	(°C)	(Hz)	(°)	(Pa)
Data Pt[1]	:	629.995	51.93	1.59E-03	76.56	1.52E+02
Data Pt[2]	:	695.639	52	1.57E-02	78.68	1.04E+03
Data Pt[3]	:	756.492	52	1.70E-02	78.28	1.14E+03
Data Pt[4]	:	765.022	52	1.56E-01	77.4	7.81E+03
Data Pt[5]	:	773.088	52	1.69E-01	73.08	8.34E+03
Data Pt[6]	:	776.454	52	8.19E-01	72.31	3.59E+04
Data Pt[7]	:	779.819	51.99	1.67E+00	62.1	4.62E+04
Data Pt[8]	:	782.945	52.01	3.98E+00	59.66	8.36E+04

Test Run[1] :
 Temperature[4]
 : 58
 Temp Run[1] :
 Last Data Point
 : 7
 Start Test Time 4331.23
 : 1

Header[1]	:	Time	Temperature	Frequency	Phase	Complex Modulus
Header[2]	:	(s)	(°C)	(Hz)	(°)	(Pa)
Data Pt[1]	:	629.998	57.93	1.59E-03	77	6.29E+01
Data Pt[2]	:	695.638	58	1.57E-02	79.2	4.34E+02
Data Pt[3]	:	756.423	58	1.70E-02	79	4.70E+02
Data Pt[4]	:	764.948	58	1.56E-01	76.9	3.37E+03
Data Pt[5]	:	773.025	58.01	1.69E-01	77.01	3.54E+03
Data Pt[6]	:	776.39	58.01	8.19E-01	66.58	1.49E+04
Data Pt[7]	:	779.726	58	1.67E+00	67.31	2.37E+04
Data Pt[8]	:	782.882	58	3.98E+00	63.53	4.45E+04

Test Run[1] :
 Temperature[5]
 : 64
 Temp Run[1] :
 Last Data Point
 : 7
 Start Test Time 5498.74
 : 8

Header[1]	:	Time	Temperature	Frequency	Phase	Complex Modulus
Header[2]	:	(s)	(°C)	(Hz)	(°)	(Pa)
Data Pt[1]	:	629.998	63.93	1.59E-03	77.1	2.69E+01
Data Pt[2]	:	695.64	63.99	1.57E-02	78.69	1.96E+02
Data Pt[3]	:	756.495	63.99	1.70E-02	78.44	2.11E+02
Data Pt[4]	:	765.03	63.99	1.56E-01	79.45	1.49E+03
Data Pt[5]	:	773.111	64	1.69E-01	78.96	1.65E+03
Data Pt[6]	:	776.466	64.01	8.19E-01	79.62	6.12E+03
Data Pt[7]	:	779.833	64.01	1.67E+00	86.01	1.10E+04
Data Pt[8]	:	783.021	64.01	3.98E+00	68.59	2.24E+04

Test Run[1] :
 Temperature[6]
 : 70
 Temp Run[1] :
 Last Data Point
 : 7
 Start Test Time 6648.86
 : 7

Header[1]	:	Time	Temperature	Frequency	Phase	Complex Modulus
Header[2]	:	(s)	(°C)	(Hz)	(°)	(Pa)
Data Pt[1]	:	629.998	69.91	1.59E-03	71.46	1.85E+01
Data Pt[2]	:	695.709	70	1.57E-02	74.62	1.00E+02
Data Pt[3]	:	756.492	70	1.70E-02	76.09	1.09E+02
Data Pt[4]	:	765.079	70	1.56E-01	79.7	7.46E+02
Data Pt[5]	:	773.159	70	1.69E-01	79.64	8.02E+02
Data Pt[6]	:	776.504	69.99	8.19E-01	78.79	3.37E+03
Data Pt[7]	:	779.878	70	1.67E+00	76.27	6.13E+03
Data Pt[8]	:	783.068	70	3.98E+00	72.91	1.21E+04

Test Run[1] :
 Temperature[7]
 : 76
 Temp Run[1] :
 Last Data Point
 : 7
 Start Test Time 7818.78
 : 6

Header[1]	Time	Temperature	Frequency	Phase	Complex Modulus
Header[2]	(s)	(°C)	(Hz)	(°)	(Pa)
Data Pt[1]	629.996	75.93	1.59E-03	61.71	1.07E+01
Data Pt[2]	695.71	76	1.57E-02	69.77	5.79E+01
Data Pt[3]	756.492	76.01	1.70E-02	71.27	6.20E+01
Data Pt[4]	765.068	76	1.56E-01	77.62	3.84E+02
Data Pt[5]	773.158	75.99	1.69E-01	77.78	4.07E+02
Data Pt[6]	776.5	75.99	8.19E-01	78.2	1.63E+03
Data Pt[7]	779.872	75.99	1.67E+00	78.37	3.26E+03
Data Pt[8]	783.08	76	3.98E+00	75.88	6.90E+03

DSR result BMR-20-5

Test Run[1] :
 Temperature[1]
 : 40
 Temp Run[1] :
 Last Data Point
 : 7
 Start Test Time
 : 1191.967

Header[1]	Time	Temperature	Frequency	Phase	Complex
Header[2]	(s)	(°C)	(Hz)	Angle	Modulus
				(°)	(Pa)
Data Pt[1]	630.002	40.05	1.59E-03	83.33	4.87E+02
Data Pt[2]	695.642	39.99	1.57E-02	79.39	3.93E+03

Data Pt[3]	:	756.5	39.99	1.70E-02	78.27	4.34E+03
Data Pt[4]	:	765.049	40	1.56E-01	63.65	2.71E+04
Data Pt[5]	:	773.125	40	1.69E-01	64.53	2.16E+04
Data Pt[6]	:	776.49	40	8.19E-01	61.29	8.01E+04
Data Pt[7]	:	779.853	39.99	1.67E+00	56.67	1.32E+05
Data Pt[8]	:	783.038	40	3.98E+00	54.07	2.24E+05

Test Run[1] :
 Temperature[2]
 : 46
 Temp Run[1] :
 Last Data Point
 : 7
 Start Test Time
 : 2331.491

Header[1]	:	Time	Temperature	Frequency	Phase	Complex
Header[2]	:	(s)	(°C)	(Hz)	Angle	Modulus
					(°)	(Pa)
Data Pt[1]	:	629.999	45.93	1.59E-03	83.95	1.64E+02
Data Pt[2]	:	695.711	46.01	1.57E-02	82.87	1.39E+03
Data Pt[3]	:	756.495	46	1.70E-02	82.26	1.52E+03
Data Pt[4]	:	765.07	46	1.56E-01	77.89	1.05E+04
Data Pt[5]	:	773.139	46	1.69E-01	74.66	1.19E+04
Data Pt[6]	:	776.495	46	8.19E-01	79.29	3.37E+04
Data Pt[7]	:	779.875	46	1.67E+00	59.87	6.60E+04
Data Pt[8]	:	783.046	46	3.98E+00	58.45	1.15E+05

Test Run[1] :
 Temperature[3]
 : 52
 Temp Run[1] :
 Last Data Point
 : 7
 Start Test Time
 : 3492.611

Header[1]	:	Time	Temperature	Frequency	Phase	Complex
Header[2]	:	(s)	(°C)	(Hz)	Angle	Modulus
					(°)	(Pa)
Data Pt[1]	:	629.997	51.92	1.59E-03	81.26	6.46E+01
Data Pt[2]	:	695.638	52.01	1.57E-02	83.5	5.21E+02

Data Pt[3]	:	756.495	52	1.70E-02	83.32	5.63E+02
Data Pt[4]	:	765.046	52	1.56E-01	78.75	4.36E+03
Data Pt[5]	:	773.122	51.98	1.69E-01	78.45	4.64E+03
Data Pt[6]	:	776.477	52	8.19E-01	80.46	2.35E+04
Data Pt[7]	:	779.848	51.99	1.67E+00	67.08	3.02E+04
Data Pt[8]	:	783.024	52	3.98E+00	63.57	5.77E+04

Test Run[1] :
 Temperature[4] : 58
 Temp Run[1] :
 Last Data Point : 7
 Start Test Time : 4640.331

Header[1]	:	Time	Temperature	Frequency	Phase	Complex
Header[2]	:	(s)	(°C)	(Hz)	Angle	Modulus
	:				(°)	(Pa)
Data Pt[1]	:	629.996	57.92	1.59E-03	76	3.13E+01
Data Pt[2]	:	695.637	58.01	1.57E-02	81.54	2.15E+02
Data Pt[3]	:	756.494	58	1.70E-02	81.8	2.29E+02
Data Pt[4]	:	765.055	58	1.56E-01	81.76	1.78E+03
Data Pt[5]	:	773.137	58	1.69E-01	81.35	1.92E+03
Data Pt[6]	:	776.482	57.99	8.19E-01	79.41	7.43E+03
Data Pt[7]	:	779.856	58	1.67E+00	78.3	1.34E+04
Data Pt[8]	:	783.038	58	3.98E+00	68.34	2.82E+04

Test Run[1] :
 Temperature[5] : 64
 Temp Run[1] :
 Last Data Point : 7
 Start Test Time : 6479.4

Header[1]	:	Time	Temperature	Frequency	Phase	Complex
Header[2]	:	(s)	(°C)	(Hz)	Angle	Modulus
	:				(°)	(Pa)
Data Pt[1]	:	630.002	64.05	1.59E-03	24.86	1.26E+06
Data Pt[2]	:	695.716	63.99	1.57E-02	83.69	7.83E+01

Data Pt[3]	:	756.569	64.01	1.70E-02	83.78	8.66E+01
Data Pt[4]	:	765.134	64.01	1.56E-01	84.78	6.98E+02
Data Pt[5]	:	773.202	64	1.69E-01	84.71	7.49E+02
Data Pt[6]	:	776.571	63.98	8.19E-01	81.81	3.35E+03
Data Pt[7]	:	779.931	63.99	1.67E+00	79.09	6.27E+03
Data Pt[8]	:	783.108	64	3.98E+00	75.35	1.33E+04

Test Run[1] :
 Temperature[6] : 70
 Temp Run[1] :
 Last Data Point : 7
 Start Test Time : 7641.722

Header[1]	:	Time	Temperature	Frequency	Phase Angle	Complex Modulus
Header[2]	:	(s)	(°C)	(Hz)	(°)	(Pa)
Data Pt[1]	:	629.995	69.93	1.59E-03	43.44	5.32E+01
Data Pt[2]	:	695.639	70	1.57E-02	79.22	3.92E+01
Data Pt[3]	:	756.493	70.01	1.70E-02	78.42	4.24E+01
Data Pt[4]	:	765.031	70.01	1.56E-01	84.05	3.29E+02
Data Pt[5]	:	773.111	70.01	1.69E-01	84.31	3.46E+02
Data Pt[6]	:	776.467	69.99	8.19E-01	82.75	1.62E+03
Data Pt[7]	:	779.84	70	1.67E+00	81.79	3.05E+03
Data Pt[8]	:	783.032	70	3.98E+00	78.93	6.62E+03

Test Run[1] :
 Temperature[7] : 76
 Temp Run[1] :
 Last Data Point : 7
 Start Test Time : 8828.836

Header[1]	:	Time	Temperature	Frequency	Phase Angle	Complex Modulus
Header[2]	:	(s)	(°C)	(Hz)	(°)	(Pa)
Data Pt[1]	:	629.998	75.92	1.59E-03	81.75	4.41E+00
Data Pt[2]	:	695.709	76	1.57E-02	66.95	2.74E+01

Data Pt[3]	:	756.492	76	1.70E-02	67.46	2.94E+01
Data Pt[4]	:	765.089	76.01	1.56E-01	79.71	1.77E+02
Data Pt[5]	:	773.146	76	1.69E-01	80.58	1.95E+02
Data Pt[6]	:	776.527	76	8.19E-01	83.44	8.03E+02
Data Pt[7]	:	779.882	76	1.67E+00	82.74	1.70E+03
Data Pt[8]	:	783.071	76.02	3.98E+00	80.84	3.63E+03

DSR result BMR-20-10

Test Run[1] :
 Temperature[1]
 : 40
 Temp Run[1] :
 Last Data Point
 : 7
 Start Test Time 620.062
 : 6

Header[1]	:	Time	Temperatur	Frequenc	Phase Angle	Complex
Header[2]	:	(s)	e	y	(°)	Modulus
			(°C)	(Hz)		(Pa)
Data Pt[1]	:	630.002	40.07	1.59E-03	80.56	3.40E+02
Data Pt[2]	:	695.714	40	1.57E-02	80.24	2.64E+03
Data Pt[3]	:	756.499	40.01	1.70E-02	79.54	2.87E+03
Data Pt[4]	:	765.082	40	1.56E-01	71.76	1.85E+04
Data Pt[5]	:	773.162	39.98	1.69E-01	66.29	1.77E+04
Data Pt[6]	:	776.599	40	8.19E-01	64.27	6.64E+04
Data Pt[7]	:	779.999	39.99	1.67E+00	60.82	1.07E+05
Data Pt[8]	:	783.196	40	3.98E+00	57.67	1.88E+05

Test Run[1] :
 Temperature[2]
 : 46
 Temp Run[1] :
 Last Data Point
 : 7
 Start Test Time 1764.98
 : 4

Header[1]	:	Time	Temperature	Frequency	Phase Angle	Complex Modulus
Header[2]	:	(s)	(°C)	(Hz)	(°)	(Pa)
Data Pt[1]	:	629.999	45.93	1.59E-03	79.07	1.24E+02
Data Pt[2]	:	695.71	46	1.57E-02	81.75	9.57E+02
Data Pt[3]	:	756.494	46	1.70E-02	81.43	1.04E+03
Data Pt[4]	:	765.079	46	1.56E-01	80.05	7.52E+03
Data Pt[5]	:	773.171	46	1.69E-01	76.46	8.25E+03
Data Pt[6]	:	776.586	46	8.19E-01	83.72	5.39E+04
Data Pt[7]	:	779.926	45.99	1.67E+00	66.26	5.07E+04
Data Pt[8]	:	783.12	46	3.98E+00	62.58	9.46E+04

Test Run[1] :
 Temperature[3] : 52
 Temp Run[1] :
 Last Data Point : 7
 Start Test Time : 2934.50
 : 3

Header[1]	:	Time	Temperature	Frequency	Phase Angle	Complex Modulus
Header[2]	:	(s)	(°C)	(Hz)	(°)	(Pa)
Data Pt[1]	:	629.997	51.94	1.59E-03	78.92	5.14E+01
Data Pt[2]	:	695.709	52	1.57E-02	81.55	3.72E+02
Data Pt[3]	:	756.567	51.99	1.70E-02	81.6	4.00E+02
Data Pt[4]	:	765.161	52	1.56E-01	79.94	3.00E+03
Data Pt[5]	:	773.23	52.01	1.69E-01	80.1	3.19E+03
Data Pt[6]	:	776.597	52	8.19E-01	72.79	1.30E+04
Data Pt[7]	:	779.957	52	1.67E+00	73	2.23E+04
Data Pt[8]	:	783.157	51.99	3.98E+00	67.46	4.51E+04

Test Run[1] :
 Temperature[4] : 58
 Temp Run[1] :
 Last Data Point : 7
 Start Test Time : 4085.62
 : 1

Header[1]	:	Time	Temperature	Frequency	Phase Angle	Complex Modulus
Header[2]	:	(s)	(°C)	(Hz)	(°)	(Pa)
Data Pt[1]	:	629.997	57.92	1.59E-03	79.66	2.30E+01
Data Pt[2]	:	695.708	58	1.57E-02	80.03	1.57E+02
Data Pt[3]	:	756.564	58	1.70E-02	79.98	1.71E+02
Data Pt[4]	:	765.15	58	1.56E-01	82.23	1.27E+03
Data Pt[5]	:	773.22	58	1.69E-01	81.75	1.35E+03
Data Pt[6]	:	776.648	58	8.19E-01	83.17	5.41E+03
Data Pt[7]	:	779.993	58	1.67E+00	78.61	9.95E+03
Data Pt[8]	:	783.19	57.99	3.98E+00	72.19	2.22E+04

Test Run[1] :
 Temperature[5]
 : 64
 Temp Run[1] :
 Last Data Point
 : 7
 Start Test Time 5259.53
 : 8

Header[1]	:	Time	Temperature	Frequency	Phase Angle	Complex Modulus
Header[2]	:	(s)	(°C)	(Hz)	(°)	(Pa)
Data Pt[1]	:	629.998	63.92	1.59E-03	70.52	9.55E+00
Data Pt[2]	:	695.709	63.99	1.57E-02	77.81	7.35E+01
Data Pt[3]	:	756.492	64	1.70E-02	78.47	7.76E+01
Data Pt[4]	:	765.077	64	1.56E-01	82.88	5.60E+02
Data Pt[5]	:	773.158	64.01	1.69E-01	83.19	6.13E+02
Data Pt[6]	:	776.585	63.99	8.19E-01	80.91	2.79E+03
Data Pt[7]	:	779.921	64	1.67E+00	79.85	5.30E+03
Data Pt[8]	:	783.125	64.01	3.98E+00	76.74	1.08E+04

Test Run[1] :
 Temperature[6]
 : 70
 Temp Run[1] :
 Last Data Point
 : 7
 Start Test Time 6424.85
 : 8

Header[1]	:	Time	Temperature	Frequency	Phase Angle	Complex Modulus
Header[2]	:	(s)	(°C)	(Hz)	(°)	(Pa)
Data Pt[1]	:	629.998	69.92	1.59E-03	68.15	6.81E+00
Data Pt[2]	:	695.638	70	1.57E-02	75.48	3.87E+01
Data Pt[3]	:	756.494	69.99	1.70E-02	76.83	4.03E+01
Data Pt[4]	:	765.058	69.99	1.56E-01	81.71	3.07E+02
Data Pt[5]	:	773.124	70.01	1.69E-01	82.49	3.08E+02
Data Pt[6]	:	776.49	70.01	8.19E-01	82.42	1.33E+03
Data Pt[7]	:	779.843	70.01	1.67E+00	81.92	2.47E+03
Data Pt[8]	:	783.054	70	3.98E+00	79.58	5.71E+03

Test Run[1] :
 Temperature[7]
 : 76
 Temp Run[1] :
 Last Data Point
 : 7
 Start Test Time 7610.77
 : 5

Header[1]	:	Time	Temperature	Frequency	Phase Angle	Complex Modulus
Header[2]	:	(s)	(°C)	(Hz)	(°)	(Pa)
Data Pt[1]	:	629.997	75.92	1.59E-03	57.6	3.88E+00
Data Pt[2]	:	695.711	76	1.57E-02	73.54	2.24E+01
Data Pt[3]	:	756.563	76	1.70E-02	72.45	2.28E+01
Data Pt[4]	:	765.175	76	1.56E-01	77	1.64E+02
Data Pt[5]	:	773.243	76.01	1.69E-01	79.42	1.61E+02
Data Pt[6]	:	776.61	75.99	8.19E-01	83.25	7.25E+02
Data Pt[7]	:	779.963	76.01	1.67E+00	82.81	1.30E+03
Data Pt[8]	:	783.177	75.99	3.98E+00	81.69	2.89E+03

DSR result BMR-20-15

Test Run[1] :
 Temperature[1]
 : 40
 Temp Run[1] :
 Last Data Point
 : 7
 Start Test Time
 : 40.0328

Header[1] :	Time	Temperature	Frequency	Phase	Complex
Header[2] :	(s)	(°C)	(Hz)	Angle	Modulus
				(°)	(Pa)
Data Pt[1] :	630.003	40.02	1.59E-03	78.66	2.99E+02
Data Pt[2] :	695.644	39.99	1.57E-02	78.17	2.08E+03
Data Pt[3] :	756.432	40.01	1.70E-02	77.67	2.25E+03
Data Pt[4] :	764.978	40.01	1.56E-01	74.65	1.42E+04
Data Pt[5] :	773.059	39.99	1.69E-01	72.59	1.56E+04
Data Pt[6] :	776.411	39.99	8.19E-01	65.82	5.13E+04
Data Pt[7] :	779.784	39.99	1.67E+00	62.11	8.65E+04
Data Pt[8] :	782.956	40.01	3.98E+00	59.33	1.55E+05

Test Run[1] :
 Temperature[2]
 : 46
 Temp Run[1] :
 Last Data Point
 : 7
 Start Test Time 1181.66
 : 5

Header[1] :	Time	Temperature	Frequency	Phase	Complex
Header[2] :	(s)	(°C)	(Hz)	Angle	Modulus
				(°)	(Pa)
Data Pt[1] :	629.996	45.93	1.59E-03	75.63	1.09E+02
Data Pt[2] :	695.638	46	1.57E-02	79.36	7.37E+02
Data Pt[3] :	756.426	46	1.70E-02	79.26	7.91E+02
Data Pt[4] :	764.946	46	1.56E-01	79.08	5.69E+03
Data Pt[5] :	773.028	46	1.69E-01	77.67	5.96E+03
Data Pt[6] :	776.375	46	8.19E-01	81.36	2.45E+04
Data Pt[7] :	779.683	46	1.67E+00	67.32	3.89E+04
Data Pt[8] :	782.806	46	3.98E+00	65.1	7.29E+04

Test Run[1] :
 Temperature[3]
 : 52
 Temp Run[1] :
 Last Data Point
 : 7
 Start Test Time 2344.97
 : 7

Header[1] :	Time	Temperature	Frequency	Phase	Complex
Header[2] :	(s)	(°C)	(Hz)	Angle	Modulus
				(°)	(Pa)
Data Pt[1] :	629.998	51.92	1.59E-03	72.06	4.50E+01
Data Pt[2] :	695.636	52	1.57E-02	77.94	2.89E+02
Data Pt[3] :	756.427	52	1.70E-02	78.11	3.10E+02
Data Pt[4] :	764.987	51.99	1.56E-01	80.06	2.20E+03
Data Pt[5] :	773.075	52.01	1.69E-01	79.67	2.36E+03
Data Pt[6] :	776.425	52.01	8.19E-01	77.52	9.14E+03
Data Pt[7] :	779.784	52.01	1.67E+00	75.58	1.65E+04
Data Pt[8] :	782.9	51.99	3.98E+00	69.46	3.45E+04

Test Run[1] :
 Temperature[4]
 : 58
 Temp Run[1] :
 Last Data Point
 : 7
 Start Test Time 3495.30
 : 3

Header[1] :	Time	Temperature	Frequency	Phase	Complex
Header[2] :	(s)	(°C)	(Hz)	Angle	Modulus
				(°)	(Pa)
Data Pt[1] :	629.996	57.92	1.59E-03	71.84	2.20E+01
Data Pt[2] :	695.639	58	1.57E-02	73.76	1.33E+02
Data Pt[3] :	756.493	58	1.70E-02	73.94	1.41E+02
Data Pt[4] :	765.021	58	1.56E-01	80.44	9.60E+02
Data Pt[5] :	773.088	58	1.69E-01	80.2	1.04E+03
Data Pt[6] :	776.442	58.01	8.19E-01	81.44	4.11E+03
Data Pt[7] :	779.755	57.99	1.67E+00	77.42	7.96E+03
Data Pt[8] :	782.885	58	3.98E+00	73.77	1.68E+04

Test Run[1] :
 Temperature[5]
 : 64
 Temp Run[1] :
 Last Data Point
 : 7
 Start Test Time 4671.22
 : 1

Header[1]	:	Time	Temperature	Frequency	Phase Angle	Complex Modulus
Header[2]	:	(s)	(°C)	(Hz)	(°)	(Pa)
Data Pt[1]	:	629.995	63.93	1.59E-03	66.42	1.37E+01
Data Pt[2]	:	695.64	63.99	1.57E-02	67.28	7.35E+01
Data Pt[3]	:	756.424	63.99	1.70E-02	67.27	7.85E+01
Data Pt[4]	:	764.946	64.01	1.56E-01	78.08	4.64E+02
Data Pt[5]	:	773.018	64.01	1.69E-01	78.46	4.95E+02
Data Pt[6]	:	776.391	63.99	8.19E-01	79.34	2.09E+03
Data Pt[7]	:	779.737	64	1.67E+00	79.62	3.97E+03
Data Pt[8]	:	782.881	64	3.98E+00	77.61	8.34E+03

Test Run[1] :
 Temperature[6]
 : 70
 Temp Run[1] :
 Last Data Point
 : 7
 Start Test Time 5829.13
 : 9

Header[1]	:	Time	Temperature	Frequency	Phase Angle	Complex Modulus
Header[2]	:	(s)	(°C)	(Hz)	(°)	(Pa)
Data Pt[1]	:	629.997	69.92	1.59E-03	57.49	9.69E+00
Data Pt[2]	:	695.639	70	1.57E-02	61.52	4.50E+01
Data Pt[3]	:	756.422	70.01	1.70E-02	61.12	4.79E+01
Data Pt[4]	:	764.948	70	1.56E-01	74.97	2.45E+02
Data Pt[5]	:	773.019	69.99	1.69E-01	75.61	2.66E+02
Data Pt[6]	:	776.386	70	8.19E-01	80.02	1.02E+03
Data Pt[7]	:	779.741	70	1.67E+00	81.49	2.08E+03
Data Pt[8]	:	782.876	70.01	3.98E+00	79.79	4.38E+03

Test Run[1] :
 Temperature[7]
 : 76
 Temp Run[1] :
 Last Data Point
 : 7
 Start Test Time 7007.45
 : 7

Header[1]	:	Time	Temperature	Frequency	Phase	Complex
Header[2]	:	(s)	(°C)	(Hz)	Angle	Modulus
	:				(°)	(Pa)
Data Pt[1]	:	629.998	75.91	1.59E-03	61.48	5.93E+00
Data Pt[2]	:	695.64	76.01	1.57E-02	58.6	2.64E+01
Data Pt[3]	:	756.423	76	1.70E-02	59.53	2.82E+01
Data Pt[4]	:	764.986	75.99	1.56E-01	69.66	1.40E+02
Data Pt[5]	:	773.054	76	1.69E-01	71.77	1.52E+02
Data Pt[6]	:	776.414	76.01	8.19E-01	80.17	5.59E+02
Data Pt[7]	:	779.779	76	1.67E+00	80.76	1.03E+03
Data Pt[8]	:	782.901	75.99	3.98E+00	80.92	2.36E+03

DSR result BMR-20-20

Test Run[1] :
 Temperature[1]
 : 40
 Temp Run[1] :
 Last Data Point
 : 7
 Start Test Time 1195.52
 : 8

Header[1]	:	Time	Temperature	Frequency	Phase	Complex
Header[2]	:	(s)	(°C)	(Hz)	Angle	Modulus
	:				(°)	(Pa)
Data Pt[1]	:	630.003	40.06	1.59E-03	79.7	1.79E+02

Data Pt[2]	:	695.644	40	1.57E-02	81.47	1.39E+03
Data Pt[3]	:	756.497	39.99	1.70E-02	81.22	1.52E+03
Data Pt[4]	:	765.062	40.01	1.56E-01	79.09	1.05E+04
Data Pt[5]	:	773.131	40.01	1.69E-01	76.3	1.20E+04
Data Pt[6]	:	776.486	39.99	8.19E-01	84.84	3.66E+04
Data Pt[7]	:	779.859	40	1.67E+00	62.38	7.01E+04
Data Pt[8]	:	783.026	40.01	3.98E+00	60.97	1.26E+05

Test Run[1] :
 Temperature[2]
 : 46
 Temp Run[1] :
 Last Data Point
 : 7
 Start Test Time 2330.64
 : 9

Header[1]	:	Time	Temperature	Frequency	Phase	Complex Modulus
Header[2]	:	(s)	(°C)	(Hz)	(°)	(Pa)
Data Pt[1]	:	629.996	45.92	1.59E-03	77.86	7.02E+01
Data Pt[2]	:	695.711	46	1.57E-02	81.39	5.38E+02
Data Pt[3]	:	756.564	46	1.70E-02	81.22	5.81E+02
Data Pt[4]	:	765.16	45.99	1.56E-01	79.52	4.47E+03
Data Pt[5]	:	773.23	46.01	1.69E-01	79.16	4.62E+03
Data Pt[6]	:	776.591	46	8.19E-01	82.22	2.43E+04
Data Pt[7]	:	779.948	46	1.67E+00	69.32	3.22E+04
Data Pt[8]	:	783.159	46	3.98E+00	65.91	6.17E+04

Test Run[1] :
 Temperature[3]
 : 52
 Temp Run[1] :
 Last Data Point
 : 7
 Start Test Time 3491.56
 : 5

Header[1]	:	Time	Temperature	Frequency	Phase	Complex Modulus
Header[2]	:	(s)	(°C)	(Hz)	(°)	(Pa)
Data Pt[1]	:	629.996	51.93	1.59E-03	72.78	3.38E+01

Data Pt[2]	:	695.708	52	1.57E-02	78.19	2.36E+02
Data Pt[3]	:	756.564	52	1.70E-02	78.44	2.53E+02
Data Pt[4]	:	765.162	52	1.56E-01	81.04	1.84E+03
Data Pt[5]	:	773.239	52	1.69E-01	80.87	1.94E+03
Data Pt[6]	:	776.595	52	8.19E-01	79.49	8.05E+03
Data Pt[7]	:	779.963	52	1.67E+00	80.08	1.44E+04
Data Pt[8]	:	783.144	51.99	3.98E+00	70.64	2.97E+04

Test Run[1] :
 Temperature[4] : 58
 Temp Run[1] :
 Last Data Point : 7
 Start Test Time : 4635.88
 : 5

Header[1]	:	Time	Temperature	Frequency	Phase	Complex Modulus
Header[2]	:	(s)	(°C)	(Hz)	(°)	(Pa)
Data Pt[1]	:	629.997	57.93	1.59E-03	69.81	1.86E+01
Data Pt[2]	:	695.709	58	1.57E-02	74.46	1.15E+02
Data Pt[3]	:	756.494	58	1.70E-02	74.38	1.22E+02
Data Pt[4]	:	765.055	58	1.56E-01	81.03	8.29E+02
Data Pt[5]	:	773.138	58	1.69E-01	81.38	9.08E+02
Data Pt[6]	:	776.501	58	8.19E-01	81.23	3.81E+03
Data Pt[7]	:	779.845	58	1.67E+00	78.07	7.52E+03
Data Pt[8]	:	783.051	58.01	3.98E+00	75.07	1.51E+04

Test Run[1] :
 Temperature[5] : 64
 Temp Run[1] :
 Last Data Point : 7
 Start Test Time : 5803.60
 : 3

Header[1]	:	Time	Temperature	Frequency	Phase	Complex Modulus
Header[2]	:	(s)	(°C)	(Hz)	(°)	(Pa)
Data Pt[1]	:	629.997	63.92	1.59E-03	70.65	1.02E+01

Data Pt[2]	:	695.709	63.99	1.57E-02	73.72	5.71E+01
Data Pt[3]	:	756.495	64.01	1.70E-02	74.46	6.19E+01
Data Pt[4]	:	765.069	64	1.56E-01	80.94	4.18E+02
Data Pt[5]	:	773.148	64	1.69E-01	81.11	4.67E+02
Data Pt[6]	:	776.499	64	8.19E-01	81.01	1.79E+03
Data Pt[7]	:	779.884	63.99	1.67E+00	80.66	3.68E+03
Data Pt[8]	:	783.064	64	3.98E+00	78.14	8.37E+03

Test Run[1] :
 Temperature[6] : 70
 Temp Run[1] :
 Last Data Point : 7
 Start Test Time : 6962.92
 : 5

Header[1]	:	Time	Temperature	Frequency	Phase	Complex Modulus
Header[2]	:	(s)	(°C)	(Hz)	(°)	(Pa)
Data Pt[1]	:	629.997	69.92	1.59E-03	62.06	5.49E+00
Data Pt[2]	:	695.64	70	1.57E-02	74.33	3.03E+01
Data Pt[3]	:	756.495	70	1.70E-02	74.21	3.18E+01
Data Pt[4]	:	765.042	70	1.56E-01	79.37	2.21E+02
Data Pt[5]	:	773.112	70.01	1.69E-01	79.69	2.25E+02
Data Pt[6]	:	776.475	70.01	8.19E-01	82.93	9.90E+02
Data Pt[7]	:	779.835	70	1.67E+00	83.35	1.76E+03
Data Pt[8]	:	783.012	69.99	3.98E+00	80.7	4.22E+03

Test Run[1] :
 Temperature[7] : 76
 Temp Run[1] :
 Last Data Point : 7
 Start Test Time : 8137.83
 : 8

Header[1]	:	Time	Temperature	Frequency	Phase	Complex Modulus
Header[2]	:	(s)	(°C)	(Hz)	(°)	(Pa)
Data Pt[1]	:	629.998	75.91	1.59E-03	66.47	4.47E+00

Data Pt[2]	:	695.639	76	1.57E-02	74.56	1.67E+01
Data Pt[3]	:	756.494	76.01	1.70E-02	72.92	1.80E+01
Data Pt[4]	:	765.032	75.99	1.56E-01	77.67	1.24E+02
Data Pt[5]	:	773.111	76	1.69E-01	78.15	1.23E+02
Data Pt[6]	:	776.471	76.02	8.19E-01	82.85	5.26E+02
Data Pt[7]	:	779.839	76.01	1.67E+00	82.8	9.10E+02
Data Pt[8]	:	783.032	76	3.98E+00	82.12	2.29E+03

DSR result BMR-20-30

Test Run[1] :
 Temperature[1]
 : 40
 Temp Run[1] :
 Last Data Point
 : 7
 Start Test Time 1256.47
 : 2

Header[1]	:	Time	Temperature	Frequency	Phase	Complex
Header[2]	:	(s)	(°C)	(Hz)	Angle	Modulus
	:				(°)	(Pa)
Data Pt[1]	:	630.004	40.05	1.59E-03	69.47	1.55E+02
Data Pt[2]	:	695.645	40	1.57E-02	78.75	9.82E+02
Data Pt[3]	:	756.431	40	1.70E-02	78.73	1.05E+03
Data Pt[4]	:	764.977	40	1.56E-01	79.86	7.46E+03
Data Pt[5]	:	773	39.99	1.69E-01	77.02	7.88E+03
Data Pt[6]	:	776.351	39.99	8.19E-01	85.9	5.76E+04
Data Pt[7]	:	779.645	39.99	1.67E+00	66.73	4.99E+04
Data Pt[8]	:	782.788	40.01	3.98E+00	63.69	9.10E+04

Test Run[1] :
 Temperature[2]
 : 46
 Temp Run[1] :
 Last Data Point
 : 7

Start Test Time : 2395.395

Header[1]	Header[2]	Time (s)	Temperature (°C)	Frequency (Hz)	Phase Angle (°)	Complex Modulus (Pa)
Data Pt[1]	:	629.997	45.92	1.59E-03	66.8	5.95E+01
Data Pt[2]	:	695.639	46	1.57E-02	77.77	3.75E+02
Data Pt[3]	:	756.421	46	1.70E-02	77.79	4.02E+02
Data Pt[4]	:	764.985	46.01	1.56E-01	79.84	2.87E+03
Data Pt[5]	:	773.042	46	1.69E-01	80.07	3.10E+03
Data Pt[6]	:	776.411	46	8.19E-01	74.11	1.22E+04
Data Pt[7]	:	779.774	46	1.67E+00	81.2	2.05E+04
Data Pt[8]	:	782.898	46.01	3.98E+00	69.68	4.48E+04

Test Run[1] :
 Temperature[3] : 52
 Temp Run[1] :
 Last Data Point : 7
 Start Test Time : 3725.699

Header[1]	Header[2]	Time (s)	Temperature (°C)	Frequency (Hz)	Phase Angle (°)	Complex Modulus (Pa)
Data Pt[1]	:	629.997	51.96	1.59E-03	63.05	3.45E+01
Data Pt[2]	:	695.64	52	1.57E-02	72.39	1.84E+02
Data Pt[3]	:	756.493	52.01	1.70E-02	72.55	1.95E+02
Data Pt[4]	:	765.023	52	1.56E-01	80.46	1.29E+03
Data Pt[5]	:	773.1	52	1.69E-01	80.2	1.38E+03
Data Pt[6]	:	776.448	52	8.19E-01	82.47	5.50E+03
Data Pt[7]	:	779.76	52.01	1.67E+00	84.67	9.04E+03
Data Pt[8]	:	782.944	52	3.98E+00	72.22	2.19E+04

Test Run[1] :
 Temperature[4] : 58
 Temp Run[1] :
 Last Data Point : 7

Start Test Time
: 4873.42

Header[1]	:	Time	Temperature	Frequency	Phase Angle	Complex Modulus
Header[2]	:	(s)	(°C)	(Hz)	(°)	(Pa)
Data Pt[1]	:	629.996	57.93	1.59E-03	57.19	2.35E+01
Data Pt[2]	:	695.637	58	1.57E-02	64.39	1.04E+02
Data Pt[3]	:	756.42	58	1.70E-02	64.26	1.11E+02
Data Pt[4]	:	764.96	58	1.56E-01	77.62	6.26E+02
Data Pt[5]	:	773.051	58	1.69E-01	77.79	6.60E+02
Data Pt[6]	:	776.398	58	8.19E-01	79.76	2.79E+03
Data Pt[7]	:	779.769	58	1.67E+00	79.58	5.14E+03
Data Pt[8]	:	782.941	58	3.98E+00	76.53	1.10E+04

Test Run[1] :
Temperature[5]
: 64
Temp Run[1] :
Last Data Point
: 7
Start Test Time 6045.73
: 8

Header[1]	:	Time	Temperature	Frequency	Phase Angle	Complex Modulus
Header[2]	:	(s)	(°C)	(Hz)	(°)	(Pa)
Data Pt[1]	:	629.996	63.93	1.59E-03	51.36	1.81E+01
Data Pt[2]	:	695.71	64.01	1.57E-02	56.45	6.68E+01
Data Pt[3]	:	756.493	64	1.70E-02	55.79	7.11E+01
Data Pt[4]	:	765.058	64.01	1.56E-01	72.98	3.23E+02
Data Pt[5]	:	773.137	64.01	1.69E-01	73.35	3.40E+02
Data Pt[6]	:	776.496	63.99	8.19E-01	79.6	1.31E+03
Data Pt[7]	:	779.836	63.99	1.67E+00	80.07	2.53E+03
Data Pt[8]	:	782.984	63.99	3.98E+00	79.11	5.50E+03

Test Run[1] :
Temperature[6]
: 70
Temp Run[1] :
Last Data Point
: 7

Start Test Time
: 7205.26

Header[1]	:	Time	Temperature	Frequency	Phase Angle	Complex Modulus
Header[2]	:	(s)	(°C)	(Hz)	(°)	(Pa)
Data Pt[1]	:	629.997	69.93	1.59E-03	48.93	1.14E+01
Data Pt[2]	:	695.636	70	1.57E-02	52.99	4.23E+01
Data Pt[3]	:	756.494	70	1.70E-02	52.66	4.37E+01
Data Pt[4]	:	765.005	70	1.56E-01	69.25	1.77E+02
Data Pt[5]	:	773.039	70	1.69E-01	69.88	1.83E+02
Data Pt[6]	:	776.385	70	8.19E-01	79.34	6.72E+02
Data Pt[7]	:	779.756	70	1.67E+00	80.57	1.31E+03
Data Pt[8]	:	782.875	70	3.98E+00	80.69	2.89E+03

Test Run[1] :
Temperature[7]
: 76
Temp Run[1] :
Last Data Point
: 7
Start Test Time 8384.17
: 7

Header[1]	:	Time	Temperature	Frequency	Phase Angle	Complex Modulus
Header[2]	:	(s)	(°C)	(Hz)	(°)	(Pa)
Data Pt[1]	:	629.998	75.92	1.59E-03	68.43	5.84E+00
Data Pt[2]	:	695.64	76	1.57E-02	51.46	2.53E+01
Data Pt[3]	:	756.422	76.01	1.70E-02	51.73	2.62E+01
Data Pt[4]	:	764.949	76	1.56E-01	67.1	1.01E+02
Data Pt[5]	:	773.029	76	1.69E-01	68.08	1.06E+02
Data Pt[6]	:	776.389	75.99	8.19E-01	78.08	3.85E+02
Data Pt[7]	:	779.747	76	1.67E+00	80.32	7.31E+02
Data Pt[8]	:	782.878	76	3.98E+00	81.51	1.66E+03

DSR result BMR-20-50

Test Run[1] :
 Temperature[1]
 : 40
 Temp Run[1] :
 Last Data Point
 : 7
 Start Test Time
 : 836.124

Header[1]	:	Time	Temperature	Frequency	Phase Angle	Complex Modulus
Header[2]	:	(s)	(°C)	(Hz)	(°)	(Pa)
Data Pt[1]	:	630.002	40.07	1.59E-03	41.78	2.81E+02
Data Pt[2]	:	695.715	39.98	1.57E-02	55.42	7.25E+02
Data Pt[3]	:	756.497	40	1.70E-02	57.14	7.07E+02
Data Pt[4]	:	765.076	40	1.56E-01	74.78	3.05E+03
Data Pt[5]	:	773.154	40.01	1.69E-01	76.93	3.10E+03
Data Pt[6]	:	776.501	40.01	8.19E-01	73.81	1.20E+04
Data Pt[7]	:	779.87	40.02	1.67E+00	85.39	1.99E+04
Data Pt[8]	:	783.061	40.01	3.98E+00	72.17	4.35E+04

Test Run[1] :
 Temperature[2]
 : 46
 Temp Run[1] :
 Last Data Point
 : 7
 Start Test Time
 : 1975.239

Header[1]	:	Time	Temperature	Frequency	Phase Angle	Complex Modulus
Header[2]	:	(s)	(°C)	(Hz)	(°)	(Pa)
Data Pt[1]	:	629.995	45.92	1.59E-03	38.68	1.86E+02
Data Pt[2]	:	695.708	46	1.57E-02	49.42	4.34E+02
Data Pt[3]	:	756.493	46	1.70E-02	50.14	4.26E+02
Data Pt[4]	:	765.057	46	1.56E-01	68.92	1.53E+03
Data Pt[5]	:	773.137	46	1.69E-01	69.5	1.56E+03
Data Pt[6]	:	776.496	46.01	8.19E-01	77.78	5.54E+03
Data Pt[7]	:	779.846	46	1.67E+00	79.62	9.60E+03
Data Pt[8]	:	783.026	46	3.98E+00	74.86	2.04E+04

Test Run[1] :
 Temperature[3]
 : 52
 Temp Run[1] :
 Last Data Point
 : 7
 Start Test Time
 : 3135.365

Header[1]	:	Time	Temperature	Frequency	Phase Angle	Complex Modulus
Header[2]	:	(s)	(°C)	(Hz)	(°)	(Pa)
Data Pt[1]	:	629.998	51.92	1.59E-03	37.77	1.24E+02
Data Pt[2]	:	695.636	51.99	1.57E-02	45.16	2.72E+02
Data Pt[3]	:	756.423	51.99	1.70E-02	46.05	2.69E+02
Data Pt[4]	:	764.972	52	1.56E-01	64.29	8.36E+02
Data Pt[5]	:	773.052	52.01	1.69E-01	64.61	8.47E+02
Data Pt[6]	:	776.414	52.01	8.19E-01	74.02	2.83E+03
Data Pt[7]	:	779.757	51.99	1.67E+00	75.89	5.01E+03
Data Pt[8]	:	782.899	52	3.98E+00	75.87	1.04E+04

Test Run[1] :
 Temperature[4]
 : 58
 Temp Run[1] :
 Last Data Point
 : 7
 Start Test Time
 : 4280.682

Header[1]	:	Time	Temperature	Frequency	Phase Angle	Complex Modulus
Header[2]	:	(s)	(°C)	(Hz)	(°)	(Pa)
Data Pt[1]	:	629.999	57.92	1.59E-03	36.75	1.01E+02
Data Pt[2]	:	695.711	58	1.57E-02	39.26	2.18E+02
Data Pt[3]	:	756.493	58.01	1.70E-02	39.73	2.17E+02
Data Pt[4]	:	765.07	58	1.56E-01	56.49	5.53E+02
Data Pt[5]	:	773.147	58	1.69E-01	56.93	5.57E+02
Data Pt[6]	:	776.502	58	8.19E-01	69.15	1.50E+03
Data Pt[7]	:	779.874	58	1.67E+00	73.21	2.75E+03
Data Pt[8]	:	783.056	58	3.98E+00	75.18	5.60E+03

Test Run[1] :
 Temperature[5]
 : 64
 Temp Run[1] :
 Last Data Point
 : 7
 Start Test Time
 : 5449.603

Header[1]	:	Time	Temperature	Frequency	Phase	Complex Modulus
Header[2]	:	(s)	(°C)	(Hz)	Angle	(Pa)
	:				(°)	
Data Pt[1]	:	629.997	63.92	1.59E-03	33.25	1.02E+02
Data Pt[2]	:	695.71	63.99	1.57E-02	34.66	1.91E+02
Data Pt[3]	:	756.495	64.01	1.70E-02	34.54	1.84E+02
Data Pt[4]	:	765.068	64.01	1.56E-01	50.43	4.11E+02
Data Pt[5]	:	773.137	64	1.69E-01	50.91	4.06E+02
Data Pt[6]	:	776.506	64	8.19E-01	64.62	9.44E+02
Data Pt[7]	:	779.868	64	1.67E+00	69.7	1.66E+03
Data Pt[8]	:	783.056	63.99	3.98E+00	72.61	3.29E+03

Test Run[1] :
 Temperature[6]
 : 70
 Temp Run[1] :
 Last Data Point
 : 7
 Start Test Time
 : 6607.723

Header[1]	:	Time	Temperature	Frequency	Phase	Complex Modulus
Header[2]	:	(s)	(°C)	(Hz)	Angle	(Pa)
	:				(°)	
Data Pt[1]	:	629.998	69.94	1.59E-03	31.67	8.33E+01
Data Pt[2]	:	695.637	70.01	1.57E-02	33.08	1.52E+02
Data Pt[3]	:	756.427	70	1.70E-02	32.13	1.50E+02
Data Pt[4]	:	764.985	70.01	1.56E-01	45.8	3.08E+02
Data Pt[5]	:	773.066	70.01	1.69E-01	46.15	2.98E+02
Data Pt[6]	:	776.421	70	8.19E-01	59.99	6.29E+02
Data Pt[7]	:	779.791	70	1.67E+00	64.88	1.05E+03
Data Pt[8]	:	782.979	70	3.98E+00	69.8	2.04E+03

Test Run[1] :
 Temperature[7]
 : 76
 Temp Run[1] :
 Last Data Point
 : 7
 Start Test Time
 : 7783.84

Header[1]	:	Time	Temperature	Frequency	Phase	Complex Modulus
Header[2]	:	(s)	(°C)	(Hz)	(°)	(Pa)
Data Pt[1]	:	629.996	75.93	1.59E-03	29.32	6.30E+01
Data Pt[2]	:	695.639	76	1.57E-02	28.83	1.18E+02
Data Pt[3]	:	756.422	75.99	1.70E-02	29.84	1.15E+02
Data Pt[4]	:	764.93	76.01	1.56E-01	42.11	2.16E+02
Data Pt[5]	:	772.959	76	1.69E-01	43.03	2.21E+02
Data Pt[6]	:	776.299	76	8.19E-01	54.96	4.26E+02
Data Pt[7]	:	779.61	76	1.67E+00	60.55	6.80E+02
Data Pt[8]	:	782.738	75.99	3.98E+00	66.46	1.24E+03